



Review article

Engineering multifunctional bioactive citrate-based biomaterials for tissue engineering

Min Wang^a, Peng Xu^{a,*}, Bo Lei^{b,c,d,e,**}^a Honghui Hospital, Xi'an Jiaotong University, Xi'an, 710000, China^b Key Laboratory of Shaanxi Province for Craniofacial Precision Medicine Research, College of Stomatology, Xi'an Jiaotong University, Xi'an, 710000, China^c Frontier Institute of Science and Technology, Xi'an Jiaotong University, Xi'an, 710000, China^d State-Key Laboratory for Mechanical Behavior of Materials, Xi'an Jiaotong University, Xi'an, 710000, China^e State Key Laboratory for Manufacturing Systems Engineering, Xi'an Jiaotong University, Xi'an, 710000, China

ARTICLE INFO

Keywords:

Bioactive materials
Bioactive polymers
Citrate-based biomaterials
Multifunctional modification
Tissue engineering

ABSTRACT

Developing bioactive biomaterials with highly controlled functions is crucial to enhancing their applications in regenerative medicine. Citrate-based polymers are the few bioactive polymer biomaterials used in biomedicine because of their facile synthesis, controllable structure, biocompatibility, biomimetic viscoelastic mechanical behavior, and functional groups available for modification. In recent years, various multifunctional designs and biomedical applications, including cardiovascular, orthopedic, muscle tissue, skin tissue, nerve and spinal cord, bioimaging, and drug or gene delivery based on citrate-based polymers, have been extensively studied, and many of them have good clinical application potential. In this review, we summarize recent progress in the multifunctional design and biomedical applications of citrate-based polymers. We also discuss the further development of multifunctional citrate-based polymers with tailored properties to meet the requirements of various biomedical applications.

1. Introduction

In recent years, the complexity and diversity of polymers have been regulated by many their molecular, aggregated, and apparent structures, which allow their wide applicability to biomedicine [1–3]. Compared to traditional nondegradable polymers, biodegradable polymers do not require subsequent surgical removal after implantation *in vivo*, expanding their range of biomedical applications, such as tissue engineering, drug/gene delivery, and bioimaging [4,5]. Polyester biomaterials, a class of synthetic biodegradable polymer materials, have become the most promising biomaterials because of their controllable mechanical properties, good biodegradation, and excellent biocompatibility [6–8].

Citric acid, an intermediate of the tricarboxylic acid cycle (TCA cycle), plays an important role in metabolism, calcium chelation, the formation of hydroxyapatite (HA), and regulation of the thickness of the bone apatite structure [9,10]. Moreover, modification of polymers using

citric acid produces antioxidant and anti-inflammatory properties, and the residual carboxyl and hydroxyl groups can be further functionally modified [11]. Therefore, citric acid is an ideal starting material for the synthesis of biodegradable polymers. In 2004, Ameer and Yang et al. synthesized a new type of biodegradable citrate-based biomedical elastomer, including poly(hexamethylene citrate) (PHC), poly(octamethylene citrate) (POC), poly(decamethylene citrate) (PDC), and poly(dodecamethylene citrate) (PDDC), using citric acid and diol and utilizing melt polymerization and vacuum thermal crosslinking technology [12]. After continuous studies, the main cross-linking routes of citrate-based polymers include thermal crosslinking (esterification and thermal click reaction) and room temperature crosslinking (HDI crosslinking, double bond crosslinking, and mussel-inspired crosslinking). It is worth noting that polyurethane-doped citrate elastomers require HDI crosslinking at room temperature and further esterification crosslinking at high temperature (Fig. 1) [13,14]. Among the abovementioned citrate-based biomedical elastomers, POC elastomers possess

Peer review under responsibility of KeAi Communications Co., Ltd.

* Corresponding author.

** Corresponding author. Key Laboratory of Shaanxi Province for Craniofacial Precision Medicine Research, College of Stomatology, Frontier Institute of Science and Technology, Xi'an Jiaotong University, Xi'an 710000, China.

E-mail addresses: sousou369@163.com (P. Xu), rayboo@xjtu.edu.cn (B. Lei).<https://doi.org/10.1016/j.bioactmat.2022.04.027>

Received 12 January 2022; Received in revised form 22 April 2022; Accepted 24 April 2022

2452-199X/© 2022 The Authors. Publishing services by Elsevier B.V. on behalf of KeAi Communications Co. Ltd. This is an open access article under the CC BY-NC-ND license (<http://creativecommons.org/licenses/by-nc-nd/4.0/>).

controllable mechanical properties, good biodegradability, and excellent biocompatibility, which is foundational to their biomedical applications [12,15]. Based on work previously published by Ameer and Yang et al., a POC-based biomaterial called “Citregen” as a new type of surgical fixation material, which can not only reconnect damaged tissues but also promote tissue healing after degradation of the citrate. Importantly, the fixation screw “Citrellock” prepared from the synthetic “Citregen” polymer and which has a tissue repair function, has been approved by the Food and Drug Administration (FDA). It is manufactured and sold by Acuitive Technologies, Inc., which further enhances the potential clinical applications of POC-based polymers.

The mechanical and degradation properties of POC elastomers can be adjusted by controlling the crosslinking temperature, crosslinking time, degree of vacuum, and molar ratio of the initial monomers during synthesis. For example, an increase in the crosslinking temperature or crosslinking time can increase the crosslinking density of POC to enhance its tensile strength and Young’s modulus, reducing the elongation at break and degradation rate. The POC elastomers exhibited a comparable tensile strength (~6.1 MPa) and Young’s modulus (0.96–16.4 MPa) to elastin from bovine ligaments (tensile strength: 2 MPa, Young’s modulus: 1.1 MPa) and a comparable maximum elongation (~265%) with arteries and veins (~260%) and elastin (~150%). POC elastomers can be completely degraded in phosphate-buffered saline (PBS) within 6 months and undergo faster degradation due to the action of various enzymes *in vivo*. In addition, POC elastomers can mediate the nonspecific adsorption of proteins to promote cell adhesion compared with other exogenous adhesion protein coatings, and they do not cause chronic inflammation *in vivo*. Importantly, POC elastomers can effectively maintain the activity and stability of encased drugs or proteins because of the mild crosslinking temperature and normal pressure during synthesis [12].

At present, the most commonly used biomedical degradable materials include poly (ϵ -caprolactone) (PCL), polylactide (PLA), and poly (glycerol sebacate) (PGS) [16–18]. In contrast to PCL and PLA, PGS is a typical elastomeric polymer prepared by a facile polycondensation reaction of glycerol and sebacic acid, which has wide applications in cardiovascular, nerve, cartilage, bone, and corneal tissue engineering

through specific chemical modifications [18]. Considering the elastomeric properties and facile synthesis of PGS, POC polymers have been reported using a similar synthesis process, including the use of citric acid and diol. Compared with traditional biodegradable synthetic polymers, POC polymers ($M_n = 1085$ g/mol) possess many advantages, including simple synthesis, controllable structure, good biocompatibility, biomimetic viscoelastic mechanical behavior, controllable biodegradability, and the capacity for further functional modification, which provide broad application prospects in soft and hard tissue regeneration and nanomedicine design, both *in vitro* and *in vivo* [12–14]. However, the conventional POC polymer is water-insoluble and limited with a narrow scope of mechanical properties, bioactivities, and functions, which pose obstacles in using it for application in tissue engineering, bioimaging and drug/gene delivery [12]. To expand their properties and biomedical applications, further functionalization of POC is necessary. In recent years, our group and others have investigated the synthesis and biomedical applications of functionalized POC polymers, which would accelerate the research and clinical applications of citrate-based polymers. In this paper, we mainly discuss the functionalization of citrate-based biomaterials and their biomedical applications (Fig. 2). The properties and benefits of different functional citrate-based polymers used in biomedical applications are summarized to guide further research. Finally, we emphasize the advantages and challenges of multifunctional citrate-based polymers in various biomedical applications.

2. Functional design for cardiovascular tissue engineering

2.1. Critical factors of biomaterials in cardiovascular tissue engineering

Myocardial tissue has a complex architecture comprising different cells, such as cardiomyocytes; fibroblasts; smooth muscle cells (SMCs); endothelial cells (ECs); and extracellular matrix (ECM), such as fibrin, collagen, and elastin, which together maintain the elastomeric mechanical properties and physiological activities of the heart [19]. ECM plays an important role in cell interconnection, signal transmission, and mechanics [20]. Typical human myocardial tissue has highly

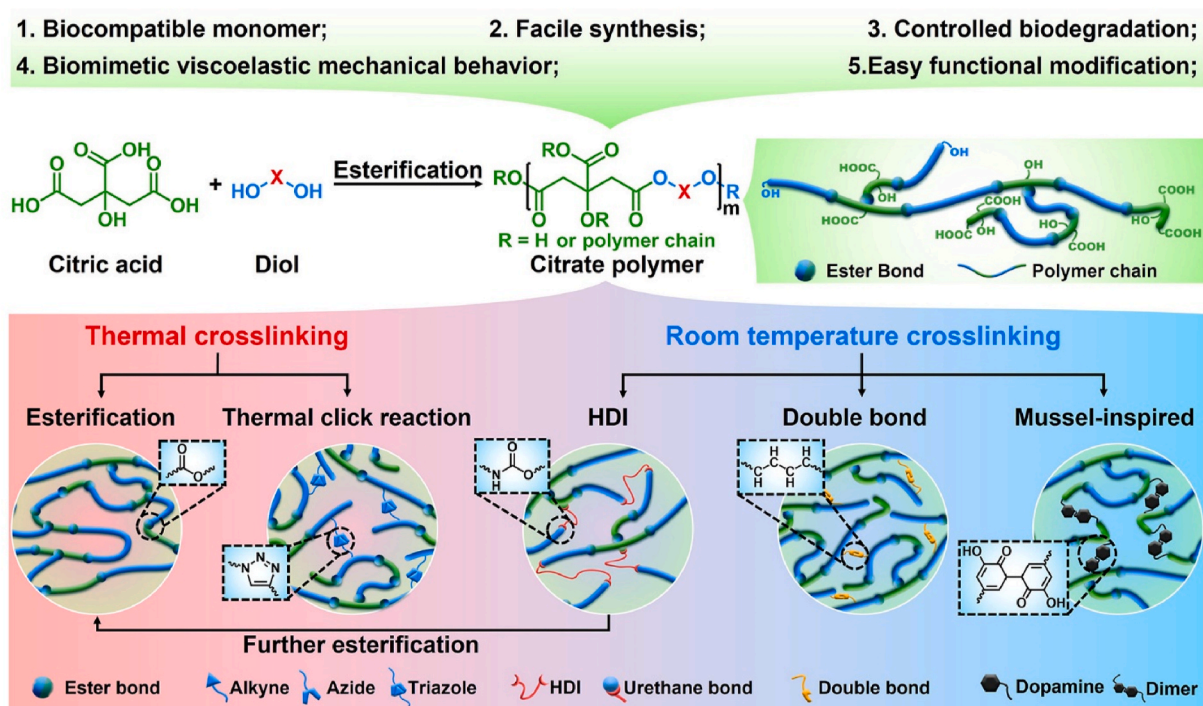


Fig. 1. Synthesis and properties of citrate prepolymer and citrate elastomers.

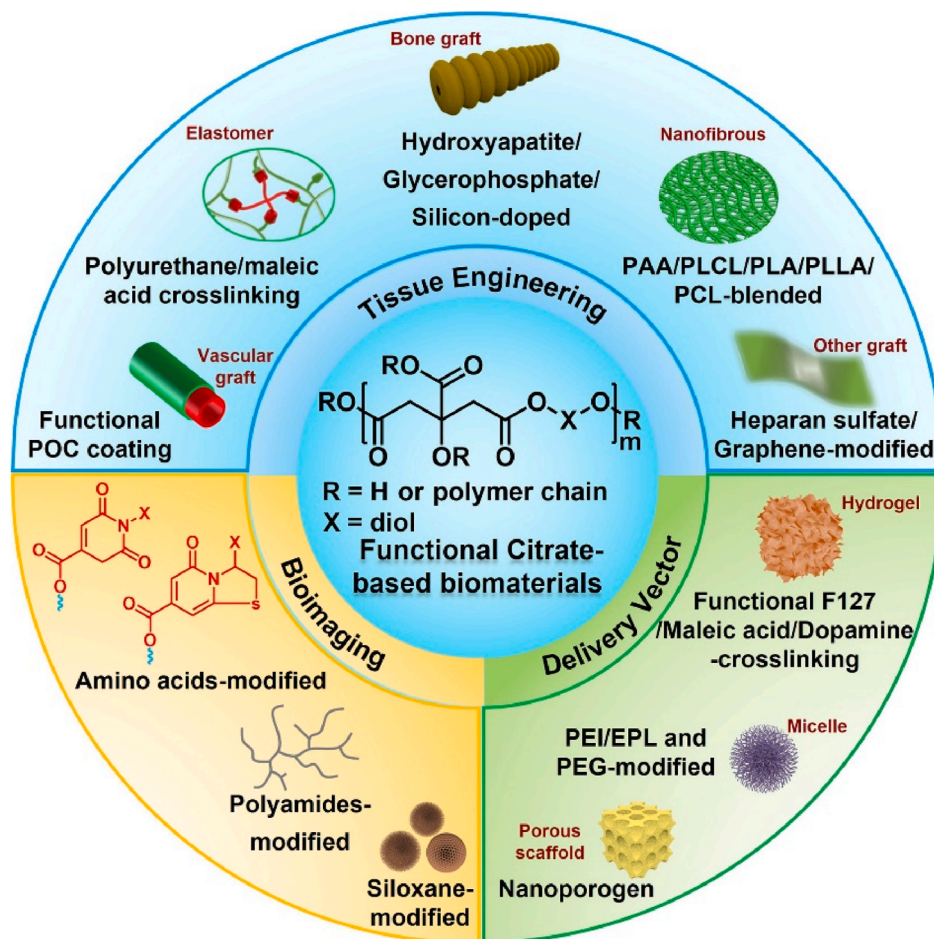


Fig. 2. Development and biomedical applications of functional citrate-based biomaterials. PAA: poly (acrylic acid); PLCL: poly (*l*-lactic acid)-co-poly-(3-caprolactone); PLA: polylactide; PLLA: poly (*l*-lactic acid); PCL: polycaprolactone; F127: Pluronic; PEI: polyethyleneimine; EPL: ϵ -polylysine; PEG: polyethylene glycol.

elastomeric mechanical properties with an end-diastolic Young's modulus between 0.2 and 0.5 MPa and tensile strength in the range of 3–15 kPa [21]. Previous studies have indicated that various factors, such as mimicking the biochemical environment of the natural myocardium, recruiting and promoting muscle cell division, enhancing tissue vascularization, and controlling the release of repair-related factors, can promote myocardial tissue repair [19,22–24]. Vascular tissue is an expandable and elastic tubular layered structure comprising different cells, proteins, and ECM [19]. The vascular intima is mainly composed of ECs, which are involved in thrombosis prevention, vasomotor regulation, inflammation regulation, and immune regulation [25]. The vascular media mainly comprises SMCs and elastin and plays an important role in vasomotor adjustment, vascular repair, and proliferative diseases [26]. Vascular adventitia mainly comprises fibroblasts, which can strengthen and protect blood vessels and fix them in the surrounding environment [27]. The typical vascular tissue has viscoelastic mechanical properties with a burst pressure up to 3000 mmHg, compliance in the range of 10–20%/100 mmHg, a tensile strength of approximately 4.3 MPa, and a special biological function that prevents platelet adhesion [28]. Previous studies have indicated that various factors can promote vascular tissue repair, such as providing a biochemical environment that mimics natural vascular tissue, inhibiting platelet adhesion, reducing inflammation, promoting endothelialization, and controlling the release of bioactive molecules [19,29,30].

Considering the structure and function of natural cardiovascular tissues, cardiovascular tissue engineering strategies have focused on the development of biomaterial scaffolds to simulate or replace natural

cardiovascular tissues, which not only provide the necessary microenvironment for cell proliferation, differentiation, and metabolism but also effectively maintain normal physiological activities. Ideal cardiovascular grafts should possess multifunctional properties, including biomimetic elastomeric mechanical properties, appropriate biodegradation, excellent biocompatibility, inhibition of thrombus and inflammatory reactions, and promotion of endothelialization [31–33]. For example, the biomimetic mechanical properties of vascular grafts can effectively simulate natural blood vessels and maintain the normal physiological activities of blood vessels [31]. Vascular grafts that inhibit thrombi and inflammatory reactions can effectively ensure normal use without thrombus formation and severe inflammatory responses [32]. In addition, endothelialization of vascular grafts can effectively prevent local thrombus formation and restenosis [33].

2.2. Functionalized citrate polymers for cardiovascular tissue engineering

Among the various biodegradable vascular grafts, such as hyaluronan (HA), PCL, and polylactic-co-glycolic acid (PLGA), POC has been extensively studied in vascular tissue engineering owing to its excellent elastomeric mechanical properties, good biodegradability, and biocompatibility (Fig. 3 and Table 1) [34–36]. Motlagh et al. evaluated the hemocompatibility and human aortic endothelial cell (HAEC) compatibility of POC polymers *in vitro*. POC exhibited good hemocompatibility, including decreased platelet adhesion and clotting, negligible hemolysis, appropriate protein adsorption, and effective support for HAEC attachment and differentiation [37]. Owing to its

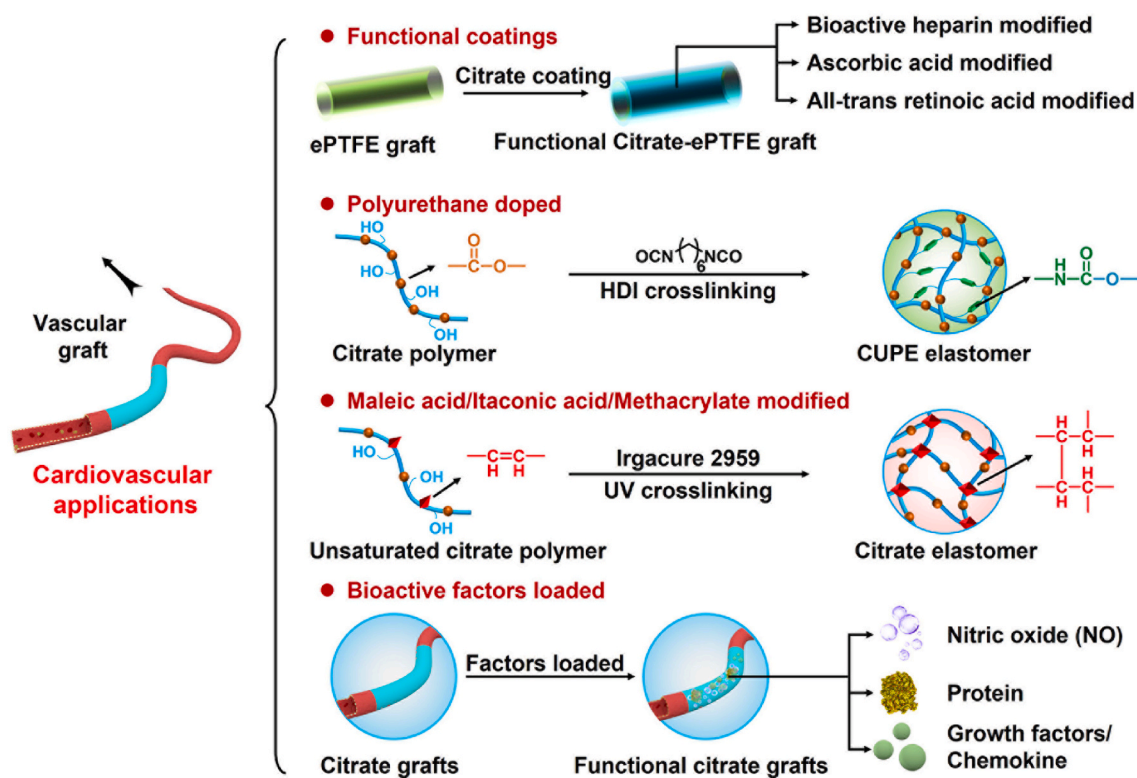


Fig. 3. Schematic diagram of further functionalized modified citrate-based polymers for vascular applications.

biomimetic mechanical properties and good hemocompatibility, POC is a good coating biomaterial and vascular implant for cardiovascular tissue engineering applications.

2.2.1. Antithrombus and endothelialization functionalized citrate coating for vascular implants

Yang et al. prepared a POC-ePTFE graft using POC coating to significantly change the surface energy of an expanded polytetrafluoroethylene (ePTFE) graft without changing its compliance. Because POC polymers can reduce the adhesion of platelets and the infiltration of macrophages, the POC-ePTFE graft can not only inhibit thrombi and inflammatory reactions, but also promote the endothelialization of grafts [38]. Kibbe et al. further evaluated the mid-term performance of the POC-ePTFE grafts. After the POC-ePTFE graft was implanted in the porcine carotid artery for 4 weeks, it remained patent without hemodynamically significant stenoses, adverse reactions, or inflammation [39]. Hoshi et al. further developed a bioactive heparin-POC-ePTFE vascular graft by incorporating heparin with antithrombogenic and anticoagulant properties into the POC-ePTFE vascular graft, which not only significantly inhibited whole blood clotting and platelet adhesion, but also supported endothelial cell proliferation and specific phenotype expression (Fig. 4A–C) [40]. Lith et al. prepared ascorbic acid-containing POC-based elastomer (POCA) with intrinsic antioxidant properties, including free-radical scavenging, iron chelation, and lipid peroxidation inhibition, and maintained a high viability of vascular cells. Importantly, POCA-coated ePTFE grafts can reduce neointimal hyperplasia in guinea pig aortic grafts [41]. Subsequently, Lith et al. prepared a biodegradable elastomer (POCR) with antioxidant and retinoid-like properties by incorporating all-trans retinoic acid (atRA) into a POC polymer network. The POCR elastomer also exhibits free radical scavenging, inhibition of lipid peroxidation, and inhibition of vascular smooth muscle cell proliferation and migration [42]. Gregory et al. further fabricated a POCR-coated ePTFE (atRA-POC-ePTFE) vascular graft, which effectively inhibited intimal formation and hastened endothelialization (Fig. 4D and E) [43]. Zailani et al. successfully

improved the hemocompatibility of polyethersulfone (PES) membranes through POC blending. POC-PES membranes exhibit reduced fibrinogen adsorption and platelet adhesion; prolonged activated partial thromboplastin time and prothrombin time; decreased TAT, C5a, and C3a activation; and increased Ca^{2+} absorption [44].

2.2.2. Biomimetic mechanics and structure functionalized citrate-based vascular implants

To develop soft, strong and completely elastic POC-based polymers for cardiovascular tissue engineering, Dey et al. reported a polyurethane-doped POC elastomer (CUPE) through 1,6-hexamethylene diisocyanate (HDI) chemical crosslinking and further thermal crosslinking, which possessed a tensile strength of approximately 41.07 MPa and a breaking elongation of approximately 222.66%. The CUPE elastomer exhibited good biocompatibility and effectively inhibited platelet adhesion according to the preliminary hemocompatibility evaluation (Fig. 4F–H) [45]. Subsequently, Dey et al. evaluated the application potential of the CUPE elastomer as a vascular graft. The CUPE vascular graft exhibited tensile strength, tunable burst pressure, and suture retention properties similar to those of native veins and arteries. Compared to poly(L-lactic acid) (PLLA), the CUPE vascular graft released less inflammatory cytokines, good blood compatibility, and antithrombosis [46]. Moreover, Dey et al. prepared a series of CUPE elastomers by varying the diol component, which had a significant difference in physicochemical properties and no influence on long-term biocompatibility *in vivo*. Therefore, CUPE elastomers may serve as viable vascular grafts for cardiovascular tissue engineering *in vivo* [47].

In addition to polyurethane-doped POC elastomers, unsaturated polyester-doped POC elastomers, including maleic acid, maleic anhydride, and itaconic acid, have been widely studied in a bid to improve their mechanical properties. Gyawali et al. reported a novel biodegradable POC-based elastomer (POMC) obtained by covalently crosslinking maleic acid for versatile biomedical applications. The POMC elastomer exhibited controllable mechanical, degradation, and swelling properties through a combination of thermal crosslinking and photocrosslinking.

Table 1
Functionalized citrate-based polymers for cardiovascular tissue engineering.

Materials	Component	Properties	Tissue engineering	Ref.
POC-ePTFE	POC; ePTFE	Hydrophilicity; Compliance	Reduce platelets adhesion and macrophage infiltration; Inhibit thrombus; Promote endothelialization	38,39
Heparin-POC-ePTFE	POC; ePTFE; Heparin	Anti-thrombogenic; Anti-coagulant	Inhibit platelets adhesion and thrombus; Supported endothelial cells proliferation and specific phenotype expression	40
POCA- ePTFE	POC; ePTFE; Ascorbic acid	Intrinsic antioxidant	Reduce neointimal hyperplasia	41
POCR-ePTFE	POC; ePTFE; atRA	Antioxidant; Retinoid-like properties	Reduce macrophage and leukocyte infiltration; Inhibit the intimal formation; Hasten endothelialization	42,43
POC-PES	POC; PES	Enhanced hemocompatibility	Reduced fibrinogen adsorption and platelet adhesion	44
CUPE	POC; Polyurethane	Similar tensile strength, tunable burst pressure and suture retention	Inhibit platelets adhesion; Reduce inflammation; Anti-thrombosis	45–47
POMC	POC; Maleic acid	Controllable mechanical and degradation; Further Modification	Good cytocompatibility; Reduce inflammation	48
CUPOMC	POC; Maleic acid; Polyurethane	Increased tensile strength; Great processability	Support the cell adhesion and proliferation	49
POMaC	POC; Maleic anhydride	Increased elongation; Controlled physical structure and properties; Good biocompatibility	Minimally invasive delivery; Soft tissue engineering	50–52
AP	POMaC; Dopamine	Spatially varying adhesive properties	Biomaterial patches of supporting damaged tissue	53
PICO	POC; Itaconic acid	Tunable elasticity	Support cardiac tissue organization and viability	54
POC-PDDC	POC; PDDC	Biphasic tubular mimicked blood vessels; Shorten cells co-culture time	Small-diameter blood vessel scaffold	55
Porous POC-ECM proteins	POC; ECM proteins	Controlled pore size, porosity and shape	Support cell adhesion	56
POC-ECM	POC; ECM	Reduce platelet adhesion, Inhibit clotting	Improve thromboresistance and recellularization properties	57
PITCO	Dimethyl itaconate, Triethyl citrate; 1,8-octanediol	Fast crosslinking time; Semi-permeable; Appropriate elastic properties	Support the cells adhesion and proliferation	59
mPDDC	PDDC; glycidyl methacrylate	Customizable; Compressible, Self-expanding, Bioabsorbable, Antioxidant	Customize specific 3D-printed vascular scaffold	60,62
POCDA/PDDCDA	POC/PDDC; NO-donor	Controllable NO release; Compliance	Controlled cytostatic or cytotoxic effects; Inhibit neointimal hyperplasia	63
MA-POC/MA-PDDC	POC; PDDC; MA; Miscible NO-donor	Strong tensile strength; Radial compressive strength; Sustained release of NO	Local sustained release of NO in the vasculature	64
MTN	CUPE; GP1b; Anti-CD34 antibodies	Inhibit platelet aggregation; Reduce neointimal hyperplasia	Re-endothelialization <i>in situ</i>	66
PPCN	Citric acid; PEG; PNIPAAm	Lower critical solution temperature; Intrinsic antioxidant properties	Sustained release of chemokine <i>SDF-1a</i> to support the proliferation of vascular cells	67
PPC-ET/PEG	Citric acid; PEG; Ethyl thioglycolate	Injectable; Sustained release of citrate and growth factors	Reduce scar formation; Increase new blood vessel formation	68

POC: poly(octamethylene citrate); ePTFE: expanded polytetrafluoroethylene; atRA: all-trans retinoic acid; PES: polyethersulfone; GP1b: glycoprotein 1b; PDDC : poly (dodecamethylene citrate); ECM: extracellular matrix; PEG: polyethylene glycol; PNIPAAm: poly-*N*-isopropylacrylamide; NO-donor: *N,N*-Bis(2-hydroxyethyl)ethylenediamine . MA: 2-aminoethyl methacrylate; Miscible NO-donor: diazeniumdiolated *N,N*-diethyldiethylenetriamine.

Moreover, the residual carboxyl and hydroxyl groups of the POMC elastomer can be further coupled with biomolecules, such as proteins, polypeptides, or antibodies, to promote cell proliferation and adhesion, and they do not cause a strong inflammatory reaction *in vivo* [48]. Zhang et al. further developed a photocrosslinkable urethane-doped POMC elastomer (CUPOMC) via HDI chemical crosslinking. The CUPOMC elastomer exhibited a drastic increase in tensile strength (~10.91 MPa) compared to the POMC elastomer (less than 1 MPa) and could support cell adhesion and proliferation. Importantly, CUPOMC prepolymers possess great processability under various conditions because of their compatibility with dual crosslinking methods, including thermocrosslinking and photocrosslinking [49]. In addition, Tran et al. developed a soft biodegradable POC-based elastomeric (POMaC) by replacing maleic acid with maleic anhydride. Compared to the POMC elastomer (elongation of 382%), the POMaC elastomer displayed a higher elongation rate of up to 534%. Moreover, the POMaC elastomer possesses good cytocompatibility and tissue biocompatibility, which supports its potential application as a soft and elastic 3D microchannel scaffold for soft tissue engineering [50]. Montgomery et al. prepared a flexible shape-memory POMaC scaffold polymer with a microfabricated lattice for the design of patches and minimally invasive delivery of functional tissues. The scaffold could effectively return to its original shape after injection without affecting the viability and function of the surrounding cells. The cardiac patch possessed vascularization, macrophage recruitment, and cell survival comparable to those of surgical patches. In addition, minimally invasive delivery to the heart, liver, and aorta has

been achieved in pigs [51]. Moreover, Montgomery et al. further fabricated POMaC scaffolds with various shapes by soft lithography and evaluated the effect of the scaffold design on scaffold elasticity, which may offer a promising strategy for precise material design due to its physical structure and properties [52]. Bannerman et al. designed an elastic polymer patch (AP) with spatially varying adhesive properties via the copolymerization of dopamine (DA) and POMaC polymers. The AP patch exhibited negligible cytotoxicity and improved adhesive strength (~0.44 N/cm²) to cardiac tissue compared to fibrin glue for the POMaC path (~0.17 N/cm²) and elastic modulus (~43 kPa) comparable to cardiac tissue (relaxed: 10–20 kPa; contracted: 200–500 kPa) [53]. In addition, Huyer et al. synthesized an unsaturated polyester bioelastomer (PICO) using itaconic acid to copolymerize a POC polymer. The PICO bioelastomer exhibited tunable elasticity in the range of 36–1476 kPa and could effectively support cardiac tissue organization and viability [54].

To mimic the intimal and medial layers of blood vessels, Yang et al. fabricated a new degradable biphasic tubular scaffold (POC-PDDC) comprising a connected POC porous phase and PDDC nonporous phase. This biphasic scaffold can shorten the coculture time of SMCs and ECs *in vitro* to reduce the risk of contamination, and it is expected to be a small-diameter blood vessel scaffold that can reduce the side effects caused by compliance mismatch with host vessels *in vivo* [55]. In addition, Hidalgo-Bastida et al. prepared a series of porous POC scaffolds with different pore sizes, porosities, and shapes and reported that a decrease in porosity can lead to an increase in the elastic modulus. These porous

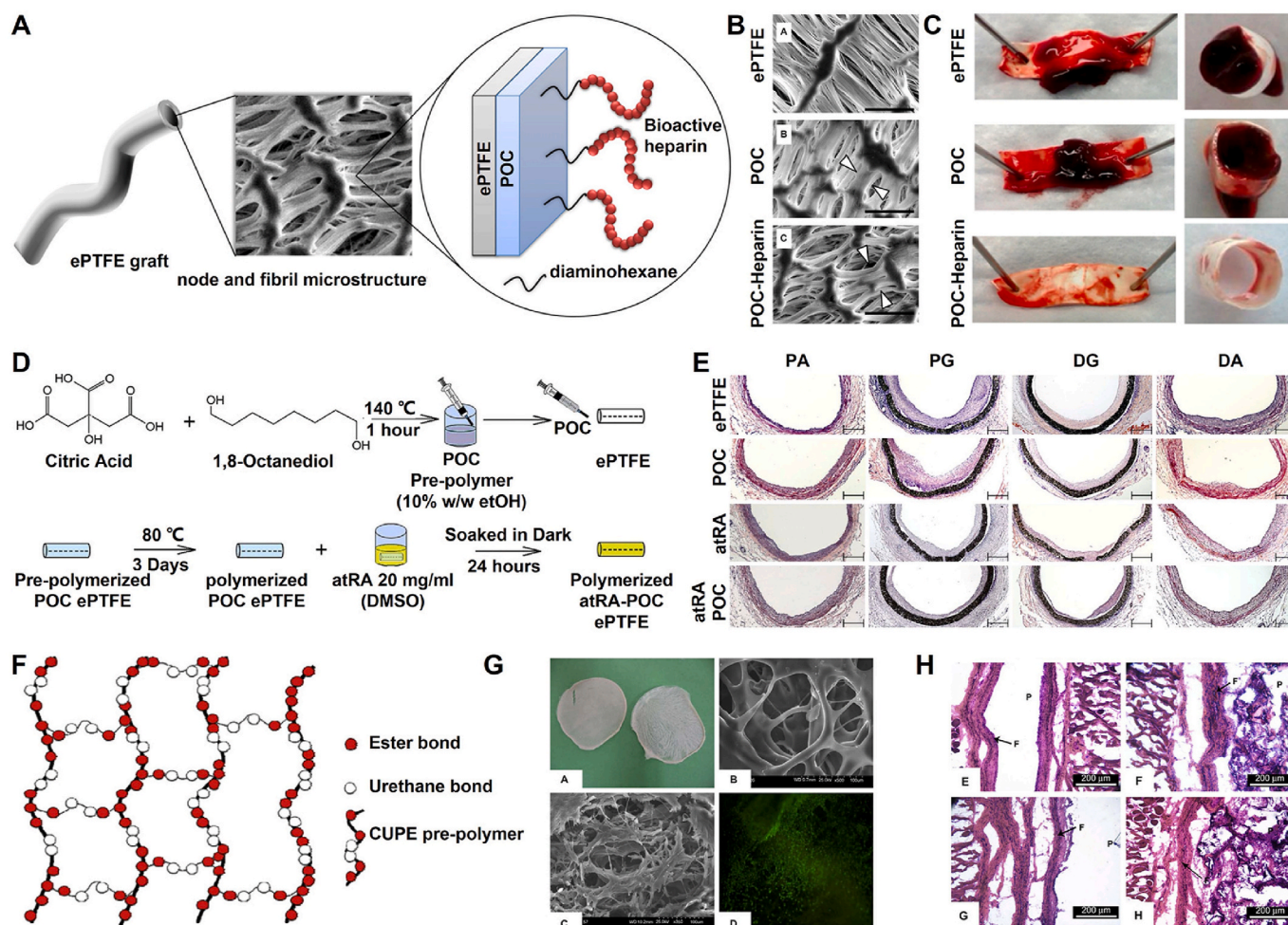


Fig. 4. Development and cardiovascular applications of functional POC-based biomaterials. (A) Synthesis schematic of the POC-Heparin ePTFE vascular graft; (B, C) SEM micrograph (B) and whole blood clot formation (C) of ePTFE, POC-coated ePTFE and POC-Heparin-coated ePTFE [40]; Copyright 2013, Elsevier. (D) Synthesis schematic of atRA-POC-ePTFE vascular graft; (E) The morphometric analysis for each graft and region, PA: proximal artery, PG: proximal graft, DG: distal graft, DA: distal artery, scale bar = 50 μm [43]; Copyright 2013, Elsevier. (F) Synthesis schematic of CUPE scaffold; (G) The morphology of CUPE scaffold and the state of fibroblast-seeded on CUPE scaffold; (H) Histology of *in vivo* response to each scaffold after 4-week [45]. Copyright 2008, Elsevier.

POC scaffolds can effectively support cell adhesion after coating with three different ECM proteins: fibronectin, laminin, and collagen [56]. Jiang et al. designed POC-based polymer-ECM composites to effectively improve their thromboresistance and recellularization properties. Compared with untreated ECM, the composites can significantly reduce platelet adhesion, inhibit clotting, and support endothelial cell adhesion [57].

2.2.3. 3D printing functionalized citrate-based vascular scaffolds

With the advent of 3D printing processes, customized patient-specific vascular grafts can be manufactured at relatively low cost [58]. Savoji et al. prepared vascular tubes (PITCO) through 3D printing using bio-elastomer prepolymers comprising dimethyl itaconate (DMI), triethyl citrate (TEC), and 1,8-octanediol (OD). The tubes possessed a fast crosslinking time (less than 100 s) and had elastic properties (modulus of 11–53 kPa) comparable to those of cardiac tissues. The tubes supported human umbilical vein endothelial cell adhesion and proliferation and were semipermeable, allowing for the exchange of oxygen, nutrients, and metabolic waste in tissue engineering applications. In addition, the endothelialized tubes can support cardiac tissue formation by human pluripotent stem cells (hPSC) [59]. Lith et al. fabricated a photopolymerizable PDDC-based 3D-printed vascular scaffold (mPDDC), including citric acid, 1,12-dodecanediol, and glycidyl methacrylate, using a custom-made microcontinuous liquid interface production

system (microCLIP). The vascular scaffold possessed customizable (20 mm length printed for approximately 70 min), compressible, self-expanding, bioabsorbable, antioxidant, and mechanical properties (500 μm thickness) comparable to those of nitinol stents, which strengthened the radial compression of porcine arteries after deployment, suggesting the possibility of preparing customized patient-specific stents in clinical applications [60]. Subsequently, Akar et al. reported mechanically functional 3D-printed bioresorbable citrate-based vascular scaffolds [61]. Ware et al. further presented a methodology that calibrated the high-resolution microcontinuous liquid interface production (μCLIP) process using a dedicated speed working curve method to optimize the high-resolution and high-speed PDDC-based 3D printed bioresorbable vascular scaffold process, including material strength/stiffness, exposure dosage, and fabrication speed. The methodology can not only shorten the fabrication time of the 2 cm-long scaffolds (layer slicing with 5, 10, and 15 μm printed within 26.5, 15.3 and 11.3 min, respectively), but also reduce the thickness (150 μm) required for radial stiffness to a value comparable to those of nitinol stents and the commercial polymer stent ABSORB GT1BVS [62].

2.2.4. Release of bioactive factors from functionalized citrate-based vascular scaffolds

Nitric oxide (NO) delivery is important for vascular applications. Serrano et al. synthesized NO-releasing elastomers (POCDA or PDDCDA)

using *N,N*-bis(2-hydroxyethyl)ethylenediamine and POC or PDDC polymer via a condensation reaction, which can effectively release NO to inhibit the proliferation of angiogenesis intima after covering the blood vessels [63]. Wang et al. synthesized photocrosslinked biodegradable POC-based elastomers (MA-POC) and PDDC-based elastomers (MA-PDDC) functionalized using 2-aminoethyl methacrylate (MA) to sustain NO release. The elastomers exhibited strong tensile strength and radial compressive strength and sustained NO release for at least one week, which provided a new approach for treating thrombosis and vascular restenosis by local sustained NO release into the vasculature [64].

Sharma et al. prepared heparan sulfate-modified POC thin films (heparin-POC) with sustained release of vascular endothelial growth factor (VEGF) to effectively promote vascular regeneration [65]. Su et al. developed a multifunctional targeted nanoscaffold (MTN) comprising a CUPE polymer, glycoprotein 1b (GP1b), and antiCD34 antibodies for *in situ* reendothelialization. Nanoscaffolds can inhibit platelet aggregation and activation, and promote endothelial progenitor cells for *in situ* endothelial regeneration. Moreover, the nanoscaffolds can reduce neointimal hyperplasia by 57% and increase endothelial cell regeneration by ~60% at vascular injury sites over 21 d [66].

Yang et al. synthesized a thermoresponsive biodegradable antioxidant hydrogel (PPCN) comprising citric acid, polyethylene glycol (PEG), and poly-*N*-isopropylacrylamide (PNIPAAm) via polycondensation and free radical polymerization. The PPCN hydrogel exhibited a lower critical solution temperature (26 °C) and intrinsic antioxidant properties, including free-radical scavenging, iron chelation, and lipid peroxidation inhibition. The PPCN hydrogel can effectively sustain the release of chemokine *SDF-1α* to support the proliferation of vascular cells [67]. Yuan et al. reported an injectable citrate-based hydrogel (PPC-ET/PEG) and investigated its performance as an angiogenic biomaterial for improving cardiac repair after myocardial infarction. In a rat myocardial infarction model, this PPC-ET/PEG hydrogel could continuously release citrate and growth factors to significantly reduce scar formation and the infarct area, increase the wall thickness and new blood vessel formation, and improve heart repair after myocardial infarction [68].

3. Bone tissue engineering

3.1. Critical factors of biomaterials in bone tissue engineering

Bone tissue is a natural nanocomposite with a hierarchical structure comprising organic proteins (mainly collagen I), inorganic minerals (mainly calcium phosphate), and multiple cells (osteoblasts, osteoclasts, stem cells, etc.) [69]. The bone ECM is mainly composed of crosslinked collagen fibers, and the bone minerals are calcium phosphate crystals located in and around the collagen fibers [70]. The outer bone tissue is composed of dense cortical bone or dense bone, whereas the interior bone is composed of cancellous or spongy bone. The composition and layered structure of bone tissue provide it with unique mechanical properties and physiological functions [69]. Previous studies have indicated that various factors can promote bone tissue repair, including good mechanical support, nutrient delivery, cell adhesion and proliferation, osteoconductivity (biomineralization deposition), and osteogenesis [69,71,72]. Therefore, bone tissue engineering materials are generally designed based on the physical structure and functional design of the bone tissue, which promotes the growth of new bone tissue and restores its functions. Ideal bone tissue engineering scaffolds should possess multifunctional properties, including biomimetic structural properties, controlled biodegradation, excellent biocompatibility and antibacterial activity, and good osteoconductivity and osteoinductivity [73–76]. For example, the antibacterial activity of scaffolds can effectively prevent related infections after being implanted [75]. The biomineralization ability and osteogenic bioactivity of scaffolds can also provide a suitable environment for bone integration, osteoblastic growth, and osteoblast differentiation, thereby facilitating excellent

bone defect repair ability [76].

3.2. Functionalized citrate for bone tissue engineering

Previous studies have shown that citrate in human bone tissue plays an important role in metabolism, calcium chelation, hydroxyapatite formation, and regulation of bone apatite structure thickness [77–80]. Therefore, citrate polymers have shown promise in bone tissue engineering (Fig. 5 and Table 2).

3.2.1. Si-functionalized citrate-based polymers for enhanced mechanics and osteogenesis

The doping of Silicon (Si) could effectively improve the mechanical properties of scaffolds and promote bone formation [81]. Ren et al. developed a series of POC/PSC composites using a POC polymer and phytic acid-derived bioactive glass (PSC). The POC/PSC composite exhibited improved mechanical performance owing to the formation of calcium dicarboxylate bridges, and its compressive strength and modulus were approximately 50 MPa and 1.3 GPa, respectively. In addition, the POC/PSC composite showed good bioactivity and cytocompatibility, integrated well with surrounding tissues, and stimulated bone regeneration in rat femoral condyle defects [82]. Chen et al. fabricated a novel ibuprofen (IBU)-loaded POC-based scaffold ($\text{SiO}_2/\beta\text{-TCP/POC}$) using silica, β -tricalcium phosphate, and a POC polymer via a 3D printing technique, which possessed a highly interconnected porous network (macropores: 350–450 nm and mesopores: 3.65 nm) with a high load and sustained release of IBU. In addition, the scaffold exhibited effective antimicrobial properties and could be used in the repair of infectious bone defects [83]. Du et al. reported a series of silica-grafted POC hybrid elastomers (SPOC), including POCAS (POC and 3-aminopropyltriethoxysilane) and POCGS (POC and 3-(2,3-glycidoxy) propyltrimethoxysilane), produced via melt polymerization and vacuum thermal crosslinking technology. SPOC hybrid elastomers possess controllable mechanical and degradation properties and can significantly promote the adhesion and proliferation of myoblasts, fibroblasts, bone marrow mesenchymal stem cells, and osteoblasts. Moreover, the POCAS elastomer exhibits a higher modulus (approximately 22.1 MPa) and elongation (approximately 134%) than the POCGS elastomer [84]. To improve the mechanical properties of POCAS elastomers, Du et al. prepared a multifunctional POC hybrid elastomer (CMSPC) through the chemical crosslinking of HDI instead of thermal crosslinking. Compared to POCAS elastomers, CMSPC elastomers exhibited better mechanical properties, including a modulus (approximately 976 MPa) and elongation (approximately 309%) comparable to that of trabecular bone and tibia tissues. In addition, the CMSPC elastomer significantly promoted the proliferation of osteoblasts, increased alkaline phosphatase activity and biomineralization deposition, and promoted the expression of osteogenic genes and osteogenic differentiation (Fig. 6A–C) [85]. In addition, Du et al. developed a series of polyhedral oligomeric silsesquioxane (POSS)-grafted POC hybrid elastomers (POC-POSS) by applying a thermal polymerization strategy. The POC-POSS elastomers exhibited highly tunable elastomeric behavior in the hydrated state, and they significantly enhanced the differentiation of osteoblasts by upregulating alkaline phosphatase (ALP) activity, calcium deposition, and the expression of osteogenic genes (Fig. 6D and E) [86]. Xi et al. developed a biomimetic antibacterial nanofibrous scaffold (GT-PCS-EPL) using gelatin (GT), POCAS prepolymer (PCS), and ϵ -polylysine (EPL) via electrospinning and facile thermal crosslinking. The GT-PCS-EPL nanofibrous scaffold exhibited biomimetic elastomeric behavior, controlled spinning diameter and degradation rate, good biocompatibility, broad-spectrum antibacterial ability, and enhanced osteogenic bioactivity capacity, making it a promising nanofibrous scaffold for smart infection-related bone-tissue regeneration applications [87]. Li et al. reported a silica nanoparticle (SN)-reinforced biodegradable PCS hybrid elastomer (PCS-SN) produced through an *in situ* nanoparticle formation process. The PCS-SN elastomer exhibited

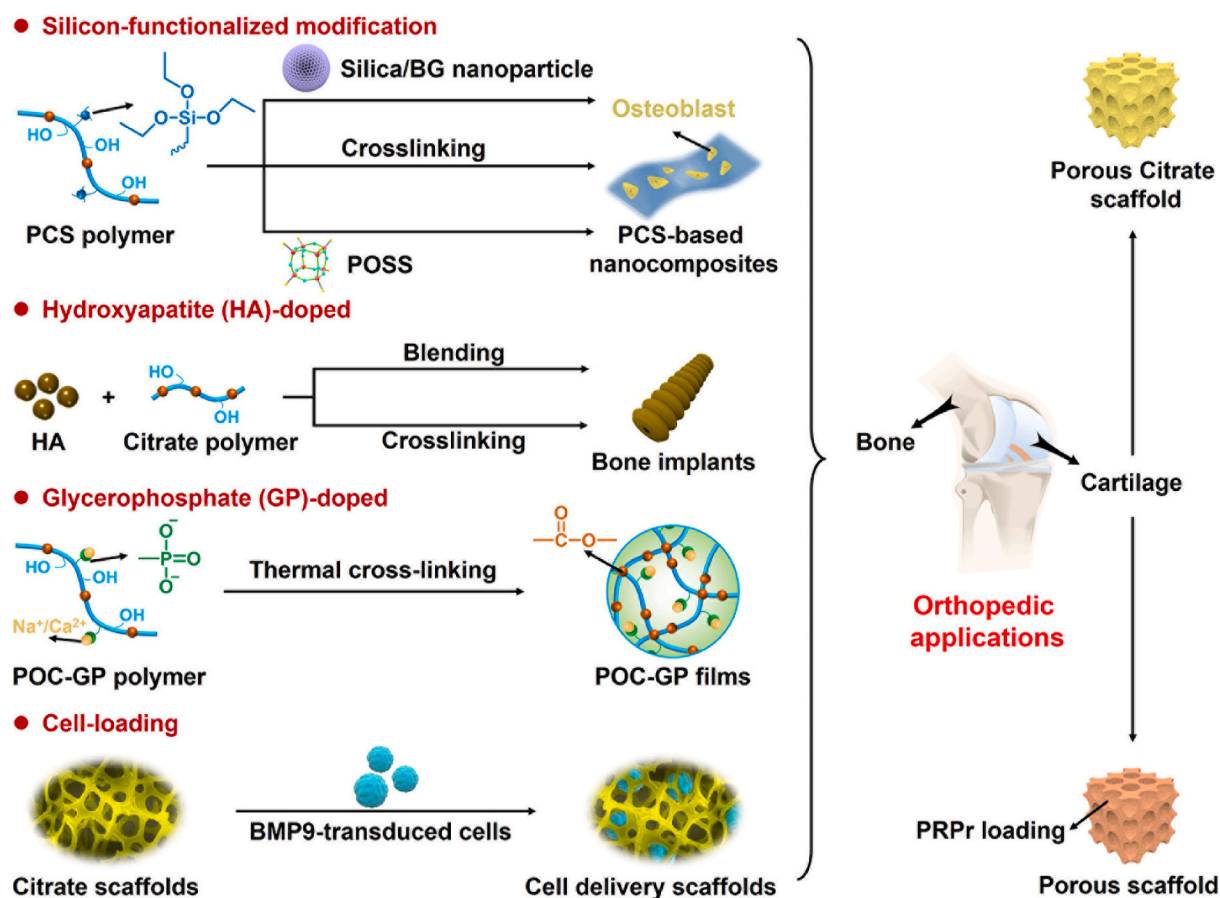


Fig. 5. Schematic diagram of further functionalized modified citrate-based polymers for orthopedic applications.

evenly distributed SNs with a uniform size and spherical morphology, and controlled elastomeric mechanical properties and biodegradation. In addition, this PCS-SN elastomer with good histocompatibility can effectively promote the adhesion and proliferation of osteoblasts [88]. Li et al. further reported a silica-based bioactive glass nanoparticle (BGN)-based PCS hybrid elastomer (PCS-BGN) with intrinsic biomineralization activity for bone tissue regeneration. The PCS-BGN elastomer showed significantly enhanced mechanical properties, low inflammatory response, and improved osteogenic differentiation (Fig. 6F and G) [89]. In addition, Zhao et al. prepared a hybrid (PEC-GS/BG) using bioactive glass (BG) and citrate (PEC-GS) at the molecular level for bone regeneration. In the rat femoral condyle critical defect model, there was no significant difference in the bone mineral density of defects between the PEC-GS/BG group ($509 \pm 21 \text{ mg/cm}^3$) and the autogenous bone group ($517 \pm 21 \text{ mg/cm}^3$), indicating that the PEC-GS/BG hybrid had angiogenesis and osteoblast differentiation comparable to that of autogenous bones [90]. Yu et al. prepared a bioactive nanofibrous scaffold (PPM) using PCL and PCS polymers via electrospinning to load miRNA complexes to promote bone regeneration. The PPM nanofibrous scaffold effectively controlled miRNA loading and release and promoted the differentiation of osteoblasts and bone regeneration *in vivo* (Fig. 6H–J) [91].

3.2.2. HA-doped functionalized citrate-based nanocomposites for enhanced osteogenesis

In addition to functional modifications, POC-based nanocomposites have broad applications in bone-tissue engineering. Qiu et al. reported a bioceramic-elastomer composite (POC-HA) with mechanical properties similar to those of natural bone using a POC polymer and hydroxyapatite (HA). Simulating the inorganic content of natural bone, the POC-HA composite containing 65% HA had the slowest degradation rate. The

POC-HA composite exhibited good osteoblast adhesion and proliferation, biocompatibility, and mineralizing effects, suggesting that it has potential applications in the fabrication of osteoconductive bone screws (Fig. 7A–C) [92]. Qulub et al. further evaluated the mechanical properties and biocompatibility of POC-HA composites with different HA contents (62%, 65%, 68%, and 71%). The hardness value of the POC-HA composite containing 62% HA was 885.57 MPa, which is close to that of natural bone (150–664 MPa). Moreover, the POC-HA composite exhibited a stable degradation rate of approximately 3.42% for 4 weeks in simulated body fluid, and the total degradation time over 109 weeks (27 months) of the composite fits well into the required fracture bone grafting and healing time (3–21 months) [93]. Subsequently, Chung et al. proved that a POC-HA composite could promote the adhesion, proliferation, and osteogenic differentiation of mesenchymal stem cells (MSCs) [94]. Chung et al. further evaluated the early tissue and long-term responses of POC-HA nanocomposites after implantation into rabbit osteochondral defects. The POC-HA nanocomposites were well integrated with the surrounding bone and cartilage without inflammation after implantation for 6 weeks, and they enhanced osseointegration and bone regeneration after implantation for 26 weeks, indicating that the POC-HA nanocomposites can be used as bone substitutes for osteochondral regeneration [95,96]. Furthermore, Chung et al. prepared a porous POC-HA scaffold using low-pressure foaming to facilitate graft fixation and tissue integration *in vivo* due to the promotion of cell migration and inward tissue growth and diffusion [97]. Chung et al. prepared a biodegradable tricomponent graft (POC-HA/PLL), including a porous POC-HA scaffold and poly(l-lactide) (PLL) braids, to promote graft fixation and anterior cruciate ligament (ACL) reconstruction. The graft exhibited porous regions and appropriate mechanical properties (maximum load: 256.2 N, modulus: 217.5 MPa) comparable to those of the rabbit ACL (maximum load: 244 N, modulus: 233.7 MPa).

Table 2
Functionalized citrate-based polymers for bone tissue engineering.

Materials	Component	Properties	Tissue engineering	Ref.
POC/PSC	POC; PSC	Improved mechanical performances	Good bioactivity; Stimulated bone regeneration	82
IBU-loaded SiO ₂ / β-TCP/POC	POC; Ibuprofen; Silica; β-tricalcium phosphate	Highly interconnected porous network; Sustained IBU release; Antimicrobial property	Infectious bone defects repair	83
SPOC	POC; AS; GS	Controllable mechanical properties and degradation	Promote cell adhesion and proliferation; Increase ALP activity; mineralization	84,85
POC-POSS	POC; POSS	Highly tunable elastomeric behavior	Enhanced osteoblasts differentiation	86
GT/PCS/EPL	Gelatin; PCS; ε-polylysine	Biomimetic elastomeric behavior; Controlled spinning diameter and degradation rate	Broad-spectrum antibacterial ability; Enhanced osteogenic bioactivity	87
PCS-SN	PCS; Silica	Uniformly distributed; Controlled elastomeric mechanical properties	Good histocompatibility; Promote osteoblasts adhesion and proliferation	88
PCS-BGN	PCS; BGN	Enhanced mechanical properties	Intrinsic biomineralization activity; Improved osteogenic differentiation	89
PEC-GS/BG	POC, BG	Improve angiogenesis and osteoblast differentiation	Enhance bone regeneration	90
PPM	PCS; PCL; miRNA complexes	Control miRNA loading and release	Enhance bone regeneration	91
POC-HA	POC; HA	Similar mechanical properties; Controlled degradation; Good biocompatibility	Good osteoblasts adhesion and proliferation; Osteogenic differentiation; mineralization	92–96
Porous POC-HA	POC; HA	Promotion of cell migration and tissue inward growth and diffusion	facilitate graft fixation and tissue integration	97
Porous POC-HA/PLL	POC; HA; poly(L-lactide)	Appropriate mechanical; Promote the infiltration and ingrowth of tissue	Promote graft fixation and anterior cruciate ligament reconstruction	98
POC-nHA	POC; smaller HA nanoparticles	Increased mechanical properties; Reduced degradation rate	Promote osteogenesis and craniofacial bone repair	99
POC-Click-HA	POC-Click; HA	Appropriate porosities; Controllable compressive strength	Promote osseointegration, periosteal remodeling and new bone formation	101
POC-M-click-HA	POC-Click; HA; MDEA	Rapidly degradable; Higher load and stiffness	Promote spinal fusion	102
CUPE-HA	CUPE; HA	Higher osteogenesis effect than POC-Click-HA	Calvarial defects repair	103
CBPBHA	CUPE; POC; HA	Higher compressive strength	Excellent osteoconductivity and osseointegration	104
CTBCs	POC; HA; Tannic acid; Silver nanoparticles	Improved compression strengths, degradation properties and antibacterial activity	Enhanced cell adhesion, proliferation and biomineralization; promote bone regeneration	105
iCMBHA-HA	Citric acid; PEG; Dopamine; HA	Good injectability and adhesion; Suitable compressive strength and degradation rate	Increase bone mass and recover bone strength	106
CMWAs	Citric acid; PEG-PPG-PEG diol; Dopamine; Magnesium whitlockite	Excellent adhesion; Enhance the strength of bone-tendon bonding	Promote bone-tendon healing	107
PEGMC-HA	Citric acid; Maleic anhydride; PEG; HA	Controllable mechanical properties and viscoelastic; Injectable	promote ALP activity and calcium deposition of osteoblasts; osteonecrosis treatment	108,109
BPLP-PSer/HA	BPLP; Phosphoserine; HA	Promote osteogenic differentiation of MSCs	Promote bone regeneration	110
POC-HA/CS	POC; HA; Chitosan	Antibacterial activity	Antibacterial biodegradable bone screw	113
POC-ZnO	POC; Zinc oxide nanoparticles	Good antibacterial properties, Controllable release kinetics profile	Drug release and antiinfection-related tissue engineering	114
PCGL/GM	Citric acid; Glycerol; Gentamicin	Enhanced antibacterial efficacy	Antiinfection-related tissue engineering	115
PPCNG/BMP9-transduced cells	PPCN; Gelatin; MSCs/iCALs/iMAD	Thermoresponsive; Good angiogenic and osteogenic differentiation	Promote cranial defects repair	116–118
PPCNG-GO	PPCN; Gelatin; Graphene oxide	Thermoresponsive; Enhanced osteoinductive ability	Promote bone repair	119
PPCN-Sr/PPCN-phos/PPCN-cRGD	PPCN; Strontium/Phosphate/Arg-Gly-Asp peptide	Thermoresponsive; Induce osteoinductive and osteogenic differentiation	Bone regenerative engineering	120
POC-GP-Ca	POC; GP-Ca	Controlled mechanical properties and degradation	promoted osteogenic differentiation and bone regeneration	121

POC: poly(octamethylene citrate); PSC: phytic acid-derived bioactive glass; AS: 3-aminopropyltriethoxysilane; GS: 3-(2,3-glycidoxy) propyltrimethoxysilane; POSS: polyhedral oligomeric silsesquioxanes; PCS: 3-aminopropyltriethoxysilane grafted POC; BGN: silica-based bioactive glasses nanoparticles; BG: bioactive glass; PCL: poly (ε-caprolactone); PPCN: thermoresponsive POC-based polymer comprised of citric acid, polyethylene glycol and poly-N-isopropylacrylamide; BMP9: bone morphogenetic protein-9; MSCs: mesenchymal stem cells; iCALs: murine-derived calvarial mesenchymal progenitor cells; iMAD: immortalized murine adipocyte; GP-Ca: calcium glycerophosphate; HA: hydroxyapatite; POC-Click: azide-alkyne modified POC polymer; MDEA: N-methyl-diethanolamine; CUPE: POC-based polymer comprised of POC and polyurethane; PEG: polyethylene glycol; PEG-PPG-PEG diol: poly(ethylene glycol)-block-poly(propylene glycol)-block-poly(ethylene glycol); ALP: alkaline phosphatase; BPLP: amino acid-modified POC.

Importantly, the graft effectively promoted the recovery of animal weight-bearing function and ACL reconstruction, and its fixation was strengthened by the infiltration and ingrowth of tissue [98]. Remarkably, *Levi-Polyachenko* et al. prepared an elastic nanocomposite (POC-nHA) using POC and smaller HA nanoparticles (~200 nm) to improve the elastic modulus and strength of POC-nHA for craniofacial contraction osteogenesis. Compared with POC, the POC/nHA composite exhibited improved mechanical properties with an elastic modulus of 1.21 MPa and a maximum load of 13.17 N and a reduced degradation rate, which is expected to promote osteogenesis and craniofacial bone repair [99]. In contrast to the PLA bioabsorbable screws with reported foreign-body reaction (FBR), including tibia and pretibial cysts, delayed FBR at lateral femoral epicondyle, delayed intra-articular inflammatory reaction, and widening of the osteolytic femoral tunnel [17]. Citrelock

based on the POC-HA composite (product: Citregein) has been sold by Acuitive Technologies, Inc. since 2020. Citrate, the main component of Citregein, is a naturally occurring metabolic molecule with antibacterial and anti-inflammatory properties [11,14]. According to previous studies and product introduction, Citregein possesses many advantages, including simple preparation, controllable mechanical properties (bending, compression, and stretching) to adapt to different bone tissues, complete degradation without chronic inflammation to reduce the risk of secondary surgery, and promotion of soft tissue and bone regeneration [92–96]. Therefore, Citregein, an unprecedented innovative bioabsorbable biomaterial, is expected to become the future of bone screws.

Guo et al. developed a new citrate-based polymer (POC-Click) that can react, through azide-alkyne cycloaddition to enhance the

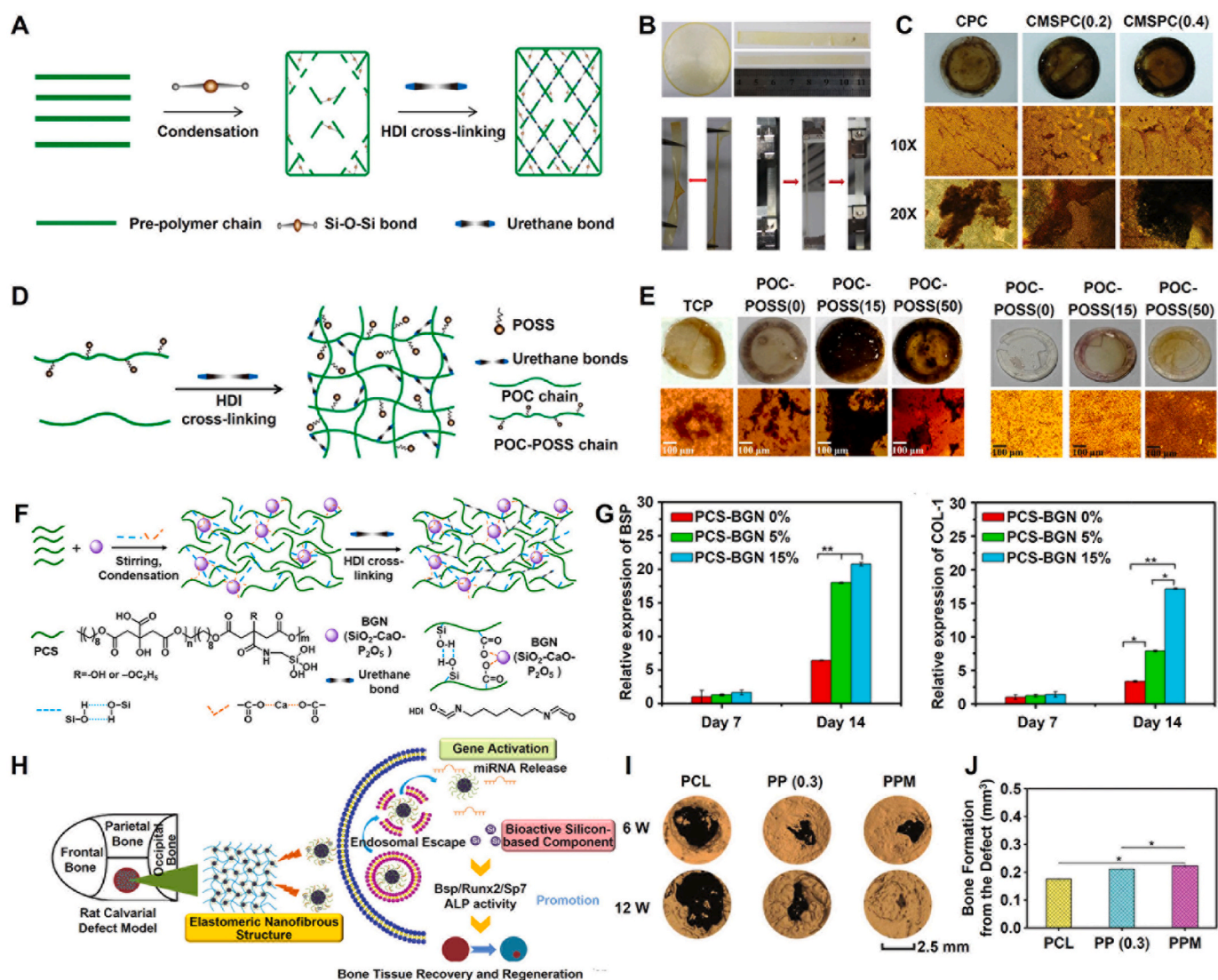


Fig. 6. Development and orthopedic applications of silicon-doped POC-based biomaterials. (A) Synthesis schematic of CMSPC elastomers; (B) Mechanical properties of CMSPC hybrid elastomers; (C) Osteogenic differentiation of MC3T3-E1 cells after culture with CMSPC elastomers [85]; Copyright 2015, John Wiley and Sons. (D) Synthesis schematic of POC-POSS elastomers; (E) Calcium deposition mineralization on different elastomers with cells (left) and without cells (right) [86]; Copyright 2016, American Chemical Society. (F) Synthesis schematic of PCS-BGN elastomers; (G) Osteoblastic genes expressions of MC3T3-E1 after culture with PCS-BGN elastomers [89]; Copyright 2018, American Chemical Society. (H) Schematic diagram of PPM nanofibrous scaffold to recover bone tissue defect; (I) Micro-CT images of new bone formation in rat calvarial defect model; (J) Bone formation from the defect in 6 weeks [91]. Copyright 2019, John Wiley and Sons. (For interpretation of the references to colour in this figure legend, the reader is referred to the Web version of this article.)

mechanical strength of the material without depleting the carboxyl groups for calcium chelation [100]. Using the POC-click polymer, Guo et al. fabricated a biomimetic POC-click-HA scaffold with a biphasic structure for to repair large segmental bone defects. The biomimetic scaffold exhibited porosities (internal: 70%, external: 5–50%) comparable to cancellous and cortical bones, with a controllable compressive strength (maximum: 37.45 MPa). Importantly, the bionic scaffold could significantly promote osseointegration, periosteal remodeling, and new bone formation in 10 mm-long rabbit segmental radial defects [101]. Tang et al. reported a rapidly degradable citrate-based scaffold (POC-M-click-HA), including *N*-methyldiethanolamine (MDEA)-modified POC-click and HA, to promote spinal fusion. The scaffold exhibited a higher maximum load (~880.8 N), stiffness (843.2 N/mm), and spinal fusion rates (80.0%) at 8 weeks postsurgery compared to the PLLA-HA scaffold (maximum load: ~712.0 N, stiffness: 622.5 N/mm, and spinal fusion rate: 71.1%) [102]. Sun et al. further evaluated the ability of two citrate porous scaffolds (CUPE-HA and POC-Click-HA) to promote calvarial regeneration. Both CUPE-HA and POC-Click-HA scaffolds

exhibited satisfactory calvarial defect repair by stimulating proximal bone formation and angiogenesis. Notably, the CUPE-HA scaffold could better promote osteogenesis than the POC-Click-HA scaffold [103].

To improve the strength of POC-HA composites in load-bearing orthopedic applications, Tran et al. prepared a biomimetic citrate-based biodegradable composite (CBPBHA) including CUPE, POC, and HA. The CBPBHA composite exhibited comparable compressive strength (~116.23 MPa) to that of human cortical bone (100–230 MPa) in contrast to the pure POC-HA composite (~88.63 MPa), high HA incorporation ability (65 wt%), and excellent osteoconductivity and osseointegration [104]. To improve the mechanical properties and biological activity of the POC-HA composite, Guo et al. prepared a series of tannin-bridged POC-HA composites (CTBCs) using a strong adhesive tannic acid (TA) to bind silver nanoparticles, and then bridged the POC polymer and HA particles through chemical binding. Compared with the POC-HA composite, the CTBCs composite exhibited greatly improved compression strengths and degradation properties, as well as enhanced cell adhesion, proliferation, biomineralization performance, and

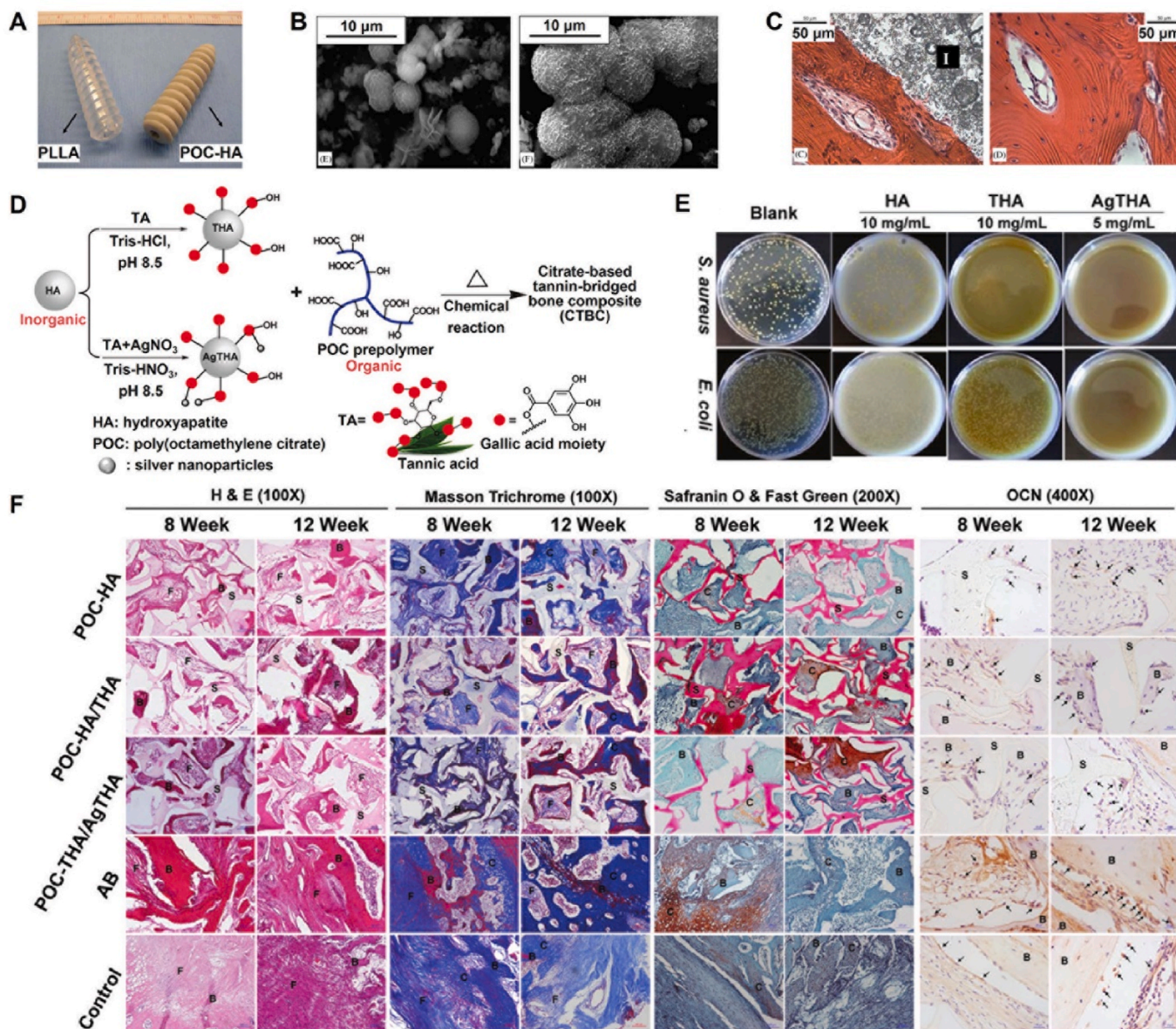


Fig. 7. Development and orthopedic applications of POC-HA complexes. (A) PLLA and POC-HA screws; (B) Mineralization in SBF for POC-HA (65 wt% HA) at 3 days (left) and 15 days (right); (C) H&E stains of decalcified tissue (left) and femur bone (right) after 6 weeks of POC-HA implantation [92]; Copyright 2006, Elsevier. (D) Synthesis schematic of CTBCs; (E) Antibacterial ability of HA, THA, and AgTHA; (F) Histological staining at week 8 and 12 of the decalcified tissue sections containing the implanted materials [105]. Copyright 2020, John Wiley and Sons.

antibacterial activity. In a lumbar fusion model, the CTBCs composite can promote bone regeneration owing to its good osteoconductivity and osteoinductivity. In addition, the immobilized TA in CTBCs composites retained certain bioconjugation sites, which suggests great potential for further modification and application in bone regeneration (Fig. 7D–F) [105].

Xie et al. prepared a novel injectable citrate-based mussel-inspired bioadhesive bone implant (iCMBA-HA), comprising a dopamine-modified citrate polymer and HA, for comminuted bone fracture therapy. The iCMBA-HA implant exhibited good injectability and adhesion, a suitable compressive strength (~ 3.2 MPa) and degradation rate (~ 30 d), and good biocompatibility and osteoinductivity, which can effectively increase bone mass and recover bone strength [106]. Yuan et al. further developed a citrate-based adhesive (CMWAs) by compositing magnesium whitlockite and an iCMBA-EPE polymer synthesized using poly(ethylene glycol)-block-poly(propylene glycol)-block-poly(ethylene glycol) (PEG-PPG-PEG diol) instead of PEG. The excellent adhesion of

CMWAs can enhance the strength of bone-tendon bonding, cartilage formation, and osteogenesis at the bone-tendon interface, which promotes bone-tendon healing [107]. Jiao et al. developed a water-soluble injectable biodegradable composite (PEGMC-HA) using citric acid, maleic anhydride, PEG, and HA and systematically studied its viscoelastic properties. The PEGMC-HA composite possesses controllable mechanical properties and is expected to have potential in bone tissue engineering [108]. Gyawali et al. further proved that the PEGMC-HA composite can effectively promote ALP activity and calcium deposition in osteoblasts *in vitro*, and it could be injected into porcine femoral head bone defects and can reinforce them for the treatment of osteonecrosis *in vivo* [109]. Ma et al. reported a citrate-based composite microparticle scaffold (BPLP-PSer/HA) composed of phosphoserine-copolymerized POC (BPLP-PSer) and HA. The BPLP-PSer/HA scaffold could promote osteogenic differentiation of MSCs by providing metabolic energy from metabonegenic regulation, and it significantly promoted bone regeneration in rat femoral condyle

and cranial defect models [110].

3.2.3. Antibacterial functionalized citrate-based polymers for anti-infective bone scaffolds

Citric acid can effectively prevent bacterial growth or enhance the antibacterial properties of other antibiotics and thus has potential applications in anti-infection-related tissue engineering [111]. Su et al. evaluated the antibacterial properties of four different biodegradable POC-based polymers against *E. coli* and *S. aureus*, including POC, POMC, CUPE, and amino acid-modified POC (BPLP). Compared with the moderate antibacterial properties of POMC, CUPE, and BPLP, the POC polymer exhibited the highest antibacterial properties because of its higher citric acid ratio and faster degradation rate [112]. Considering the antibacterial properties of POC-based polymers, Widiyanti et al. evaluated the antibacterial activity and biocompatibility of a POC-HA composite with 62% HA coated with different amounts of chitosan (1%, 3%, and 5%), and the composite with 3% chitosan coating exhibited the best antibacterial activity [113]. Kompany et al. prepared a novel composite material (POC–ZnO) composed of POC and zinc oxide nanoparticles (ZnO NPs), which exhibited good antibacterial properties and controllable physical characteristics (strength/elasticity), and the release kinetics profiles suggested potential use in controlled drug release and tissue engineering [114]. In addition, Halpern et al. prepared a biodegradable thermoset polymer (PCGL) using citric acid and glycerol by esterification, which exhibited significantly enhanced antibacterial efficacy against *S. aureus* after loading with gentamicin [115].

3.2.4. Cell/bioactive factors delivery of functionalized citrate-based scaffolds for bone formation

Using the abovementioned thermoresponsive biodegradable antioxidant PPCNG polymer, Ye et al. prepared a thermoresponsive scaffold (PPCNG) comprised of PPCN and gelatin for the delivery of bone morphogenetic protein-9 (BMP9)-transduced MSCs to promote local bone formation. Owing to the presence of gelatin, the PPCNG scaffold exhibited enhanced cell adhesion and survival rates and good angiogenic and osteogenic differentiation [116]. Dumanian et al. and Lee et al. further utilized a PPCNG scaffold to deliver BMP9-transduced murine-derived calvarial mesenchymal progenitor cells (iCALs) or BMP9-transduced immortalized murine adipocyte progenitor cells (iMAD), which can promote cranial defect repair by inducing bone formation *in vivo* [117,118]. Zhao et al. reported that graphene oxide could enhance the osteoinductive ability of PPCNG scaffolds [119].

To effectively eliminate the performance differences in the natural material (gelatin) due to batch-to-batch heterogeneity, Morochnik et al. prepared three different functionalized PPCN-based hydrogels, strontium (PPCN–Sr), phosphate (PPCN–phos), and the cell adhesion peptide Arg–Gly–Asp (RGD) (PPCN–cRGD), for bone regenerative engineering. All hydrogels exhibited thermoresponsive and inductive abilities for osteogenic differentiation of MSCs. Importantly, the PPCN–Sr hydrogel exhibited superior osteoinductive and osteogenic differentiation compared to the PPCN–phos and PPCN–cRGD hydrogels [120]. The above reports suggest that functionalized PPCN-based scaffolds may be promising cell delivery scaffolds for bone tissue engineering.

Moreover, He et al. reported a new class of osteopromotive bioactive biodegradable composites (POC–GP) using a POC polymer and glycerophosphate salts (GP–Ca and β GP–Na) through a one-pot condensation reaction. Compared to the POC– β GP–Na composites, the POC–GP–Ca composite exhibited better cytocompatibility, improved osteogenic differentiation of MSCs *in vitro*, and promoted bone regeneration in a rabbit femoral condyle defect model [121].

4. Cartilage tissue engineering

4.1. Critical factors of biomaterials in cartilage tissue engineering

Cartilage is a connective tissue that plays important supportive and

protective roles in the musculoskeletal system. Cartilage tissue comprises chondrocytes; ECM; and fibers without blood vessels, lymphatic vessels, or nerves [122]. The cartilage ECM mainly consists of collagen (mainly collagen II), glycosaminoglycans (hyaluronic acid, chondroitin sulfate, keratan sulfate, dermatan sulfate, etc.), and glycoproteins [123]. Cartilage tissue generally includes hyaline cartilage, elastic cartilage and fibrocartilage [124]. The articular cartilage is located on the surface of the movable joint, which reduces the friction between adjacent bones and acts as a buffer to maintain the normal movement of the bones. In addition, with the deepening of the articular cartilage layer, the content of chondrocytes gradually decreases, the content of proteoglycans gradually increases, and the collagen fibers change from thin to thick. Meanwhile, the direction of the collagen fibers changes from parallel to the cartilage surface (superficial) to random (middle) to perpendicular to the articular surface (deep) [122]. The unique structure of articular cartilage plays an important role in maintaining tissue moisture, tensile properties, and pressure resistance. Previous studies have indicated that various factors can promote cartilage tissue repair, such as promotion of cell attachment and proliferation, maintenance of chondrocyte morphology and phenotype, induction of cell cartilage differentiation, and synthesis of cartilage ECM [124–127]. Therefore, cartilage tissue engineering materials based on the structure and function of cartilage tissue are generally needed to ensure normal joint movement and promote cartilage regeneration. Ideal cartilage tissue engineering scaffolds should possess multifunctional properties, including suitable pore shape and permeability, excellent mechanical properties, enhanced chondrocyte differentiation, and cartilage tissue formation [128–130]. For example, a suitable pore shape and permeability of scaffolds can effectively enhance cellular colonization and matrix deposition [128]. The excellent mechanical properties of scaffolds can effectively replace defective cartilage and maintain normal joint activity [129]. The chondrogenic activity of scaffolds can also provide a suitable microenvironment for chondrocytes and promote the formation of new cartilage [130].

4.2. Porous citrate-based scaffolds for enhanced chondrocyte differentiation and cartilage formation

For the repair of cartilage damage, compared with conventional tissue-engineered scaffolds including agarose, alginate, polyglycolic acid (PGA), PLLA and PLGA are prone to plastic deformation after cyclic compressive strain due to their limited strength and elasticity [131–133]. Notably, the POC-based polymer scaffolds showed a certain application potential in cartilage tissue engineering, as shown in Fig. 5.

Kang et al. prepared a porous POC scaffold using a salt leaching method for cartilage tissue engineering. The POC scaffold exhibited a recovery ratio higher than 98% after compression compared with the recovery ratios of alginate gel scaffolds (72%), PGA (88%), and PLLA (85%). The POC scaffold can also effectively promote the adhesion, proliferation, and differentiation of chondrocytes and increase the glycosaminoglycan (GAG) and collagen content of chondrocytes cocultured after 28 d in bovine knee cartilage explants, which promotes the formation of cartilage tissue. Therefore, the POC scaffold showed remarkable potential for application as a biodegradation scaffold for cartilage tissue engineering [134]. Jeong et al. examined the influence of pore shape and permeability of two different POC scaffolds, including low-permeability spherical pores and high-permeability cubical pores, on the mechanical properties, matrix production, and mRNA gene expression of chondrocytes. The results showed that low-permeability spherical pores exhibited higher matrix production and mRNA expression than high-permeability cubical pores [135]. Jeong et al. subsequently evaluated the influence of the pore shape and permeability of two different POC scaffolds on cartilage formation of primary chondrocytes *in vivo*. After 6 weeks, the POC scaffold with low-permeability spherical pores exhibited significantly increased cartilage matrix production, such as sulfated glycosaminoglycan (sGAG), which provided a

better microenvironment for chondrogenesis than the high-permeability cubical pores [136]. In addition, Jeong et al. compared the effects on cartilage regeneration for three different scaffolds with the same controlled architecture, including POC, PCL, and PGS. Compared with the PCL and PGS scaffolds, the POC scaffold exhibited the highest sGAG contents and differentiation index and the corresponding DNA and the lowest hypertrophic mRNA expression and matrix degradation after 4 weeks *in vitro*. Moreover, PCL and PGS scaffolds can promote the proliferation of chondrocytes and the expression of genes related to cartilage formation and promote the expression of genes related to cartilage destruction and ossification, which greatly limit their applications in cartilage repair. Therefore, the POC scaffold is suitable for cartilage repair, and its structure may be critical to clinical cartilage repair [137].

In addition, Rothan et al. reported an elastomeric polycaprolactone triol–citrate (PCLT–CA) porous scaffold loaded with platelet-rich plasma releasates (PRPr) to promote chondrogenic phenotypes and cartilage ECM formation. The PCLT–CA porous scaffold enriched with PRPr showed significantly increased sGAG and collagen II contents, which provided a good microenvironment for cartilage formation [138].

5. Muscle tissue engineering

5.1. Critical factors of biomaterials in muscle tissue engineering

Muscle tissue is a soft tissue that maintains body movements, homeostatic function, and postural support, and it protects internal organs [139]. Muscle tissue is formed by specially differentiated muscle cells combined with connective tissue, capillaries, and nerve fibers [140]. The main characteristic of muscle tissue is its relaxation and contraction behavior [141]. Muscle tissue can be divided into three types: skeletal muscle tissue for force generation and body movements, myocardial tissue for pumping blood to the whole body, and smooth muscle tissue for gastrointestinal peristalsis [142]. Previous studies have indicated

that various factors can promote muscle tissue repair, including maintaining the microenvironment for cell adhesion and proliferation, reducing scar tissue formation, as well as promoting myotube formation, and myogenic differentiation [143–145]. Biomaterial-based strategies have exhibited promising applications in muscle tissue repair owing to their bioactivity and biocompatibility. Ideal muscle repair biomaterials should possess multifunctional properties, including controllable mechanical properties, an appropriate degradation rate, a specific 3D structure and porosity, and promotion of myogenic differentiation [146–149]. Controllable mechanical properties can ensure that the biomaterials match the compliance of the native muscle tissue, avoiding fatigue and failure under stress [146]. The degradation rate matching the tissue regeneration rate can effectively provide continued support throughout the repair process and allow for gradual resorption [147]. An appropriate 3D structure and porosity can effectively ensure the infiltration and integration of biomaterials with muscle tissue [148]. Muscle differentiation can effectively promote the formation of new muscle tissue [149].

5.2. Functionalized citrate polymers for muscle tissue engineering

5.2.1. Controllable mechanics functionalized citrate-based polymers for biomimetic milieu

Among various biomaterials, POC-based polymers exhibit application potential in muscle tissue engineering, as shown in Fig. 8 and Table 3 [150,151]. Sharma et al. seeded MSCs onto POC elastomeric thin films (POCfs) to provide a suitable milieu for partial bladder regeneration. The POCfs film exhibited a high uniaxial elastic potential, and its Young's modulus and elongation were 138 kPa and 137%, respectively. The POCfs film can also promote the formation of muscle bundles and the expression of bladder smooth muscle contractile proteins; the muscle/collagen was approximately 1.75 times that of the pure cell control group at 10 weeks, indicating that the POCfs film has great

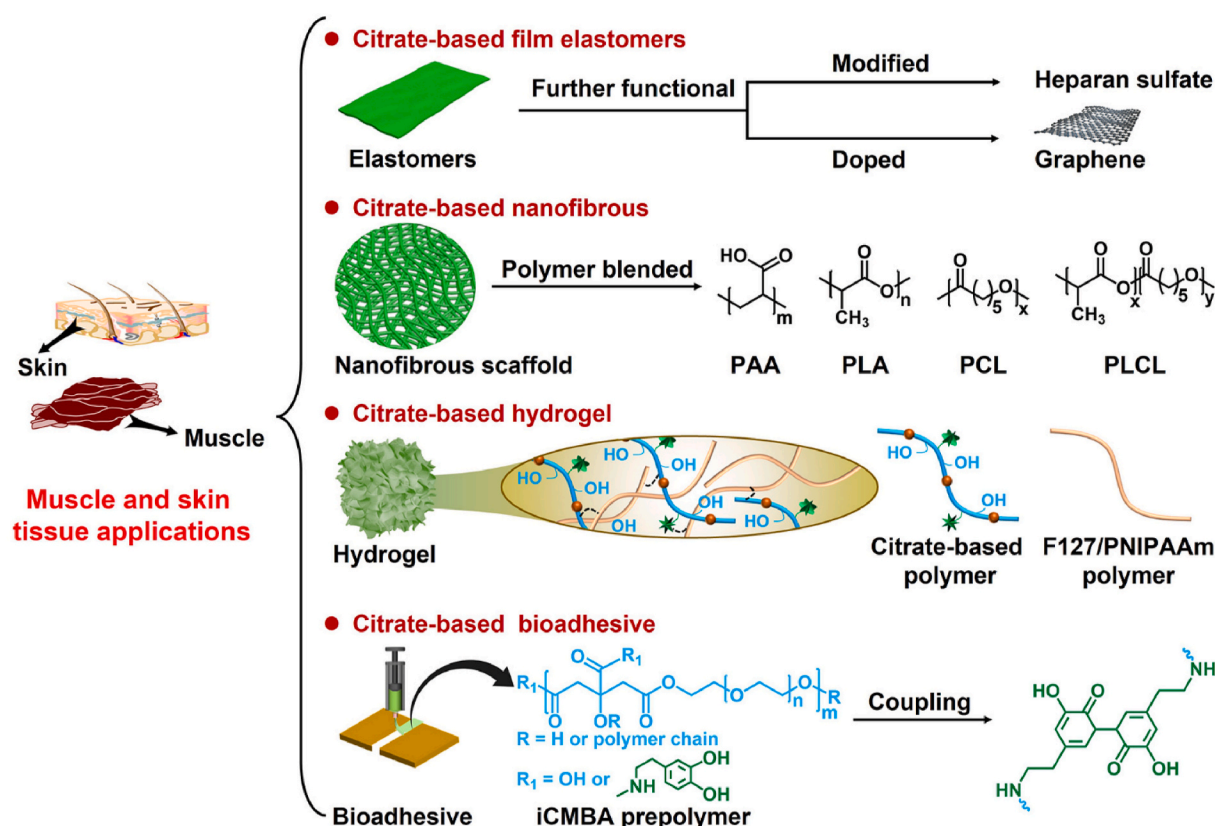


Fig. 8. Schematic diagram of further functionalized modified citrate-based polymers for muscle and skin tissue applications.

Table 3
Functionalized citrate-based polymers for muscle tissue engineering.

Materials	Component	Properties	Tissue engineering	Ref.
POCfs	POC	High uniaxial elastic potential; MSCs loading and release	Promote muscle bundles formation and proteins expression; Bladder smooth muscle repair	152
POC/PLCL	POC; PLCL	Controllable mechanical property and degradation;	Promote myoblasts adhesion and proliferation; Myocardial tissue repair	153
PCEG	POC; Graphene; PEG	Controlled biodegradability; Enhanced elastomeric; Electrochemical conductivity	Promote myogenic differentiation and skeletal muscle regeneration	154
POCG-PEI600	POC; PEG; PEI	Biodegradation and Biocompatibility	Enhance myotubes formation; Increase gene expression and protein level;	155
FPCP	POC; PEG; PEI; F127; PPy@PDA	Injectable; Adhesive;	Increase myogenic genes expression and MHC protein; Promote skeletal muscle regeneration	156

POC: poly(octamethylene citrate); PLCL: poly (L-lactic acid)-co-poly-(3-caprolactone); MSCs: mesenchymal stem cells; VEGF: vascular endothelial growth factor; PEG: polyethylene glycol; PEI: polyethyleneimine; F127: Pluronic F-127; PPy@PDA: polypyrrole@polydopamine; MHC: myosin heavy chain.

potential for applications in bladder smooth muscle repair [152]. Prabhakaran et al. prepared a biocompatible and elastomeric nanofibrous scaffold (POC/PLCL) using a POC polymer and poly (L-lactic acid)-co-poly-(3-caprolactone) (PLCL) using electrospinning technology for cardiac tissue engineering. The POC/PLCL scaffold possessed controllable mechanical properties and degradation behavior, and its tensile strength and Young's modulus were approximately 1.04 MPa and 0.51 MPa, respectively, when the weight ratio of POC to PLCL was 40:60, which is comparable to that of native cardiac tissue. In addition, the POC/PLCL scaffold can effectively promote the adhesion and proliferation of myoblasts, laying the foundation for its use as a myocardial tissue repair scaffold [153].

5.2.2. Conductive/polyamides functionalized citrate-based polymers for myogenic differentiation

Du et al. first prepared highly elastomeric, conductive, and biodegradable nanocomposites (PCEG) using graphene-doped and PEG-copolymerized POC polymers to promote myogenic differentiation and skeletal muscle regeneration. The PCEG nanocomposites possessed controlled biodegradability, electrochemical conductivity, and significantly enhanced elastomeric behavior. Moreover, PCEG nanocomposites effectively promoted the proliferation and differentiation of myoblasts and significantly enhanced the regeneration of blood vessels and muscle fibers in a rat skeletal muscle lesion model (Fig. 9A and B) [154]. Guo et al. reported a biodegradable and biocompatible cationic citrate polymer (POCG-PEI600), including polyethyleneimine (PEI, 600 Da) and polyethylene glycol (PEG)-modified POC (POCG), for skeletal muscle regeneration. The POCG-PEI600 polymer enhanced myotube formation, gene expression, and protein levels to significantly accelerate myoblast proliferation and differentiation *in vitro* and *in vivo*. Significantly, the POCG-PEI600 polymer can effectively facilitate myoblast differentiation of myoblasts (C2C12 cells) by activating the p38 MAPK γ signaling pathway to upregulate p-p38 protein levels, which provides great potential for muscle-related tissue regeneration [155]. Subsequently, Zhou et al. developed an injectable muscle-adhesive hydrogel

(FPCP) using the abovementioned POCG-PEI600 polymer, Pluronic F-127 (F127), and polypyrrole@polydopamine (PPy@PDA) to promote skeletal muscle regeneration *in vivo*. The FPCP hydrogel can increase the expression of myogenic genes and myosin heavy chain (MHC) protein to enhance the proliferation and differentiation of C2C12 cells and myofiber formation and angiogenesis capacity to promote full-thickness skeletal muscle regeneration *in vivo* [156].

6. Skin tissue engineering

6.1. Critical factors of biomaterials in skin tissue engineering

The skin is one of the largest organs in the body and plays important roles in protection, excretion, regulation of body temperature, and external stimulation perception [157]. Skin tissue exhibits softness, smoothness, and good elasticity and comprises an epidermis, dermis, and subcutaneous fat layer. The dermis and subcutaneous fat layer contain blood vessels, lymphatic vessels, nerves, sweat glands, and hair follicles, and there are free nerve endings in the epidermis without blood vessels [158]. However, the skin is often severely damaged by trauma, abrasion, burns, and surgical operations [159–161]. Wound healing can usually be divided into four stages: hemostasis, inflammation, proliferation, and tissue remodeling. The process is affected by various external factors, such as bacterial infection, temperature, pH, and sugar levels [162,163]. Previous studies have indicated that various factors can effectively regulate and accelerate wound healing, such as good hemostasis, removal of pathogenic microorganisms, inhibition of inflammation, regulation of the wound microenvironment, reduction of scar formation, and promoting vascularization. Therefore, wound dressings that can accelerate healing are extremely useful [164–167]. Ideal wound dressings should possess multifunctional properties, including excellent tissue adhesion and porosity, controlled mechanical properties, hemostatic ability, antibacterial activity, anti-inflammatory properties, and sustained bioactive molecule release [168–172]. The tissue adhesion and porosity of the dressing can effectively maintain a local moist environment around the wound and promote good gas transmission [168]. The controlled mechanical properties of the dressing can provide good operability and maintain the stability of the structure [169]. The hemostatic ability of the dressing can effectively control bleeding caused by trauma [170]. Antibacterial and anti-inflammatory properties can effectively prevent microbial infection and regulate the inflammatory microenvironment around wounds [171]. The sustained release of bioactive molecules can effectively promote cell migration and angiogenesis, which accelerate wound healing [172].

6.2. Functionalized citrate polymers for skin tissue engineering

6.2.1. Antibacterial functionalized citrate-based scaffolds for infected wound repair

According to previous reports, citrate-based polymers possess excellent biocompatibility and angiogenesis ability and have potential applications in wound healing, as shown in Fig. 8 and Table 4. Goins et al. developed a novel nanofibrous scaffold (POC/PAA) consisting of a POC polymer and poly (acrylic acid) (PAA) using electrospinning technology for wound healing applications. The POC/PAA scaffolds possessed a structural geometry that mimicked that of the natural dermis, had intrinsic antibacterial activity, and delivered growth factors. Additionally, POC/PAA scaffolds can enhance the adhesion and proliferation of skin fibroblasts, suggesting that they have potential applications in the healing of infected wounds [173]. Xi et al. developed a biomimetic elastomeric polypeptide-based nanofibrous matrix (PCE/PCL) consisting of ϵ -polylysine (EPL)-modified POC polymer (PCE) and polycaprolactone (PCL) to overcome multidrug-resistant bacteria (MDRB) and enhance full-thickness wound healing. The PCE/PCL matrix exhibited a good tensile elastomeric modulus, which was comparable to that of normal skin tissue; optimized hydrophilicity;

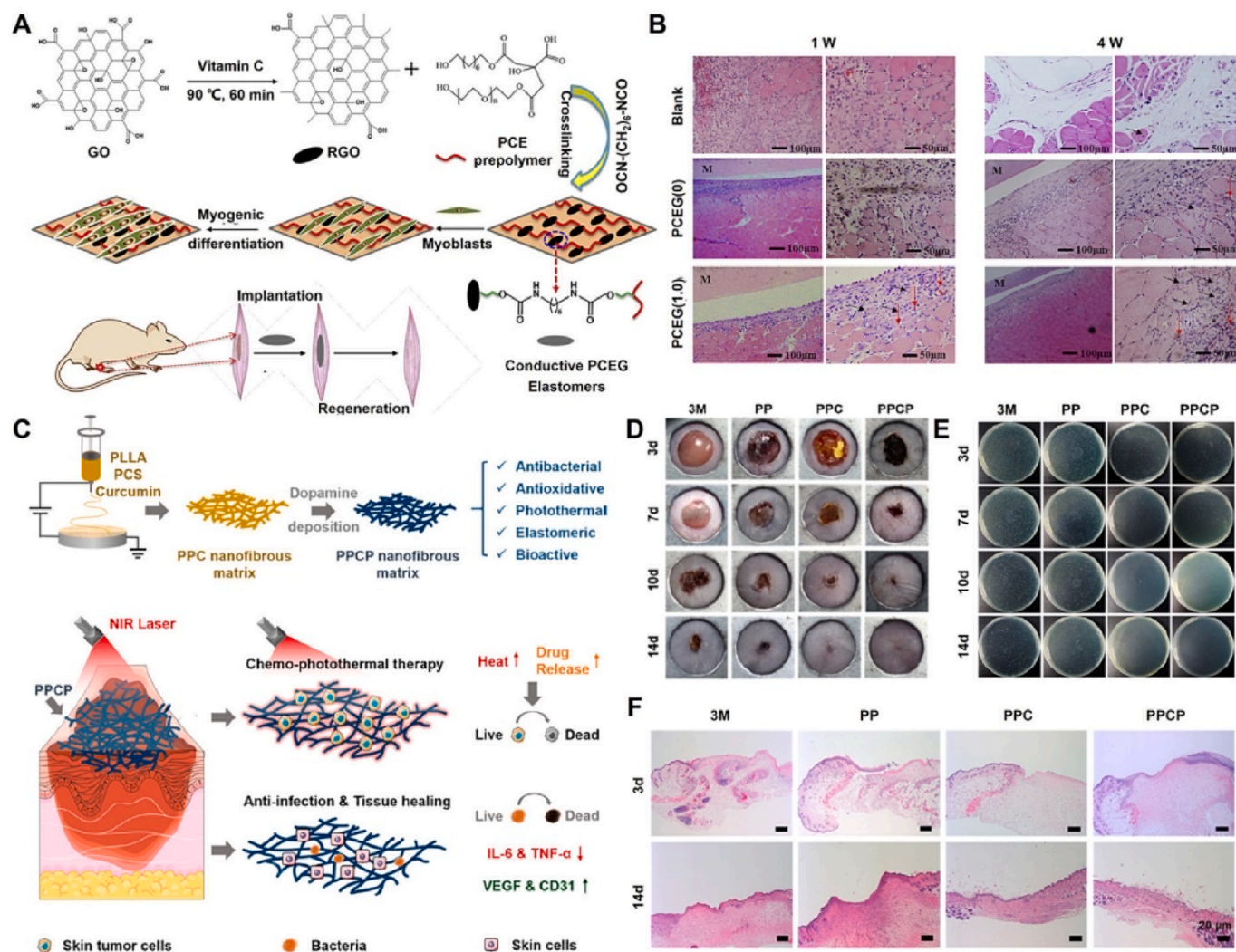


Fig. 9. Development and muscle and skin tissue applications of functional citrate-based biomaterials. (A) Synthesis schematic of conductive PCEG elastomers; (B) H&E staining of PCEG elastomers after implantation for 1 week and 4 weeks [154]; Copyright 2018, Elsevier. (C) Synthesis schematic of conductive PPCP nanofibrous matrix; (D) Photographs of *S. aureus*-infected wounds at 3, 7, 10, and 14 days; (E) Colonies derived from infected wound; (F) H&E stained images of wounds [175]. Copyright 2020, American Chemical Society.

and highly efficient broad-spectrum antibacterial activity against *E. coli* and *P. aeruginosa* (gram-negative bacteria), *S. aureus* and *E. faecalis* (gram-positive bacteria), and *MRSA* (multidrug-resistant gram-positive bacteria), which can effectively prevent MDRB wound infection and accelerate wound healing by promoting collagen deposition; angiogenesis; related gene expression; and the formation of epidermis, dermis, and hair follicle tissues [174]. Xi et al. prepared a multifunctional nanofibrous dressing (PPCP) consisting of a PCS polymer, PLLA, curcumin, and polydopamine for cutaneous tumor therapy and infection-induced wound healing. The PPCP nanofibrous dressing exhibited good antioxidant, anti-inflammatory, and broad-spectrum antibacterial properties, effectively enhancing chronic wound healing by preventing bacterial infections, reducing proinflammation, promoting angiogenesis, and stimulating collagen deposition (Fig. 9C–F) [175].

García-Argüelles et al. successfully prepared a series of biodegradable POC-based polyesters (POC-C, POC-T, POC-H, and POC-M) by deep eutectic solvent-assisted incorporation of quaternary ammonium (choline chloride, tetraethylammonium bromide, and hexadecyltrimethylammonium bromide) or phosphonium (methyltriphenylphosphonium bromide) into a POC polymer network. These polyesters exhibited good antibacterial efficacy against *E. coli* and cytocompatibility. Importantly, the POC-M polyester possessed an

appropriate Young's modulus (~ 0.27 MPa) for applications in soft tissues, such as the skin, and is a potential candidate material for antimicrobial wound dressings [176].

6.2.2. Anti-inflammatory functionalized citrate-based scaffolds for wound repair

Xie et al. demonstrated that the POCG polymer could polarize macrophages into an anti-inflammatory (M2) phenotype and downregulate proinflammatory cytokine (*Tnf- α* , *IL-1 β* and *IL-6*) expression while upregulating angiogenic factor (*Vegf* and *CD31*) expression in endothelial cells. Furthermore, CG hydrogel (chitosan and β -glycerophosphate)-loaded POCG can inhibit acute inflammation and induce early angiogenesis to accelerate wound repair [177]. Liu et al. reported a bioactive anti-inflammatory antibacterial dressing (FEA-PCEI) consisting of an ibuprofen (IBU)-modified POCG-PEI polymer (PCEI) and an FEA hydrogel prepared with EPL-modified F127 (F127-EPL) and sodium alginate to accelerate wound healing and hair follicle neogenesis. The PCEI polymer exhibited excellent anti-inflammatory properties by increasing the number of anti-inflammatory M2 macrophages and inhibiting the expression of inflammatory factors. The FEA-PCEI dressing can efficiently enhance wound healing by reducing inflammation and scar formation, and promoting hair follicle regeneration in a mouse

Table 4
Functionalized citrate-based polymers for skin tissue engineering.

Materials	Component	Properties	Tissue engineering	Ref.
POC/PAA	POC; PAA	Mimicked dermis structure; Antibacterial activity; Enhance fibroblasts adhesion and proliferation	Bacterial infection wound healing	173
PCE/PCL	POC; EPL; PCL	Good tensile elastomeric; Hydrophilicity; Antibacterial ability; Promote collagen deposition and angiogenesis	Bacterial infection wound healing	174
PPCP	PCS; PLLA; Curcumin; Polydopamine	Antioxidant, Anti-inflammatory; Broad-spectrum antibacterial	Cutaneous tumor therapy and infection-induced wound healing	175
POC-C/POC-T/ POC-H/POC-M	POC; Quaternary ammonium; Phosphonium	Good antibacterial efficacy; appropriate mechanical properties	Antimicrobial wound dressings	176
CG-POCG	POC; PEG; chitosan; β -glycerophosphate	Downregulate the pro-inflammatory cytokines; Upregulate angiogenic factors	Accelerate skin wound repair	177
FEA-PCEI	POC; PEG; PEI; Ibuprofen; F127; EPL; Sodium alginate	Injectable; Antibacterial; Increase anti-inflammatory M2 macrophage; Inhibiting inflammatory factors expression;	Accelerate wound healing and hair follicle neogenesis	178
FEPCGS	POC; PEG; Siloxane; F127; EPL	Injectable; antibacterial; anti-inflammatory; Promote fibroblasts proliferation and endothelial cells migration	MDRB-infected wound healing	179
iCMBA	Citric acid; PEG; Dopamin	High adhesion strength; Controllable mechanical properties and degradation properties	Hemostatic adhesive and wound closure	180,181
iCMBA-EPE/MgO	Citric acid; PEG-PPG-PEG diol; Magnesium oxide	High adhesive strength; Low swelling ratio; Good antibacterial and hemostatic ability	Promote wound closure and potential bone regeneration	182
AbAf iCs	iCMBA; 10-undecylenic acid	Strong wet tissue adhesion; Long-term antibacterial and antifungal abilities	Bacterial or fungal infections tissue engineering	183
POC/PLA	POC; PLA	Elastic; Hydrophilic; Sustained release aspirin	Wound dressing	184
H-HKUST-1	PPCN; HKUST-1 NPs	Sustained release of copper ions; Antioxidant property; Promotion of collagen deposition and angiogenesis	Accelerate diabetic wound healing	185

POC: poly(octamethylene citrate); PAA: poly (acrylic acid); PLA: polylactic acid; EPL: ϵ -polylysine; PCL: poly caprolactone; PCS: 3-aminopropyltriethoxysilane grafted POC; PLLA: poly (L-lactic acid); PEG: polyethylene glycol; PEI: polyethyleneimine; F127: Pluronic F-127; MDRB: multidrug resistant-bacteria; PEG-PPG-PEG diol: poly (ethylene glycol)-block-poly(propylene glycol)-block-poly(ethylene glycol); PPCN: thermoresponsive POC-based polymer comprised of citric acid, polyethylene glycol and poly-N-isopropylacrylamide; HKUST-1 NPs: copper metal-organic framework nanoparticles.

full-thickness cutaneous wound model [178]. In addition, Cheng et al. developed an injectable antibacterial anti-inflammatory hydrogel (FEPCGS) consisting of a siloxane-modified water-soluble citrate (PCGS) polymer and an F127-EPL polymer for wound healing in MDRB-infected wounds. The FEPCGS hydrogel exhibited broad-spectrum antibacterial activity, significantly preventing MDRB infection in wounds. Moreover, the FEPCGS hydrogel could effectively promote the proliferation of fibroblasts and the migration of endothelial cells *in vitro*, reinforce early angiogenesis, and decrease inflammation to enhance wound healing and skin appendage construction [179].

6.2.3. Adhering functionalized citrate-based scaffolds for hemostasis and wound repair

Mehdizadeh et al. reported an injectable mussel-inspired tissue bioadhesive (iCMBA) with a high wet strength using a dopamine covalently crosslinked water-soluble citrate polymer for sutureless wound closure. The iCMBA bioadhesive exhibited controllable mechanical and degradation properties and an 8.0 fold adhesion strength (approximately 123.2 kPa) to wet tissue compared with the clinically used fibrin glue (approximately 15.4 kPa). Compared with fibrin glue, the iCMBA bioadhesive not only effectively stopped bleeding and closed wounds in Sprague–Dawley rats but also significantly enhanced wound healing without any serious inflammatory response [180]. Guo et al. further improved the wet adhesion strength and prolonged the degradation time of the iCMBA bioadhesive through convenient copper-catalyzed azide-alkyne cycloaddition (CuAAC, click chemistry) for further surgical applications. The modified iCMBA bioadhesive showed high adhesive strength (approximately 223.11 kPa) and considerable antibacterial and antifungal properties, which enhanced its potential application as a hemostatic adhesive in wound treatment [181]. To reduce the swelling rate of iCMBA, Lu et al. prepared a magnesium oxide (MgO)-crosslinked low-swelling citrate-based mussel-inspired tissue adhesive (iCMBA-EPE/MgO). The iCMBA-EPE/MgO adhesive exhibited high adhesive strength, a low swelling ratio, tunable mechanical and degradation properties, and good antibacterial and hemostatic abilities, and it could effectively promote wound closure. In addition, the iCMBA-EPE/MgO adhesive may have potential applications in promoting bone regeneration owing to the presence of Mg ions [182]. Further, Guo et al.

successfully prepared a new family of iCMBA-based polymers (AbAf iCs) through the cocrosslinking of 10-undecylenic acid. AbAf iCs exhibited strong wet tissue adhesion, good cytocompatibility, and long-term antibacterial and antifungal abilities, which could greatly expand their applications in bacterial or fungal infection tissue engineering [183].

6.2.4. Release of bioactive factors from functionalized citrate-based scaffolds for wound repair

Zou et al. also prepared a series of elastic, hydrophilic, and controllable biodegradation nanofibrous membranes (POC/PLA) using a POC polymer and PLA through electrospinning technology for potential wound dressing applications. Compared with the pure PLA membrane, the POC/PLA membrane with a POC/PLA ratio of 25/75 exhibited better tensile deformation, hydrophilicity, and swelling properties, and the breaking strain was improved by nearly 2.5 fold. Moreover, the POC/PLA membrane can effectively load and sustain the release of aspirin, which has potential applications in wound dressings [184]. Xiao et al. prepared a novel composite (H-HKUST-1) comprising the above-mentioned thermoresponsive biodegradable antioxidant PPCN hydrogels and copper metal–organic framework nanoparticles (HKUST-1 NPs). The H-HKUST-1 composite exhibited a sustained release of Cu ions to reduce its cytotoxicity; increase its antioxidant properties; and promote cell migration, collagen deposition, and angiogenesis, which can accelerate diabetic wound healing [185].

7. Nerve and spinal cord tissue engineering

7.1. Critical factors of biomaterials in nerve and spinal cord tissue engineering

The nervous system is divided into the central nervous system (CNS), which comprises the brain and spinal cord, and peripheral nervous system (PNS), which comprises sensory and motor neurons, and it plays an important role in the transmission of various types of information *in vivo* [186]. Axons are formed by extending the cell body from neurons and are then wrapped by the myelin sheath, which plays an important role in the targeted transmission of signals to distant tissues and organs [187]. The myelin sheath in the PNS is formed by Schwann cells, which

promote nerve regeneration and repair, whereas the myelin sheath in the CNS is formed by oligodendrocytes that inhibit nerve repair [188, 189]. Previous studies have indicated that various factors can effectively promote nerve regeneration and rebuild nerve function, such as the maintenance of endogenous nerve cell attachment and proliferation, electrical stimulation, nerve growth factors, and vascular endothelial growth factors [190–192]. Therefore, nerve tissue engineering scaffolds have been extensively studied as a means of promoting nerve repair [193,194]. Unfortunately, their application is greatly restricted owing to the limited area of cell growth and the lack of a specific spatial arrangement, as well as their inability to rebuild nerve function [195, 196]. Ideal nerve scaffolds should possess multifunctional properties, including biomimetic mechanical properties, controlled biodegradation and porosity, and excellent biocompatibility [197,198]. The mechanical properties of scaffolds can allow them to effectively resist physiological loads *in vivo* [197]. Controlled biodegradation of the scaffolds can effectively match the growth rate of nerve regeneration, and porosity can ensure the transportation of nutrients and gases [198].

The spinal cord, as an important part of the central nervous system, plays an important role in maintaining vital signs, including the sensory and motor systems [199]. The human spinal cord is a cylindrical structure composed of gray and white matter and surrounded by bones (vertebrae), intervertebral discs, muscles, and ligaments [200,201]. In addition to neurons, the spinal cord possesses glial cells, including astrocytes, which maintain the stability of the chemical environment in the spinal cord, oligodendrocytes that form myelin for more effective electrical signal transduction, and microglia that remove cell debris [202]. Traumatic spinal cord injury (SCI) not only causes devastating damage to neurons, axons, and glial cells, but also changes the inflammatory microenvironment, causing secondary spinal cord injury [203]. Previous studies have indicated that various factors can effectively promote spinal cord repair, such as promoting axon growth and neuronal relay formation, regulating immune and inflammatory responses, reducing scar tissue, improving vascularization, and applying anisotropic and gradient biomaterial scaffolds [204–207]. Compared with current drug treatments, surgical treatments, and rehabilitation techniques, biomaterial scaffolds are a promising treatment method for the repair of spinal cord injury [208,209]. However, traditional biomaterials cannot precisely regulate the microenvironment in SCI, making them ineffective in the repair of spinal cord injury [210]. Ideal spinal cord repair scaffolds should possess multifunctional properties, including biomimetic mechanical properties and a porous structure, controlled biodegradation and biocompatibility, the ability to promote axonal growth and neurogenesis, a reduction of glial and fibrotic scar formation, and the necessary nutrient supply [211,212]. The biomimetic mechanical properties and porous structure of the scaffold can mimic the extracellular matrix and provide cell connectivity, which effectively promotes the reconstruction of neural circuits and recovery of nerve function after SCI to coordinate the regeneration of axons and neurons *in situ* [211]. The degradation rate of scaffolds should match the spinal cord regeneration rate, which promotes axonal regeneration without impeding the axon growth cone [212].

7.2. Biomimetic functionalized citrate-based nerve guides for nerve tissue engineering

Tran et al. fabricated biomimetic multi-channeled crosslinked POC polyester tissue-engineered (CUPE) nerve guides simulating natural microtubules and epineurium structures for nerve tissue repair. The CUPE nerve guides possessed a precisely controllable channel number and diameter, porosity, and mechanical properties, with an ultimate peak stress of approximately 1.38 MPa and an elongation of approximately 22.76% comparable to native nerve tissue. In addition, the CUPE nerve guides displayed a fiber quantity and density equivalent to nerve autografts after 8 weeks of treatment in 10 mm rat sciatic nerve defects, suggesting potential applications in tissue engineering scaffolds for

nerve repair [213]. Subsequently, Kim et al. prepared a folic acid-doped CUPE nerve guidance conduit (fCUPE) by dip-coating to promote 22 mm rat sciatic nerve defect repair in Wistar rats. The fCUPE conduit exhibited a good remediation effect on PNS regeneration and functional recovery, comparable to autografts. Moreover, the fCUPE conduit has good application prospects in neural tissue engineering because of the important role of folic acid in regulating the behavior of different nerve cells and the excellent mechanical properties and biocompatibility of the CUPE conduit [214].

7.3. Extracellular vesicles-doped functionalized citrate-based polymers for spinal cord repair

Wang et al. prepared an injectable adhesive anti-inflammatory hydrogel (FE) consisting of the abovementioned POCG-PEI600 polymer and F127 to sustain the release of extracellular vesicles (EVs) to enhance the repair of SCI. The FE@EVs hydrogel can efficiently suppress inflammation and fibrotic scar formation and promote remyelination and axonal regeneration after orthotopic injection in T10 complete transection of the spinal cord [215]. Hoshi et al. reported a series of nanoporous POC-based elastomers using poly (ethylene glycol) dimethyl ether (PEGDM) as a nanoporogen through phase separation during polymerization. The nanoporous POC elastomers exhibited a low modulus (~0.11 MPa) and high elongation (~405%). The highly interconnected porous structure and its internal surface area and porosity are approximately 91.73 m²/g and 86.8%, respectively. Moreover, nanoporous POC elastomers can safely and effectively encapsulate and produce sustained-release drugs under physiological conditions, providing a promising drug delivery platform for soft tissue engineering applications for the spinal cord and blood vessels [216].

8. Multifunctional POC biomaterials for bioimaging and drug/gene delivery in tissue engineering

8.1. Bioimaging

Biodegradable fluorescent biomaterials have been extensively studied as vectors in tissue engineering. Ideal fluorescent biomaterials should possess multifunctional properties, including controlled and stable fluorescence, excellent fluorescence penetration, good biodegradability and biocompatibility, and simple synthetic routes [217]. However, the most frequently reported biomaterials were prepared by combining fluorescent dye molecules and quantum dots with degradable polymers. POC-based polymers exhibit good photoluminescence characteristics after further functional modification owing to their special chemical structures, as shown in Fig. 10 and Table 5.

8.1.1. Amino acids modified citrate-based polymers for bioimaging

Yang et al. first reported a family of biodegradable polymers (BPLPs) as both implant and fluorescent imaging probes using POC polymers and various amino acids *via* a polycondensation reaction. Subsequently, CBPLPs films were prepared through the crosslinking of BPLPs polymers. Compared with traditional fluorescent organic dyes and quantum dots, BPLPs polymers exhibit many advantages, such as tunable fluorescence emission (279–725 nm), photostability, controlled degradation, good processability, and biocompatibility. Significantly, the BPLP-cysteine (BPLP-Cys) polymer possessed a high fluorescence quantum yield of up to 62%, and the highest tensile strength, initial modulus, compressive modulus, and elongation of the CBPLP-Cys film were approximately 6.5 MPa, 7.02 MPa, 39.6 MPa, and 240%, respectively. In addition, the BPLP-serine (BPLP-Ser) polymer, with an emission wavelength of 725 nm, can be used as a biodegradable fluorescent imaging probe for bioimaging *in vitro* and *in vivo*. This study provides a new direction for developing biodegradable materials for tissue engineering, drug delivery, and bioimaging [218]. Subsequently, Serrano et al. explored the fluorescence mechanism of BPLPs polymers by analyzing

their molecular structure. The results showed that BPLPs polymers possess a six-membered ring structure with planarity consisting of the side carboxylic and germinal hydroxyl groups of citric acid and the amino and carboxyl groups of amino acids, which may cause the appearance of fluorescence without a large conjugate structure [219]. Xie et al. further explored in detail the photoluminescence mechanism of citrate polymers, including the thiazolopyridine family (conjugated TPA structures) with high quantum yields, long lifetimes, and excellent photostability by reacting them with primary amines containing β - or γ -aminothiols, and the dioxypyridine family (nonconjugated DPR structures) with low quantum yields, multiple lifetimes, and solvent-dependent band-shift behavior by reacting with primary amines without thiol groups [220]. Moreover, Zhang et al. summarized the fluorescence mechanism and design criteria for fluorescent biodegradable polymers for biomedical applications. Although traditional biodegradable polymers can efficiently enhance the fluorescence performance of fluorescent dyes, including anti-photobleaching, stability, retention, and functionalization, BPLPs polymers with intrinsic fluorescence have promise in biomedical applications owing to their simple preparation, easy modification, good biocompatibility, and low cost [221]. In addition, Wang et al. reported a photoluminescent water-soluble BPLP polymer (PCGA) using water-soluble BPLP polymer and arginine for targeted live-cell bioimaging. The PCGA polymer exhibited a high quantum yield of 11.0% compared to the water-insoluble BPLP-arginine polymer (0.9%). Importantly, the PCGA polymer not only possessed good biocompatibility and enhanced cell proliferation but also selectively stained lysosomes in cells, indicating its potential application in bioimaging [222]. Jiang et al. prepared a mechano-compatible BPLP-Cys-based polymer-ECM composite (BPLP-Cys/ECM) for vascular tissue engineering. Importantly, the composite (BPLP-ECM-Hep) with immobilized heparin achieved by maleimide-thiol click chemistry can effectively reduce platelet adhesion and intimal hyperplasia, and inhibit vascular graft calcification with enhanced antioxidant activity [223,224]. Wadajkar et al. prepared a series of fluorescent nanoparticles (DICT-NPs) consisting of water-soluble BPLP (WBPLP)-conjugated magnetic nanoparticles (WBPLP-MNPs) and water-insoluble BPLP-conjugated magnetic nanoparticles (BPLP-MNPs)

for dual-bioimaging of fluorescence and magnetic resonance (MR). The DICT-NPs exhibited good dual-mode bioimaging and tumor-targeting selectivity, which provides a potential application for the diagnosis of cancer and other diseases [225].

8.1.2. Functionalized BPLP-based polymers for bioimaging

BPLPs with low molecular weights are prone to nanoparticle aggregation under physiological conditions, which limits their use as imaging probes. Xie et al. synthesized a biodegradable photoluminescent polylactone (BPLP-PLLA) by copolymerizing L-lactide (LA) into a BPLP polymer network. BPLP-PLLA exhibited intrinsic and stable fluorescence properties, good processability and thermal properties, and biocompatibility, which were comparable to those of commercial polylactones. Importantly, BPLP-PLLA could track its degradation by fluorescence imaging *in vivo* [226]. Xie et al. further reported an immune cell-mediated biodegradable theranostic nanoparticle by loading muramyl tripeptide (MTP)-modified BPLP-PLLA nanoparticles with the drug (PLX4032) into macrophages (THP-1). Nanoparticles allow tumor-targeted delivery of drugs to achieve tracking and tumor therapy *in vivo* [227]. Subsequently, Li et al. fabricated a biodegradable photoluminescent nanobubble as an ultrasound contrast agent (UCA) using a selective neuropeptide Y₁ ligand-conjugated photoluminescent polymer (BPLP-PLLA) to specifically target overexpressed Y₁ receptors in breast tumors. The nanobubble possessed a uniform size, good dispersion and photostability, negligible biotoxicity, excellent breast cancer targeting ability, and an enhanced ultrasound imaging effect, which provided a new targeted UCA for early breast cancer diagnosis [228]. Hu et al. synthesized a series of novel biodegradable photoluminescent polymers (BPLP-PLGA) by copolymerizing different molar ratios of L-lactide (LA) and glycolide (GA) into a BPLP polymer network. BPLP-PLGA possessed the inherent photoluminescence properties of BPLP, controllable biodegradability (8–16 weeks), good cytocompatibility, and histocompatibility. Moreover, BPLP-PLGA can be prepared with various morphologies, including films, nanoparticles, and porous scaffolds, which possess fluorescence imaging capabilities [229].

Zhang et al. further developed a new type of urethane-doped BPLP-based biodegradation photoluminescent polymer (UBPLP) and its

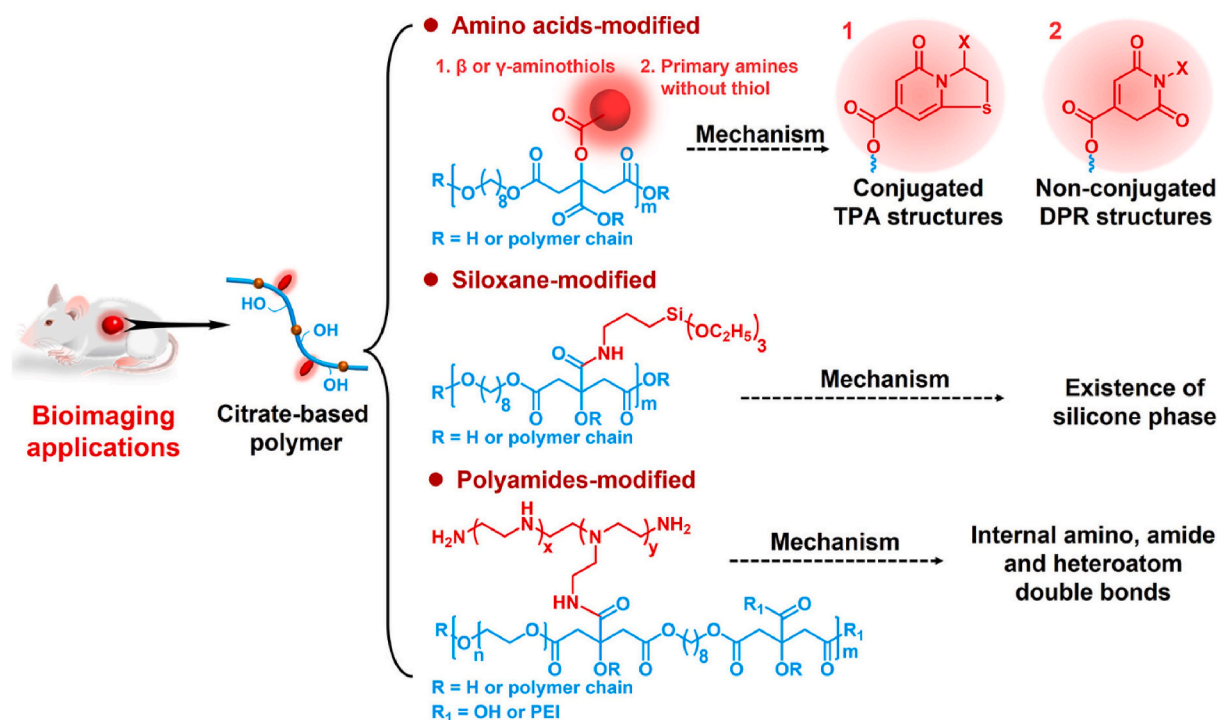


Fig. 10. Schematic diagram of further functionalized modified citrate-based polymers for bioimaging applications.

Table 5
Functionalized citrate-based polymers for bioimaging.

Materials	Component	Properties	Tissue engineering	Ref.
BPLPs	POC; Amino acids	Tunable fluorescence emission; Photostability, Controlled degradation, Good processability; Biocompatibility	Fluorescent imaging probes	218,219
BPLP-Cys	POC; Cysteine	High fluorescence quantum yield	Bioimaging	218
BPLP-Ser	POC; Serine	Emission of 725 nm	Biodegradation quantum dots for bioimaging	218
PCGA	POC; PEG; Arginine	Water-soluble; Photoluminescence	Enhanced cell proliferation and Bioimaging	222
BPLP-Cys/ ECM-Hep	POC; Cysteine; ECM; Heparin	Photoluminescence; Reduce platelet adhesion and intimal hyperplasia; Antioxidant activity	Vascular tissue engineering	223,224
DICT-NPs	Water-soluble/insoluble	Dual-bioimaging of fluorescence and magnetic resonance; Tumor targeting selectivity	Diagnosis of cancer and other diseases	225
BPLP-PLLA	BPLP; MNPs	Intrinsic and stable fluorescence properties; Good processability	Tracking degradation <i>in vivo</i>	226
BPLP-PLLA-MTP	BPLP; L-lactide; Muramyl tripeptide	Tumor-targeted delivery of drugs	Tracking the delivery of drug and tumor therapy <i>in vivo</i>	227
BPLP-PLLA-PNBL-NPY	BPLP; L-lactide; PNBL-NPY ligand	Uniform size; Good dispersion; photostability; Target breast tumors; Ultrasound imaging effect	Diagnosis of early breast cancer	228
BPLP-PLGA	BPLP; L-lactide; Glycolide	Inherent photoluminescence properties; Controllable biodegradability; Good processability	Tracking degradation <i>in vivo</i>	229
UBPLP	POC; Cysteine; Urethane	Photoluminescent; Stable; Load and sustained release drug; elastic, Soft; Strong mechanical properties	Non-invasive real-time assays and drug delivery	230
BPLPAT	BPLP; Aniline tetramer	Intrinsic dual-mode imaging; Electrical conductivity; Excellent processability	Tissue engineering, bioimaging, drug delivery and cancer therapy	231
CHPO-ET/PEG	PHC; Cysteine/Serine; thiol acid; Multi-arm PEG	Injectability; Strong and tunable fluorescence properties; Sustained release of drugs	Fluorescence imaging <i>in vivo</i>	232
PSC-based	POC; AS; CSNW/SN/BGN	Controlled mechanical properties and Biodegradation; Tunable fluorescence emission; Photostability	Bioimaging and tissue regeneration	233,235,87-89
POCG-PEI	POC; PEG; PEI	Strong blue light emission; High photostability	Bioimaging	234
PCE	POC; EPL	High elongation and recovery rate; Antibacterial	Bioimaging	237

POC: poly(octamethylene citrate); PEG: polyethylene glycol; MNPs: magnetic nanoparticles; PHC: poly(hexamethylene citrate); AS: 3-aminopropyltriethoxysilane; CSNW: ultralong copper sulfide nanowire; SN: Silica; BGN: silica-based bioactive glasses nanoparticles; EPL: ϵ -polylysine..

crosslinked elastomers (CUBPLP) for noninvasive real-time assays in the fields of tissue engineering and drug delivery. UBPLP polymers can be prepared as stable nanoparticles with an average size of 103 nm that exhibit high-efficiency anticancer drug loading and sustained release capabilities. The CUBPLP elastomers have elastic, soft, and strong mechanical properties with a tensile strength of approximately 49.41 MPa and an elongation of 334.87%. In addition, both UBPLP nanoparticles and CUBPLP elastomers exhibited a quantum yield up to 38.65% to achieve noninvasively detected *in vivo* [230]. Shan et al. successfully prepared a citrate-based dual-imaging biodegradable electroactive polymer (BPLPAT) by adding a conductive aniline tetramer (AT) to the BPLP networks. The BPLPAT polymer exhibited intrinsic dual-mode fluorescence/photoacoustic (PA) imaging capability, tunable mechanical and degradation properties, excellent processability (films, scaffolds, and nanoparticles), photothermal properties, electrical conductivity, and the promotion of P12 cell proliferation and differentiation. Accordingly, the BPLPAT polymer exhibits good application prospects in tissue engineering, bioimaging, drug delivery, and cancer therapy [231]. Tsou et al. reported a dopant-free photoluminescent biodegradable hydrogel (CHPO-ET/PEG) using thiol-acid-modified CHPO (PHC-serine or PHC-cysteine) and multiarm PEG maleimides or acrylates through conjugate addition Michael additions, respectively. This hydrogel possesses injectability, strong and tunable fluorescence properties, drug loading and sustained-release capability, and good biocompatibility. Importantly, the degradation of these hydrogels can be tracked using fluorescence imaging *in vivo* [232].

8.1.3. Siloxane/polyamides polymers modified citrate-based polymers for bioimaging

In addition to the abovementioned photoluminescent BPLP polymers formed by modifying POC polymers with amino acids, POC polymers modified with siloxane and cationic polymers also exhibit photoluminescence properties [233,234]. Du et al. reported 3-aminopropyltriethoxysilane grafted POC hybrid elastomers (PSC) with thermal polymerization for bioimaging and tissue regeneration. The PSC elastomers possessed controlled mechanical properties and biodegradation,

tunable fluorescence emission from 400 nm to 590 nm, good photostability, a fluorescent lifetime of approximately 10 ns, and a quantum yield up to 35%. Additional studies have shown that the photoluminescence properties of PSC elastomers are due to the presence of organic silicon phases. Importantly, PSC elastomers exhibit good cytocompatibility and minimal inflammatory responses compared to quantum dots and fluorescent dyes [233]. Consequently, many PSC-based elastomers with intrinsic photoluminescent properties and biocompatibility have been extensively studied for bioimaging applications. Li et al. reported PSC-based nanocomposite elastomers (PCS-CSNW) by doping ultralong copper sulfide nanowires. The PCS-CSNW elastomers exhibited controllable mechanical properties and electrical conductivity, good broad-spectrum antibacterial activity, photoluminescence ability, and near-infrared photothermal effects, which could be effectively used to detect their degradation *in vivo* through bioimaging [235]. In addition, the abovementioned GT-PCS-EPL nanofibers, PCS-SN elastomers, and PCS-BGN elastomers all had good fluorescence properties for potential applications in bioimaging [87–89]. In addition, Wang et al. synthesized a series of PEI (600 Da, 1.8 kDa, and 10 kDa) modified water-soluble POC-based polymers (POCG-PEI) with photoluminescent capacity and biocompatibility for bioimaging applications. The POCG-PEI polymer exhibited strong blue light emission at 440 nm, depending on the molecular weight of PEI, and significantly higher photostability compared to fluorescent dyes [234]. In recent years, some nonconjugated polyamide polymers have shown excellent fluorescence, and their internal amino, amide, and heteroatom double bonds can improve their photoluminescence properties; however, the detailed photoluminescent mechanism is still under study [236]. Li et al. reported ϵ -polylysine (EPL)-modified POC-based biomedical elastomers (PCE) for bioimaging and tissue regeneration applications. The PCE elastomers exhibited a higher emission of approximately 525 nm relative to the POCG-PEI polymer (440 nm) owing to the presence of EPL. Moreover, PCE elastomers exhibit good mechanical properties with an elongation of approximately 300%, a recovery rate of up to 100%, broad-spectrum antibacterial activity, and biocompatibility, which indicate potential applicability to real-time noninvasive detection *in vivo* [237].

8.2. Drug/gene delivery

Biomaterials have been extensively studied for controlled release of drugs and genes. Ideal delivery vectors should possess multifunctional properties including high loading rates, maintenance of biological activity, controlled and microenvironmental responsiveness (e.g. pH, magnetic, and reactive oxygen species), sustained release, targeted delivery, and good biodegradation and biocompatibility, which ensure the safety of the vectors *in vivo* and improve the therapeutic effect of drugs/genes [238–241]. POC elastomers play an important role in tissue engineering owing to their biodegradability, controlled mechanical properties, and biocompatibility. Unfortunately, POC elastomers prepared through thermal or chemical crosslinking require the use of organic solvents and temperatures greater than 80 °C, which may affect the activity of drugs, genes, and growth factors. Therefore, various scaffolds, including amphiphilic micelles, porous elastomers, nanofibers, and hydrogels based on POC polymers, have been extensively studied for the delivery of drugs and genes, as shown in Fig. 11 and Table 6.

8.2.1. Functionalized photoluminescence citrate-based nanoparticles for drug delivery

Kim et al. reported a drug delivery system (CTNDDS) that used doxorubicin (DOX)-loaded fluorescent BPLP-PLLA copolymer nanoparticles (DOX-BPLP-PLLA NPs) and chimeric antigen receptor (CAR) T cells modified with a targeted quadruple-mutant of interleukin-13 (TQM-13) to achieve targeted drug delivery to cancers. The CTNDDS exhibited a high targeting ability to glioblastoma cells owing to the presence of IL-13-receptor- α 2 (*IL13Ra2*), high-efficiency DOX loading, pH-responsive sustained release of DOX, and good killing ability of U87Luc cells. Furthermore, the inherent fluorescence properties of BPLP-PLLA may provide a potential diagnostic modality for tumor therapy applications through fluorescence bioimaging [242]. Jiang et al. prepared a novel photoluminescent BPLP polymer-based micelle (AP&SP-BWM-SPION/DOX) comprising the Y₁R ligand (AP), anti-phagocytosis (SP)-modified WBPLP-polyurethane polymer (BWM), superparamagnetic iron oxide nanoparticles (SPION), and DOX. The micelles could reduce material accumulation in the liver and kidney and

enhance the specific targeting and high retention of SPION or DOX in tumors, which enhances tumor magnetic resonance imaging and therapy with prolonged survival time [243]. Pandey et al. prepared a novel thermoresponsive fluorescent nanoparticle (TFP-MNPs) for tumor bioimaging and therapy by conjugating a fluorescent polymer (TFP) comprising WBPLP, PNIPAAm, and allylamine (AH) to the surface of iron oxide magnetic nanoparticles (MNP). The TFP-MNPs exhibited good colloidal stability and multifunctional properties, including superparamagnetism, fluorescence, and thermal responsiveness. Moreover, the TFP-MNPs exhibited fluorescent and MR imaging capabilities, magnetically targeted delivery of drugs to tumors, and thermoresponsive sustained release of drugs, which could effectively inhibit tumor growth [244]. Iyer et al. prepared a series of nanoparticle eluting-angioplasty balloons using BPLP-PLGA or CUPE nanoparticles by layer-by-layer (LbL) coating and hydrogel coating to improve nanoparticle retention. The BPLP-PLGA and CUPE nanoparticles were effectively loaded and sustained the release of bovine serum albumin (BSA) or coumarin-6. Compared to the LbL coating, the hydrogel coating significantly improved the delivery and retention of nanoparticles within the arterial lumen [245]. In addition, Kuriakose et al. prepared a series of BPLPL-based NPs including BPLP-co-poly (L-lactic acid) (BPLPL-PLLA) and BPLP-co-poly (lactic-co-glycolic acid) copolymers (BPLPL-PLGA). All the BPLPL-based NPs were less than 160 nm in size and had photoluminescence properties and tunable release kinetics. BPLPL-PLGA NPs exhibited optimal uptake characteristics, good biocompatibility, and greater stability under physiological conditions than BPLPL-PLLA NPs, suggesting applicability to fluorescent vascular drug delivery [246].

8.2.2. Maleic acid-crosslinked functionalized citrate-based hydrogels for drug delivery

The injectability of drug vectors can not only deliver the drug to a specific site through minimally invasive surgery, but also fill the defect site well, which provides good application prospects in the field of biomedicine [247,248]. Gyawali et al. prepared the first biodegradable citrate-based elastic hydrogel (PPEGMC) by crosslinking with maleic acid and replacing the original 1,8-octanediol with PEG for cell delivery.

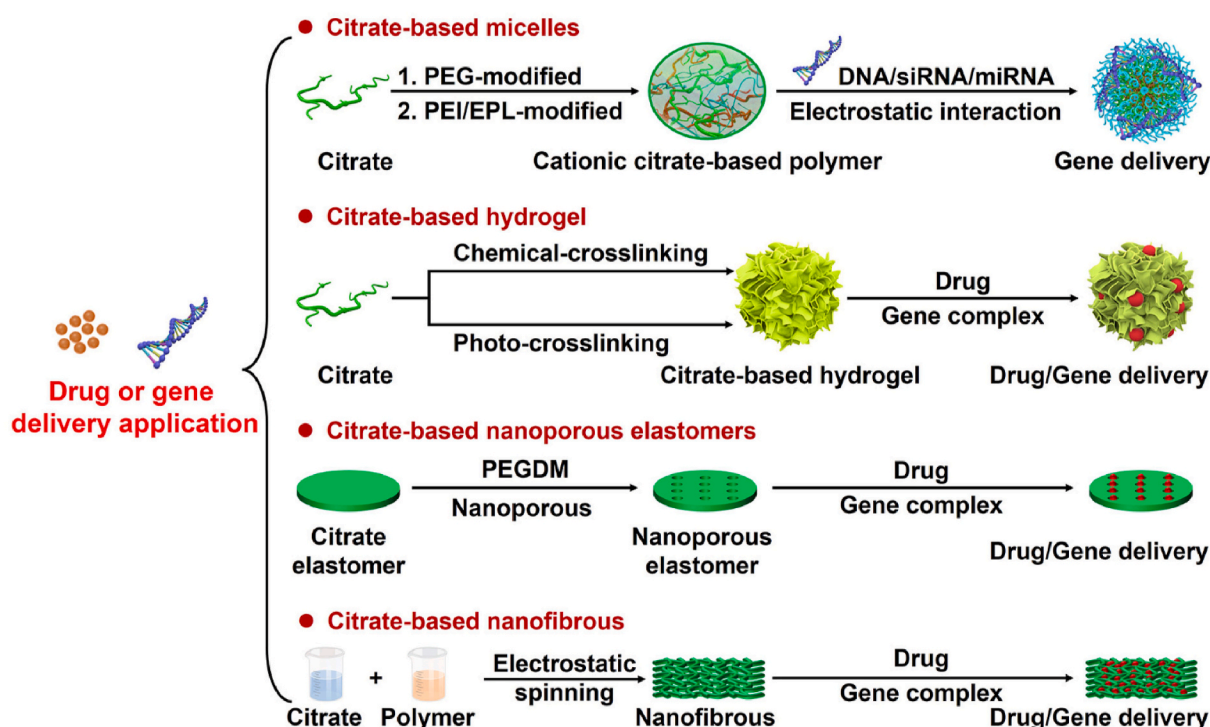


Fig. 11. Schematic diagram of further functionalized modified citrate-based polymers for drug or gene delivery applications.

Table 6
Functionalized citrate-based polymers for drug/gene delivery.

Materials	Component	Properties	Tissue engineering	Ref.
Nanoporous POC	POC	Nanoporous; Low modulus; High elongation; Highly interconnected porous structure; sustained drug release	Drug delivery	216
CTNDDS	BPLP-PLLA; CAR T cells; DOX	Targeting ability to glioblastoma cells; pH-responsive drug sustained release	Tumor therapy and diagnosis	242
AP&SP-BWM-SPION/DOX	WBPLP-polyurethane; SPION; AP/SP, DOX	Reduce accumulation in the liver and kidney; Tumor targeted and magnetic resonance imaging	Tumor therapy and diagnosis	243
TFP-MNPs	WBPLP; PNIPAAm; Allylamine; MNP	Dual mode imaging; Magnetic targeted delivery; thermo-responsive sustained release of drugs	Tumor bioimaging and therapy	244
POC-based balloons	BPLP-PLGA or CUPE	Improve the delivery and retention of nanoparticles	Protein and drug delivery	245
BPLPL-based NPs	BPLP; PLLA; PLGA	Photoluminescence and tunable release kinetics	Fluorescent vascular drug delivery	246
PPEGMC	POC; Maleic acid PEG	Injectable; Controllable mechanical and degradation properties; Good compression recovery	Cell and drug delivery	249
NCH	PPEGMC; PEGDA; PC NPs	Excellent swelling and compressive strength; Good antibacterial ability; pH-responsive drug release	Skin cancer treatment and wound healing	250
Polyplex-containing POC	POC; PEI; pDNA	Higher loading and slower release pDNA	pDNA delivery and transfection	251
POCG-PEI	POC; PEG; PEI	Injectable; Water-soluble; Genes binding, delivery, protection and release	Gene delivery	234
PPFR	POC; PEG; PEI; RB; FA	Stable fluorescence properties; High siRNA transfection efficiency	Targeted label and gene therapy	252
FPRC	POC; PEG; PEI; RB; F127; CMC	Injectability; Self-healing ability; Stable red fluorescence emission; pH-responsive drug release	Tracking and melanoma therapy	253
PPM@POCG-PEI/miRNA	PCS; PCL; POC; PEG; PEI; miRNA	Enhance elastomeric mechanical properties; Controlled miRNA loading and release	Promote bone regeneration	91
PCG-EPL	POC; PEG; EPL; miRNA	Effectively delivery miRNA33 agonist into adipocytes	Gene therapy of obesity	254

POC: poly(octamethylene citrate); PEI: polyethyleneimine; PEG: polyethylene glycol; PEGDA: PEG-diacrylate; PC NPs: PLGA-carboxymethyl chitosan nanoparticles; RB: rhodamine B; FA: folic acid; F127: Pluronic F-127; CMC: carboxymethyl chitosan; PCS: 3-aminopropyltriethoxysilane grafted POC; PCL: poly caprolactone; EPL: ϵ -polylysine; CAR T cells: chimeric antigen receptor (CAR) T cells modified with targeted quadruple-mutant of interleukin-13; DOX: doxorubicin; SPION: super-paramagnetic iron oxide nanoparticle; AP: Y₁R ligand; SP: antiphagocytosis; PNIPAAm: poly-N-isopropylacrylamide; MNP: iron oxide magnetic nanoparticles; PLLA: poly (L-lactic acid); PLGA: poly (lactic-co-glycolic acid).

The PPEGMC hydrogel possessed controllable mechanical properties and degradation properties and could be compressed to 75% deformation without permanent deformation. In addition, the PPEGMC hydrogel not only exhibited excellent cytocompatibility *in vitro* but also exhibited a minimal inflammatory response and complete degradation within 30 d *in vivo*, laying a foundation for its use as an injectable hydrogel in tissue engineering and drug delivery applications [249]. Gonsalves et al. prepared a novel pH-responsive drug-releasing nanocomposite hydrogel (NCH) containing a PPEGMC polymer, polyethylene glycol diacrylate (PEGDA), and PLGA-carboxymethyl chitosan nanoparticles (PC NPs) for skin cancer treatment and wound healing. The NCH hydrogel exhibited excellent swelling (~283%) and compressive strength (~5.34 MPa), good antibacterial ability, pH-responsive drug release and tumor cell (A431 and G361) killing ability [250].

8.2.3. Polyamides polymers modified citrate-based vectors for gene delivery

Zhang et al. reported a nanoporous POC elastomer that was used as a vector by loading a polyplex formed by pDNA and PEI for pDNA delivery and transfection. Compared to the naked pDNA-containing POC elastomer, the polyplex-containing POC scaffolds exhibited higher loading, slower initial rates of release, and enhanced transfection efficiency, indicating that the POC elastomer may be a suitable vector for gene delivery [251]. However, the aforementioned POC-based elastomers cannot be used in injectable strategies because of their lack of injectability. Wang et al. reported a series of water-soluble POC-based polymer gene vectors (POCG-PEI) by covalent crosslinking between PEG and PEI for the delivery of various genes, including DNA, small interfering RNA (siRNA), and miRNA. POCG-PEI polymers exhibited efficient injectability and various gene binding, delivery, protection, and release capabilities. Compared with commercial transfection agents, such as Lipofectamine 2000 and PEI 25 K, POCG-PEI polymers possessed good cytocompatibility and higher transfection efficiency [234]. To achieve targeted gene delivery and tumor imaging *in vivo*, Wang et al. further developed a multifunctional bioactive POCG-PEI-based polymer vector (PPFR) by covalent crosslinking with folic acid and rhodamine B. The PPFR polymer exhibited stable fluorescence properties and high siRNA transfection efficiency for targeted labeling and gene therapy of tumor tissue *in vivo* [252]. Subsequently, Wang et al. prepared an injectable biodegradation-visual POCG-PEI-based hydrogel (FPRC) drug carrier through a Schiff base reaction between rhodamine B-modified POCG-PEI polymer, aldehyde F127, and carboxymethyl chitosan for tracking and melanoma therapy *in vivo*. The FPRC hydrogel exhibited multifunctional properties, including injectability, self-healing ability, stable red fluorescence emission, and pH-responsive drug release, which could be tracked and monitored through fluorescent changes and suppression of tumor growth *in vivo* [253]. Yu et al. prepared a bioactive nanofibrous scaffold (PPM) using PCL and PCS polymers through electrospinning technology to load complexes formed by the POCG-PEI polymer and miRNA-5106 to promote bone regeneration. Compared with PCL and PCL-PCS nanofibrous scaffolds, PPM nanofibrous scaffolds can significantly enhance their elastomeric mechanical properties, control miRNA loading and release, promote the proliferation and differentiation of osteoblasts, and promote bone regeneration *in vivo* [91]. In addition, Zhang et al. prepared a safe and effective gene vector (PCG-EPL) by replacing PEI with EPL to effectively bind and deliver a miRNA33 agonist for high-fat diet-induced obesity therapy. The PCG-EPL polymer can effectively deliver a miRNA33 agonist into adipocytes to decrease related gene expression *in vitro*. Importantly, the PCG-EPL/miRNA33 agonist complex can significantly reduce body weight by enhancing lipid metabolism and reducing the expression of inflammatory factors *in vivo* [254].

9. Conclusion and further perspectives

In this article, we reviewed the progress in designing multifunctional citrate-based polymers for biomedical applications, including tissue

Table 7
The mechanical properties of citrate-based scaffolds.

Elastomers	Young's modulus/MPa	Ultimate tensile strength/MPa	Ultimate elongation/%	Ref.
POC	0.92–16.4	~6.1	~265	12
CUPE	2.53–29.82	~41.07	~222	45
POMC	0.07–1.3	~0.37	~322	48
CUPOMC	0.94–5.60	~10.91	~300	49
POMaC	0.04–1.52	~0.99	~441	50
PICO	0.04–1.48	~0.30	~40	54
POC/PDDC	1.1–1.3	~2.20	~310	55
Porous POC	0.0002–0.003	/	~165	56
PITCO	0.01–0.05	~0.03	~115	59
POCDA	~8.00	~3.50	~290	63
PDDCDA	~2.8	~2.70	~195	63
MA-POC	/	~10.60	~30.9	64
MA-PDDC	/	~6.50	~50.2	64
POCAS (PCS)	5.0–22.1	~14.7	~134	84
POCGS	3.9–12.8	~6.3	~64	84
CMSPC	4.21–976.93	~25.0	~309	85
POC-POSS	2.54–66.21	~5.98	~336	86
PCS-SN	8.06–19.18	~9.37	~80	88
PCS-BGN	67.51–190.70	~5.48	~175	89
PCS-CSNW	27.40–70.83	~10.74	~146.03	235
POC-Click	10.00–280.00	~42	~350	100
POCfs	~0.138	/	~137	152
POC-C/T/H	0.30–1.06	/	/	176
POC-M	~0.27	/	/	176
iCMBA	0.356–33.4	~8.52	~1582.5	180
iCMBA-EPE/ MgO	1.98–8.70	~4.40	~244.8	182
AbAf iCs	0.19–51.56	~3.31	~415	183
Nanoporous POC	~0.11	/	~405	216
BPLP-PLGA	14.29–72.08	~14.96	~297.48	229
CUBPLP	13.29–18.87	~49.41	~334.87	230
BPLPAT film	6–40	~7.00	~80	231
BPLPAT scaffold	0.20–0.63	0.48	/	231
PCE	3.10–3.80	~6.5	~305	237

POC: poly(octamethylene citrate); CUPE: polyurethane-doped POC; POMC: maleic acid-crosslinked POC; CUPOMC: urethane-doped POMC; POMaC: maleic anhydride-crosslinked POC; PICO: itaconic acid-crosslinked POC; PDDC: poly(dodecamethylene citrate); POCDA: amine-containing POC; PDDCDA: amine-containing PDDC; MA-POC: methacrylated POC; MA-PDDC: methacrylated PDDC; POCAS (PCS): 3-aminopropyltriethoxysilane-modified POC; POCGS: 3-(2,3-glycidoxy) propyltrimethoxysilane-modified POC; CMSPC: HDI-crosslinked PCS; POC-POSS: POSS-doped POC; PCS-SN: silica nanoparticles-doped PCS; PCS-BGN: bioactive glass nanoparticles-doped PCS; PCS-CSNW: copper sulfide nanowire-doped PCS; POC-Click: azide-alkyne modified POC; POCfs: POC elastomeric thin film; iCMBA: dopamine cross-linked citrate; AbAf iCs: 10-undecylenic acid cross-linked iCMBA; POC-C/T/H: quaternary ammonium incorporated POC; POC-M: phosphonium incorporated POC; BPLP-PLGA: L-lactide and glycolide cross-linked BPLP; BPLPAT: aniline tetramer modified BPLPs; PCE: ϵ -polylysine modified POC.

engineering, bioimaging, and delivery vectors. We provide an overview of the multifunctional properties of citrate-based polymers, including their structure and biodegradation, as well as mechanical, antibacterial, antioxidant, anti-inflammatory, and fluorescence properties, for biomedical applications. In addition, we reviewed various citrate-based polymer scaffold strategies, including amphiphilic micelles, porous elastomers, nanofibers, and hydrogels, to deliver cells, bioactive factors, drugs, and genes for tissue repair and disease treatment. Citrate-based polymers with good hemocompatibility can be used to prepare appropriate vascular grafts to simulate native veins and arteries for cardiovascular engineering applications. By doping HA, GP-Ca, and silicon or regulating their structures, citrate-based materials can effectively promote bone regeneration and cartilage matrix production in bone and cartilage engineering applications. Citrate-based elastomers/nanofibrous scaffolds/hydrogels exhibit good application prospects in muscle and skin tissue repair owing to their suitable mechanical properties and

biological activity. Citrate-based vectors can also effectively deliver and protect various drugs and genes in delivery applications. Moreover, citrate-based polymers exhibit good fluorescent properties for bioimaging applications owing to their unique structures. The mechanical properties of the various citrate-based materials are listed in Table 7.

Multifunctional citrate-based polymers have been extensively studied to meet the requirements of various biomedical applications by improving their water solubility, regulating their mechanical properties and biodegradation, and enhancing their biocompatibility and bioactivity. Significantly, citrate-based polymers have good properties and could meet the needs of various biomedical applications; however, further detailed studies on material preparation, functionalization, performance, and biomedical applications are required. The future challenges and perspectives of functional citrate-based biomaterials include the following: 1) the development of new synthesis strategies for preparing POC with a high molecular weight to expand their applications as strong implants, including bone plates, intramedullary nails, spinal internal fixation implants, artificial joints, and other osteoarticular implants; 2) the expansion of their application range in tissue engineering. Studies on tissue engineering applications of functional citrate biomaterials in the nerve, cartilage, and muscle are few. The functional importance of citrate in cerebrospinal fluid and the regulation of neurons, chondrocyte differentiation, and myoblast differentiation remain elusive; 3) The molecular mechanism of functional POC-based polymers in tissue repair needs to be further studied in detail. The mechanisms by which polymers regulate cell behavior and the tissue microenvironment should be carefully investigated. Citrate-based polymers with a tunable degradation rate and citric acid release were further designed based on the relationship between the presence of citrate in citrate-based polymers and cell or tissue fates, which influence tissue regeneration; 4) The specific metabolic pathways of citrate-based polymers *in vivo* should be clarified for more targeted functional modification. By solving the above problems, we believe that POC-based polymers will be transformed into more clinically applicable products in the field of biomedicine, along with the cross-integration of regenerative medicine and materials science and the development of new treatment strategies and clinical applications.

Ethics approval and consent to participate

This is a review article which does not contain the animal or human experiment.

Declaration of competing interest

The authors declare no conflict of interest.

Acknowledgements

This work was jointly supported by the National Natural Science Foundation of China (grant No. 52172288), Special Support Program for High Level Talents of Shaanxi Province of China (grant No. TZ0278), the key R&D plan of Shaanxi Province of China (grant No. 2021GXLH-Z-052), State Key Laboratory for Manufacturing Systems Engineering of China (grant No. sklms2021006), Young Talent Support Plan of Xi'an Jiaotong University of China (grant No. QY6J003), the Fundamental Research Funds for the Central Universities (grant No. zxy012021075), China Postdoctoral Science Foundation (grant No. 2021M702644).

References

- 1] N. Peng, D. Huang, C. Gong, Y. Wang, J. Zhou, C. Chang, Controlled arrangement of nanocellulose in polymeric matrix: from reinforcement to functionality, *ACS Nano* 14 (12) (2020) 16169–16179.
- 2] K. Wang, S. Strandman, X.X. Zhu, A mini review: shape memory polymers for biomedical applications, *Front. Chem. Sci. Eng.* 11 (2) (2017) 143–153.

- [3] R. Song, M. Murphy, C. Li, K. Ting, C. Soo, Z. Zheng, Current development of biodegradable polymeric materials for biomedical applications, *Drug Des. Dev. Ther.* 12 (2018) 3117–3145.
- [4] M. Alizadeh-Osgouei, Y.C. Li, C.E. Wen, A comprehensive review of biodegradable synthetic polymer-ceramic composites and their manufacture for biomedical applications, *Bioact. Mater.* 4 (2019) 22–36.
- [5] G.A. Martau, M. Mihai, D.C. Vodnar, The use of chitosan, alginate, and pectin in the biomedical and food sector-biocompatibility, bioadhesiveness, and biodegradability, *Polymers* 11 (11) (2019) 1837.
- [6] X. Liu, X.S. Fan, L. Jiang, X.J. Loh, Y.L. Wu, Z.B. Li, Biodegradable polyester unimolecular systems as emerging materials for therapeutic applications, *J. Mater. Chem. B* 6 (35) (2018) 5488–5498.
- [7] P. Piszko, B. Kryszyk, A. Piszko, K. Szustakiewicz, Brief review on poly(glycerol sebacate) as an emerging polyester in biomedical application: structure, properties and modifications, *Polim. Med.* 51 (1) (2021) 43–50.
- [8] H. Ye, K. Zhang, D. Kai, Z. Li, X.J. Loh, Polyester elastomers for soft tissue engineering, *Chem. Soc. Rev.* 47 (12) (2018) 4545–4580.
- [9] J. Guo, D.Y. Nguyen, R.T. Tran, Z. Xie, X. Bai, J. Yang, Design strategies and applications of citrate-based biodegradable elastomeric polymers, *Nat. Synth. Biomed. Polym.* (2014) 259–285.
- [10] R. Salihi, S.I. Abd Razak, N.A. Zawawi, M.R.A. Kadir, N.I. Ismail, N. Jusoh, et al., Citric acid: a green cross-linker for biomaterials for biomedical applications, *Eur. Polym. J.* 146 (2021), 110271.
- [11] X.P. Wu, H.L. Dai, C. Xu, L.L. Liu, S.P. Li, Citric acid modification of a polymer exhibits antioxidant and anti-inflammatory properties in stem cells and tissues, *J. Biomed. Mater. Res.* 107 (11) (2019) 2414–2424.
- [12] J. Yang, A.R. Webb, G.A. Ameer, Novel citric acid-based biodegradable elastomers for tissue engineering, *Adv. Mater.* 16 (6) (2004) 511–516.
- [13] C. Ma, E. Gerhard, D. Lu, J. Yang, Citrate chemistry and biology for biomaterials design, *Biomaterials* 178 (2018) 383–400.
- [14] R.T. Tran, J. Yang, G.A. Ameer, Citrate-based biomaterials and their applications in regenerative engineering, *Annu. Rev. Mater. Res.* 45 (2015) 277–310.
- [15] C.Y. Ma, E. Gerhard, Q.L. Lin, S.L. Xia, A.D. Armstrong, J. Yang, *In vitro* cytocompatibility evaluation of poly(octamethylene citrate) monomers toward their use in orthopedic regenerative engineering, *Bioact. Mater.* 3 (1) (2018) 19–27.
- [16] S.M. Espinoza, H.I. Patil, E.S. Martinez, R.C. Pimentel, P.P. Ige, Poly- ϵ -caprolactone (PCL), a promising polymer for pharmaceutical and biomedical applications: focus on nanomedicine in cancer, *Int. J. Polym. Mater. Polym. Biomater.* 69 (2) (2020) 85–126.
- [17] Y. Ramot, M. Haim-Zada, A.J. Domb, A. Nyska, Biocompatibility and safety of PLA and its copolymers, *Adv. Drug Deliv. Rev.* 107 (2016) 153–162.
- [18] L. Vogt, F. Ruther, S. Salehi, A.R. Boccaccini, Poly(glycerol sebacate) in biomedical applications—a review of the recent literature, *Adv. Healthc. Mater.* 10 (9) (2021), 200206.
- [19] C.V.C. Bouten, P.Y.W. Dankers, A. Driessen-Mol, S. Pedron, A.M.A. Brizard, F.P. T. Baaijens, Substrates for cardiovascular tissue engineering, *Adv. Drug Deliv. Rev.* 63 (4–5) (2011) 221–241.
- [20] P. Akhyari, H. Kamiya, A. Haverich, M. Karck, A. Lichtenberg, Myocardial tissue engineering: the extracellular matrix, *Eur. J. Cardio. Thorac. Surg.* 34 (2) (2008) 229–241.
- [21] K. Roshanbinfar, L. Vogt, F. Ruther, J.A. Roether, A.R. Boccaccini, F.B. Engel, Nanofibrous composite with tailorabe electrical and mechanical properties for cardiac tissue engineering, *Adv. Funct. Mater.* 30 (7) (2020), 1908612.
- [22] S. Pecha, T. Eschenhagen, H. Reichenspurner, Myocardial tissue engineering for cardiac repair, *J. Heart Lung Transplant.* 35 (3) (2016) 294–298.
- [23] Y.Y. Wang, Y. Li, J. Feng, W.J. Liu, Y.D. Li, J. Liu, et al., Myd88 promotes cardiomyocyte proliferation and neonatal heart regeneration, *Theranostics* 10 (20) (2020) 9100–9112.
- [24] B. Ferraro, G. Leoni, R. Hinkel, S. Ormanns, N. Paulin, A. Ortega-Gomez, et al., Pro-angiogenic macrophage phenotype to promote myocardial repair, *J. Am. Coll. Cardiol.* 73 (23) (2019) 2990–3002.
- [25] S.W. Xu, I. Ilyas, P.J. Little, H. Li, D. Kamato, X.Y. Zheng, et al., Endothelial dysfunction in atherosclerotic cardiovascular diseases and beyond: from mechanism to pharmacotherapies, *Pharmacol. Rev.* 73 (3) (2021) 924–967.
- [26] A. Rosseitsch, N. Smart, K.N. Dube, M. Turner, P.R. Riley, Essential role for thymosin β 4 in regulating vascular smooth muscle cell development and vessel wall stability, *Circ. Res.* 111 (4) (2012) e89–e102.
- [27] D.H. Wang, N. Rabhi, S.F. Yet, S.R. Farmer, M.D. Layne, Aortic carboxypeptidase-like protein regulates vascular adventitial progenitor and fibroblast differentiation through myocardin related transcription factor A, *Sci. Rep.* 11 (1) (2021) 1–13.
- [28] M.J. Moore, R.P. Tan, N. Yang, J. Rnjak-Kovacina, S.G. Wise, Bioengineering artificial blood vessels from natural materials, *Trends Biotechnol.* (2021), <https://doi.org/10.1016/j.tibtech.2021.11.003>.
- [29] X. Lin, F. Tang, S. Jiang, H. Khamis, A. Bongers, J.M. Whitelock, et al., A biomimetic approach toward enhancing angiogenesis: recombinantly expressed domain V of human perlecan is a bioactive molecule that promotes angiogenesis and vascularization of implanted biomaterials, *Adv. Sci.* 7 (17) (2020), 2000900.
- [30] Y. Zhuang, C. Zhang, M. Cheng, J. Huang, Q. Liu, G. Yuan, et al., Challenges and strategies for *in situ* endothelialization and long-term lumen patency of vascular grafts, *Bioact. Mater.* 6 (6) (2021) 1791–1809.
- [31] F. Liu, X. Liao, C.H. Liu, M.Y. Li, Y.K. Chen, W.L. Shao, et al., Poly(L-lactide-co-caprolactone)/tussah silk fibroin nanofiber vascular scaffolds with small diameter fabricated by core-spun electrospinning technology, *J. Mater. Sci.* 55 (16) (2020) 7106–7119.
- [32] H. Qiu, Q. Tu, P. Gao, X. Li, M.F. Maitz, K. Xiong, et al., Phenolic-amine chemistry mediated synergistic modification with polyphenols and thrombin inhibitor for combating the thrombosis and inflammation of cardiovascular stents, *Biomaterials* 269 (2021), 120626.
- [33] C. Liang, Y. Hu, H. Wang, D. Xia, Q. Li, J. Zhang, et al., Biomimetic cardiovascular stents for *in vivo* re-endothelialization, *Biomaterials* 103 (2016) 170–182.
- [34] H.T. Bui, A.R. Friederich, E. Li, D.A. Prawl, S.P. James, Hyaluronan enhancement of expanded polytetrafluoroethylene cardiovascular grafts, *J. Biomater. Appl.* 33 (1) (2018) 52–63.
- [35] M.C. Serrano, E.J. Chung, G.A. Ameer, Advances and applications of biodegradable elastomers in regenerative medicine, *Adv. Funct. Mater.* 20 (2) (2010) 192–208.
- [36] Q.Y. Liu, L. Jiang, R. Shi, L.Q. Zhang, Synthesis, preparation, *in vitro* degradation, and application of novel degradable bioelastomers—a review, *Prog. Polym. Sci.* 37 (5) (2012) 715–765.
- [37] D. Motlagh, J. Allen, R. Hoshi, J. Yang, K. Lui, G. Ameer, Hemocompatibility evaluation of poly(diols citrate) *in vitro* for vascular tissue engineering, *J. Biomed. Mater. Res.* 82a (4) (2007) 907–916.
- [38] J. Yang, D. Motlagh, J.B. Allen, A.R. Webb, M.R. Kibbe, O. Aalami, et al., Modulating expanded polytetrafluoroethylene vascular graft host response via citric acid-based biodegradable elastomers, *Adv. Mater.* 18 (12) (2006) 1493–1498.
- [39] M.R. Kibbe, J. Martinez, D.A. Popowich, M.R. Kapadia, S.S. Ahanchi, O. Aalami, et al., Citric acid-based elastomers provide a biocompatible interface for vascular grafts, *J. Biomed. Mater. Res.* 93a (1) (2010) 314–324.
- [40] R.A. Hoshi, R. Van Lith, M.C. Jen, J.B. Allen, K.A. Lapidus, G. Ameer, The blood and vascular cell compatibility of heparin-modified ePTFE vascular grafts, *Biomaterials* 34 (1) (2013) 30–41.
- [41] R. van Lith, E.K. Gregory, J. Yang, M.R. Kibbe, G.A. Ameer, Engineering biodegradable polyester elastomers with antioxidant properties to attenuate oxidative stress in tissues, *Biomaterials* 35 (28) (2014) 8113–8122.
- [42] R. van Lith, X. Wang, G. Ameer, Biodegradable elastomers with antioxidant and retinoid-like properties, *ACS Biomater. Sci. Eng.* 2 (2) (2016) 268–277.
- [43] E.K. Gregory, A. Webb, J.M. Vercammen, M.E. Kelly, B. Akar, R. van Lith, et al., Inhibiting intimal hyperplasia in prosthetic vascular grafts via immobilized all-trans retinoic acid, *J. Contr. Release* 274 (2018) 69–80.
- [44] M.Z. Zailani, A.F. Ismail, S.H. Sheikh Abdul Kadir, M.H. Othman, P.S. Goh, H. Hasbullah, et al., Hemocompatibility evaluation of poly(1,8-octanediol citrate) blend polyethersulfone membranes, *J. Biomed. Mater. Res.* 105 (5) (2017) 1510–1520.
- [45] J. Dey, H. Xu, J.H. Shen, P. Thevenot, S.R. Gondi, K.T. Nguyen, et al., Development of biodegradable crosslinked urethane-doped polyester elastomers, *Biomaterials* 29 (35) (2008) 4637–4649.
- [46] J. Dey, H. Xu, K.T. Nguyen, J.A. Yang, Crosslinked urethane doped polyester biphasic scaffolds: potential for *in vivo* vascular tissue engineering, *J. Biomed. Mater. Res.* 95 (2) (2010) 361–370.
- [47] J. Dey, R.T. Tran, J.H. Shen, L.P. Tang, J. Yang, Development and long-term *in vivo* evaluation of a biodegradable urethane-doped polyester elastomer, *Macromol. Mater. Eng.* 296 (12) (2011) 1149–1157.
- [48] D. Gyawali, R.T. Tran, K.J. Guleserian, L.P. Tang, J.A. Yang, Citric-acid-derived photo-cross-linked biodegradable elastomers, *J. Biomater. Sci. Polym. Ed.* 21 (13) (2010) 1761–1782.
- [49] Y. Zhang, R.T. Tran, D. Gyawali, J. Yang, Development of photocrosslinkable urethane-doped polyester elastomers for soft tissue engineering, *Int. J. Biomater. Res. Eng.* 1 (1) (2011) 18–31.
- [50] R.T. Tran, P. Thevenot, D. Gyawali, J.C. Chiao, L. Tang, J. Yang, Synthesis and characterization of a biodegradable elastomer featuring a dual crosslinking mechanism, *Soft Matter* 6 (11) (2010) 2449–2461.
- [51] M. Montgomery, S. Ahadian, L. Davenport Huyer, M. Lo Rito, R.A. Civitarese, R. D. Vanderlaan, et al., Flexible shape-memory scaffold for minimally invasive delivery of functional tissues, *Nat. Mater.* 16 (10) (2017) 1038–1046.
- [52] M. Montgomery, L.D. Huyer, D. Bannerman, M.H. Mohammadi, G. Conant, M. Radisic, Method for the fabrication of elastomeric polyester scaffolds for tissue engineering and minimally invasive delivery, *ACS Biomater. Sci. Eng.* 4 (11) (2018) 3691–3703.
- [53] A.D. Bannerman, L.D. Huyer, M. Montgomery, N. Zhao, C. Velikonja, T.P. Bender, et al., Elastic biomaterial scaffold with spatially varying adhesive design, *Adv. Biosyst.* 4 (8) (2020), 2000046.
- [54] L.D. Huyer, A.D. Bannerman, Y. Wang, H. Savoji, E.J. Knee-Walden, A. Brissenden, et al., One-pot synthesis of unsaturated polyester bioelastomer with controllable material curing for microscale designs, *Adv. Healthc. Mater.* 8 (16) (2019), 1900245.
- [55] J. Yang, D. Motlagh, A.R. Webb, G.A. Ameer, Novel biphasic elastomeric scaffold for small-diameter blood vessel tissue engineering, *Tissue Eng.* 11 (11–12) (2005) 1876–1886.
- [56] L.A. Hidalgo-Bastida, J.J.A. Barry, N.M. Everitt, F.R.A.J. Rose, L.D. Buttery, I. P. Hall, et al., Cell adhesion and mechanical properties of a flexible scaffold for cardiac tissue engineering, *Acta Biomater.* 3 (4) (2007) 457–462.
- [57] B. Jiang, B. Akgun, R.C. Lam, G.A. Ameer, J.A. Wertheim, A polymer-extracellular matrix composite with improved thromboresistance and recellularization properties, *Acta Biomater.* 18 (2015) 50–58.
- [58] Y. Lei, X. Chen, Z. Li, L. Zhang, W. Sun, L. Li, et al., A new process for customized patient-specific aortic stent graft using 3D printing technique, *Med. Eng. Phys.* 77 (2020) 80–87.
- [59] H. Savoji, L.D. Huyer, M.H. Mohammadi, B.F. Lun Lai, N. Rafatian, D. Bannerman, et al., 3D printing of vascular tubes using bioelastomer

- prepolymers by freeform reversible embedding, *ACS Biomater. Sci. Eng.* 6 (3) (2020) 1333–1343.
- [60] R. van Lith, E. Baker, H. Ware, J. Yang, A.C. Farsheed, C. Sun, et al., 3D-printing strong high-resolution antioxidant bioresorbable vascular stents, *Adv. Mater. Technol.* 1 (9) (2016), 1600138.
- [61] B. Akar, H.O.T. Ware, A.C. Farsheed, C. Duan, X. Chen, C. Sun, et al., Mechanically functional 3D-printed bioresorbable vascular scaffolds, *Tissue Eng.* 23 (2017) S14.
- [62] H.O.T. Ware, A.C. Farsheed, B. Akar, C.W. Duan, X.F. Chen, G. Ameer, et al., High-speed on-demand 3D printed bioresorbable vascular scaffolds, *Mater. Today Chem.* 7 (2018) 25–34.
- [63] M.C. Serrano, A.K. Vavra, M. Jen, M.E. Hogg, J. Murar, J. Martinez, et al., Poly (diol-co-citrate)s as novel elastomeric perivascular wraps for the reduction of neointimal hyperplasia, *Macromol. Biosci.* 11 (5) (2011) 700–709.
- [64] Y. Wang, M.R. Kibbe, G.A. Ameer, Photo-crosslinked biodegradable elastomers for controlled nitric oxide delivery, *Biomater. Sci.* 1 (6) (2013) 625–632.
- [65] A.K. Sharma, M.I. Bury, N.J. Fuller, D.I. Rozkiewicz, P.V. Hota, D.M. Kollhoff, et al., Growth factor release from a chemically modified elastomeric poly(1,8-octanediol-co-citrate) thin film promotes angiogenesis *in vivo*, *J. Biomed. Mater. Res.* 100 (3) (2012) 561–570.
- [66] L.C. Su, H. Xu, R.T. Tran, Y.T. Tsai, L.P. Tang, S. Banerjee, et al., *In situ* re-endothelialization via multifunctional nanoscaffolds, *ACS Nano* 8 (10) (2014) 10826–10836.
- [67] J. Yang, R. van Lith, K. Baler, R.A. Hoshi, G.A. Ameer, A thermoresponsive biodegradable polymer with intrinsic antioxidant properties, *Biomacromolecules* 15 (11) (2014) 3942–3952.
- [68] Z.Z. Yuan, Y.H. Tsou, X.Q. Zhang, S.X. Huang, Y. Yang, M.Z. Gao, et al., Injectable citrate-based hydrogel as an angiogenic biomaterial improves cardiac repair after myocardial infarction, *ACS Appl. Mater. Interfaces* 11 (42) (2019) 38429–38439.
- [69] G.L. Koons, M. Diba, A.G. Mikos, Materials design for bone-tissue engineering, *Nat. Rev. Mater.* 5 (8) (2020) 584–603.
- [70] G.M. Cunniffe, P.J. Diaz-Payno, E.J. Sheehy, S.E. Critchley, H.V. Almeida, P. Pitacco, et al., Tissue-specific extracellular matrix scaffolds for the regeneration of spatially complex musculoskeletal tissues, *Biomaterials* 188 (2019) 63–73.
- [71] D.B. Raina, I. Qayoom, D. Larsson, M.H. Zheng, A. Kumar, H. Isaksson, et al., Guided tissue engineering for healing of cancellous and cortical bone using a combination of biomaterial based scaffolding and local bone active molecule delivery, *Biomaterials* 188 (2019) 38–49.
- [72] X.F. Wang, J. Fang, W.W. Zhu, C.X. Zhong, D.D. Ye, M.Y. Zhu, et al., Bioinspired highly anisotropic, ultrastrong and stiff, and osteoconductive mineralized wood hydrogel composites for bone repair, *Adv. Funct. Mater.* 31 (20) (2021), 2010068.
- [73] X. Pei, L.N. Wu, C.C. Zhou, H.Y. Fan, M.L. Gou, Z.Y. Li, et al., 3D printed titanium scaffolds with homogeneous diamond-like structures mimicking that of the osteocyte microenvironment and its bone regeneration study, *Biofabrication* 13 (1) (2021), 015008.
- [74] J.H. Huang, X. Xia, Q. Zou, J.Q. Ma, S.E. Jin, J.D. Li, et al., The long-term behaviors and differences in bone reconstruction of three polymer-based scaffolds with different degradability, *J. Mater. Chem. B* 7 (48) (2019) 7690–7703.
- [75] Y. Wu, Q. Liao, L. Wu, Y. Luo, W. Zhang, M. Guan, et al., ZnL2-BPs integrated bone scaffold under sequential photothermal mediation: a win-win strategy delivering antibacterial therapy and fostering osteogenesis thereafter, *ACS Nano* 15 (11) (2021) 17854–17869.
- [76] C. Shuai, W. Yang, P. Feng, S. Peng, H. Pan, Accelerated degradation of HAP/ PLLA bone scaffold by PGA blending facilitates bioactivity and osteoconductivity, *Bioact. Mater.* 6 (2) (2021) 490–502.
- [77] H.A. Krebs, W.A. Johnson, The role of citric acid in intermediate metabolism in animal tissues, *FEBS Lett.* 117 (S1) (1980) K1–K10.
- [78] F. Dickens, The citric acid content of animal tissues, with reference to its occurrence in bone and tumour, *Biochem. J.* 35 (8–9) (1941) 1011–1023.
- [79] Y.Y. Hu, A. Rawal, K. Schmidt-Rohr, Strongly bound citrate stabilizes the apatite nanocrystals in bone, *Proc. Natl. Acad. Sci. U. S. A* 107 (52) (2010) 22425–22429.
- [80] S.H. Rhee, J. Tanaka, Effect of citric acid on the nucleation of hydroxyapatite in a simulated body fluid, *Biomaterials* 20 (22) (1999) 2155–2160.
- [81] Y. Yamada, T. Inui, Y. Kinoshita, Y. Shigemitsu, M. Honda, K. Nakano, et al., Silicon-containing apatite fiber scaffolds with enhanced mechanical property express osteoinductivity and high osteoconductivity, *J. Asian Ceram Soc.* 7 (2) (2019) 101–108.
- [82] H.H. Ren, H.Y. Zhao, Y. Cui, X. Ao, A.L. Li, Z.M. Zhang, et al., Poly(1,8-octanediol citrate)/bioactive glass composite with improved mechanical performance and bioactivity for bone regeneration, *Chin. Chem. Lett.* 28 (11) (2017) 2116–2120.
- [83] F.P. Chen, Z.Y. Song, L. Gao, H. Hong, C.S. Liu, Hierarchically macroporous/mesoporous POC composite scaffolds with IBU-loaded hollow SiO₂ microspheres for repairing infected bone defects, *J. Mater. Chem. B* 4 (23) (2016) 4198–4205.
- [84] Y.Z. Du, J. Ge, Y.P. Shao, P.X. Ma, X.F. Chen, B. Lei, Development of silica grafted poly(1,8-octanediol-co-citrate)s hybrid elastomers with highly tunable mechanical properties and biocompatibility, *J. Mater. Chem. B* 3 (15) (2015) 2986–3000.
- [85] Y.Z. Du, M. Yu, J. Ge, P.X. Ma, X.F. Chen, B. Lei, Development of a multifunctional platform based on strong, intrinsically photoluminescent and antimicrobial silica-poly(citrate)s-based hybrid biodegradable elastomers for bone regeneration, *Adv. Funct. Mater.* 25 (31) (2015) 5016–5029.
- [86] Y.Z. Du, M. Yu, X.F. Chen, P.X. Ma, B. Lei, Development of biodegradable poly(citrate)-polyhedral oligomeric silsesquioxanes hybrid elastomers with high mechanical properties and osteogenic differentiation activity, *ACS Appl. Mater. Interfaces* 8 (5) (2016) 3079–3091.
- [87] Y.W. Xi, Y. Guo, M. Wang, J. Ge, Y.L. Liu, W. Niu, et al., Biomimetic bioactive multifunctional poly(citrate-siloxane)-based nanofibrous scaffolds enable efficient multidrug-resistant bacterial treatment/non-invasive tracking *in vitro/in vivo*, *Chem. Eng. J.* 383 (2020), 123078.
- [88] Y.N. Li, Y. Guo, J. Ge, P.X. Ma, B. Lei, *In situ* silica nanoparticles-reinforced biodegradable poly(citrate-siloxane) hybrid elastomers with multifunctional properties for simultaneous bioimaging and bone tissue regeneration, *Appl. Mater. Today* 10 (2018) 153–163.
- [89] Y.N. Li, Y. Guo, W. Niu, M. Chen, Y.M. Xue, J. Ge, et al., Biodegradable multifunctional bioactive glass-based nanocomposite elastomers with controlled biomineralization activity, real-time bioimaging tracking, and decreased inflammatory response, *ACS Appl. Mater. Interfaces* 10 (21) (2018) 17722–17731.
- [90] H.Y. Zhao, H.H. Ren, J. Zhang, L. Wang, A.L. Li, J.J. Tang, et al., Bioactive glass-poly(citrate) hybrid with osteogenic ability comparable to autogenous bone, *J. Biomed. Nanotechnol.* 15 (3) (2019) 581–592.
- [91] M. Yu, Y.Z. Du, Y. Han, B. Lei, Biomimetic elastomeric bioactive siloxane-based hybrid nanofibrous scaffolds with miRNA activation: a joint physico-chemical-biological strategy for promoting bone regeneration, *Adv. Funct. Mater.* 30 (4) (2020), 1906013.
- [92] H.J. Qiu, J. Yang, P. Kodali, J. Koh, G.A. Ameer, A citric acid-based hydroxyapatite composite for orthopedic implants, *Biomaterials* 27 (34) (2006) 5845–5854.
- [93] F. Qulub, P. Widiyanti, J. Ady, Synthesis and characterization of composite poly(1,8 octanediol-co-citrate) (POC)/nano-hydroxyapatite as candidate biodegradable bone screw, *J. Biomimetics, Biomater. Biomed. Eng.* 27 (2016) 36–43.
- [94] E.J. Chung, M.J. Sugimoto, G.A. Ameer, The role of hydroxyapatite in citric acid-based nanocomposites: surface characteristics, degradation, and osteogenicity *in vitro*, *Acta Biomater.* 7 (11) (2011) 4057–4063.
- [95] E.J. Chung, H.J. Qiu, P. Kodali, S. Yang, S.M. Sprague, J. Hwang, et al., Early tissue response to citric acid-based micro- and nanocomposites, *J. Biomed. Mater. Res.* 96a (1) (2011) 29–37.
- [96] E.J. Chung, P. Kodali, W. Laskin, J.L. Koh, G.A. Ameer, Long-term *in vivo* response to citric acid-based nanocomposites for orthopaedic tissue engineering, *J. Mater. Sci. Mater. Med.* 22 (9) (2011) 2131–2138.
- [97] E.J. Chung, M. Sugimoto, J.L. Koh, G.A. Ameer, Low-pressure foaming: a novel method for the fabrication of porous scaffolds for tissue engineering, *Tissue Eng., Part C* 18 (2) (2012) 113–121.
- [98] E.J. Chung, M.J. Sugimoto, J.L. Koh, G.A. Ameer, A biodegradable tri-component graft for anterior cruciate ligament reconstruction, *J. Tissue Eng. Regen. Med.* 11 (3) (2017) 704–712.
- [99] N. Levi-Polyachenko, T. Rosenbalm, N. Kuthirummal, J. Shelton, W. Hardin, M. Teruel, et al., Development and characterization of elastic nanocomposites for craniofacial contraction osteogenesis, *J. Biomed. Mater. Res., Part B* 103 (2) (2015) 407–416.
- [100] J.S. Guo, Z.W. Xie, R.T. Tran, D.H. Xie, D.D. Jin, X.C. Bai, et al., Click chemistry plays a dual role in biodegradable polymer design, *Adv. Mater.* 26 (12) (2014) 1906–1911.
- [101] Y. Guo, R.T. Tran, D.H. Xie, Y.C. Wang, D.Y. Nguyen, E. Gerhard, et al., Citrate-based biphasic scaffolds for the repair of large segmental bone defects, *J. Biomed. Mater. Res.* 103 (2) (2015) 772–781.
- [102] J.J. Tang, J.S. Guo, Z. Li, C. Yang, D.H. Xie, J. Chen, et al., A fast degradable citrate-based bone scaffold promotes spinal fusion, *J. Mater. Chem. B* 3 (27) (2015) 5569–5576.
- [103] D.W. Sun, Y.H. Chen, R.T. Tran, S. Xu, D.H. Xie, C.H. Jia, et al., Citric acid-based hydroxyapatite composite scaffolds enhance calvarial regeneration, *Sci. Rep.* 4 (2014) 6912.
- [104] R.T. Tran, L. Wang, C. Zhang, M. Huang, W. Tang, C. Zhang, et al., Synthesis and characterization of biomimetic citrate-based biodegradable composites, *J. Biomed. Mater. Res.* 102 (8) (2014) 2521–2532.
- [105] J.S. Guo, X.G. Tian, D.H. Xie, K. Rahn, E. Gerhard, M.L. Kuzma, et al., Citrate-based tannin-bridged bone composites for lumbar fusion, *Adv. Funct. Mater.* 30 (27) (2020), 2002438.
- [106] D.H. Xie, J.S. Guo, M.R. Mehdizadeh, R.T. Tran, R.S. Chen, D.W. Sun, et al., Development of injectable citrate-based bioadhesive bone implants, *J. Mater. Chem. B* 3 (3) (2015) 387–398.
- [107] X.W. Yuan, Y.T. Zhao, J.T. Li, X.C. Chen, Z.H. Lu, L.Y. Li, et al., Citrate-based mussel-inspired magnesium whitlockite composite adhesives augmented bone-to-tendon healing, *J. Mater. Chem. B* 9 (39) (2021) 8202–8210.
- [108] Y. Jiao, D. Gyawali, J.M. Stark, P. Akcora, P. Nair, R.T. Tran, et al., A rheological study of biodegradable injectable PEGMC/HA composite scaffolds, *Soft Matter* 8 (5) (2012) 1499–1507.
- [109] D. Gyawali, P. Nair, H.K.W. Kim, J. Yang, Citrate-based biodegradable injectable hydrogel composites for orthopedic applications, *Biomater. Sci.* 1 (1) (2013) 52–64.
- [110] C.Y. Ma, X.G. Tian, J.P. Kim, D.H. Xie, X. Ao, D.Y. Shan, et al., Citrate-based materials fuel human stem cells by metabonegenic regulation, *Proc. Natl. Acad. Sci. U. S. A* 115 (50) (2018) E11741–E11750.
- [111] A. Ogita, K. Fujita, T. Tanaka, Salinomycin and citric acid in combination demonstrate bactericidal activity against gram-negative bacteria, *Ann. Microbiol.* 59 (3) (2009) 611–614.
- [112] L.C. Su, Z. Xie, Y. Zhang, K.T. Nguyen, J. Yang, Study on the antimicrobial properties of citrate-based biodegradable polymers, *Front. Bioeng. Biotechnol.* 2 (2014) 23.

- [113] P. Widiyanti, I. Sholikah, A. Isfandiari, N.A.F. Hasbiyani, M.B. Lazuardi, R. D. Laksana, Poly (1,8 octanediol-co-citrate) hydroxyapatite composite as antibacterial biodegradable bone screw, *IOP Conf. Ser. Mater. Sci. Eng.* 202 (1) (2017), 012082.
- [114] K. Company, E.H. Mirza, S. Hosseini, B. Pingguan-Murphy, I. Djordjevic, Polyoctanediol citrate-ZnO composite films: preparation, characterization and release kinetics of nanoparticles from polymer matrix, *Mater. Lett.* 126 (2014) 165–168.
- [115] J.M. Halpern, R. Urbanski, A.K. Weinstock, D.F. Iwig, R.T. Mathers, H.A. von Recum, A biodegradable thermoset polymer made by esterification of citric acid and glycerol, *J. Biomed. Mater. Res.* 102 (5) (2014) 1467–1477.
- [116] J.X. Ye, J. Wang, Y.X. Zhu, Q. Wei, X. Wang, J. Yang, et al., A thermoresponsive polydiolcitrate-gelatin scaffold and delivery system mediates effective bone formation from BMP9-transduced mesenchymal stem cells, *Biomed. Mater.* 11 (2) (2016), 025021.
- [117] Z.P. Dumanian, V. Tollemar, J.X. Ye, M.P. Lu, Y.X. Zhu, J.Y. Liao, et al., Repair of critical sized cranial defects with BMP9-transduced calvarial cells delivered in a thermoresponsive scaffold, *PLoS One* 12 (3) (2017), 0172327.
- [118] C.S. Lee, E.S. Bishop, Z. Dumanian, C. Zhao, D.Z. Song, F.G. Zhang, et al., Bone morphogenetic protein-9-stimulated adipocyte-derived mesenchymal progenitors entrapped in a thermoresponsive nanocomposite scaffold facilitate cranial defect repair, *J. Craniofac. Surg.* 30 (6) (2019) 1915–1919.
- [119] C. Zhao, Z.Y. Zeng, N.T. Qazvini, X.Y. Xu, R.Y. Zhang, S.J. Yan, et al., Thermoresponsive citrate-based graphene oxide scaffold enhances bone regeneration from BMP9-stimulated adipose-derived mesenchymal stem cells, *ACS Biomater. Sci. Eng.* 4 (8) (2018) 2943–2955.
- [120] S. Morochnik, Y.X. Zhu, C.W. Duan, M. Cai, R.R. Reid, T.C. He, et al., A thermoresponsive, citrate-based macromolecule for bone regenerative engineering, *J. Biomed. Mater. Res.* 106 (6) (2018) 1743–1752.
- [121] Y. He, Q.Y. Li, C.Y. Ma, D.H. Xie, L.M. Li, Y.T. Zhao, et al., Development of osteopromotive poly (octamethylene citrate glycerophosphate) for enhanced bone regeneration, *Acta Biomater.* 93 (2019) 180–191.
- [122] W.Y. Wei, H.L. Dai, Articular cartilage and osteochondral tissue engineering techniques: recent advances and challenges, *Bioact. Mater.* 6 (12) (2021) 4830–4855.
- [123] B. Han, Q. Li, C. Wang, P. Patel, S.M. Adams, B. Doyran, et al., Decorin regulates the aggrecan network integrity and biomechanical functions of cartilage extracellular matrix, *ACS Nano* 13 (10) (2019) 11320–11333.
- [124] Y. Krishnan, A.J. Grodzinsky, Cartilage diseases, *Matrix Biol.* 71 (2018) 51–69.
- [125] A.C. Hall, The role of chondrocyte morphology and volume in controlling phenotype-implications for osteoarthritis, cartilage repair, and cartilage engineering, *Curr. Rheumatol. Rep.* 21 (8) (2019) 1–13.
- [126] M. Morille, K. Toupet, C.N. Montero-Menei, C. Jorgensen, D. Noel, PLGA-based microcarriers induce mesenchymal stem cell chondrogenesis and stimulate cartilage repair in osteoarthritis, *Biomaterials* 88 (2016) 60–69.
- [127] J. Kisiday, M. Jin, B. Kurz, H. Hung, C. Semino, S. Zhang, et al., Self-assembling peptide hydrogel fosters chondrocyte extracellular matrix production and cell division: implications for cartilage tissue repair, *Proc. Natl. Acad. Sci. U. S. A* 99 (15) (2002) 9996–10001.
- [128] S. Scaglione, L. Ceseracciu, M. Aiello, L. Coluccino, F. Ferrazzo, P. Giannoni, et al., A novel scaffold geometry for chondral applications: theoretical model and *in vivo* validation, *Biotechnol. Bioeng.* 111 (10) (2014) 2107–2119.
- [129] J.A. Hendriks, L. Moroni, J. Riesle, J.R. de Wijn, C.A. van Blitterswijk, The effect of scaffold-cell entrapment capacity and physico-chemical properties on cartilage regeneration, *Biomaterials* 34 (17) (2013) 4259–4265.
- [130] R.S. Tigli, M. Gumusderelioglu, Evaluation of RGD- or EGF-immobilized chitosan scaffolds for chondrogenic activity, *Int. J. Biol. Macromol.* 43 (2) (2008) 121–128.
- [131] W. Wei, Y. Ma, X. Yao, W. Zhou, X. Wang, C. Li, et al., Advanced hydrogels for the repair of cartilage defects and regeneration, *Bioact. Mater.* 6 (4) (2021) 998–1011.
- [132] B. Balakrishnan, R. Banerjee, Biopolymer-based hydrogels for cartilage tissue engineering, *Chem. Rev.* 111 (8) (2011) 4453–4474.
- [133] R. Yang, F. Chen, J. Guo, D. Zhou, S. Luan, Recent advances in polymeric biomaterials-based gene delivery for cartilage repair, *Bioact. Mater.* 5 (4) (2020) 990–1003.
- [134] Y. Kang, J. Yang, S. Khan, L. Anissian, G.A. Ameer, A new biodegradable polyester elastomer for cartilage tissue engineering, *J. Biomed. Mater. Res.* 77 (2) (2006) 331–339.
- [135] C.G. Jeong, S.J. Hollister, Mechanical and biochemical assessments of three-dimensional poly(1,8-octanediol-co-citrate) scaffold pore shape and permeability effects on *in vitro* chondrogenesis using primary chondrocytes, *Tissue Eng.* 16 (12) (2010) 3759–3768.
- [136] C.G. Jeong, H.N. Zhang, S.J. Hollister, Three-dimensional poly(1,8-octanediol-co-citrate) scaffold pore shape and permeability effects on sub-cutaneous *in vivo* chondrogenesis using primary chondrocytes, *Acta Biomater.* 7 (2) (2011) 505–514.
- [137] C.G. Jeong, S.J. Hollister, A comparison of the influence of material on *in vitro* cartilage tissue engineering with PCL, PGS, and POC 3D scaffold architecture seeded with chondrocytes, *Biomaterials* 31 (15) (2010) 4304–4312.
- [138] H.A. Rothan, S.A. Mahmood, I. Djordjevic, M. Golpich, R. Yusof, S. Snigh, Polycaprolactone triol-citrate scaffolds enriched with human platelet releasates promote chondrogenic phenotype and cartilage extracellular matrix formation, *Tissue Eng. Regen. Med.* 14 (2) (2017) 93–101.
- [139] W. Park, G. Gao, D.W. Cho, Tissue-specific decellularized extracellular matrix bioinks for musculoskeletal tissue regeneration and modeling using 3D bioprinting technology, *Int. J. Mol. Sci.* 22 (15) (2021) 7837.
- [140] L. Gao, L. Ma, X.h. Yin, Y.c. Luo, H.y. Yang, B. Zhang, Nano- and microfabrication for engineering native-like muscle tissues, *Small Methods* 4 (3) (2020), 1900669.
- [141] M.E. Heroux, I. Anderman, S. Nykvist Vouis, J. Diong, P.W. Stubbs, R.D. Herbert, History-dependence of muscle slack length in humans: effects of contraction intensity, stretch amplitude, and time, *J. Appl. Physiol.* 129 (4) (2020) 957–966.
- [142] H.L. Sweeney, D.W. Hammers, Muscle contraction, cold spring harbor perspect, *Biol.* 10 (2) (2018), a023200.
- [143] J.H. Kim, I. Kim, Y.J. Seol, L.K. Ko, J.J. Yoo, A. Atala, et al., Neural cell integration into 3D bioprinted skeletal muscle constructs accelerates restoration of muscle function, *Nat. Commun.* 11 (1) (2020) 1–12.
- [144] S. Jimi, S. Koizumi, K. Sato, M. Miyazaki, A. Saparov, Collagen-derived dipeptide Pro-Hyp administration accelerates muscle regenerative healing accompanied by less scarring after wounding on the abdominal wall in mice, *Sci. Rep.* 11 (1) (2021) 18750.
- [145] M.M. Smoak, K.J. Hogan, K.J. Grande-Allen, A.G. Mikos, Bioinspired electrospun decm scaffolds guide cell growth and control the formation of myotubes, *Sci. Adv.* 7 (20) (2021), eabg4123.
- [146] K.H. Nakayama, M. Shayan, N.F. Huang, Engineering biomimetic materials for skeletal muscle repair and regeneration, *Adv. Healthc. Mater.* 8 (5) (2019), 1801168.
- [147] M.M. Carleton, M.V. Sefton, Injectable and degradable methacrylic acid hydrogel alters macrophage response in skeletal muscle, *Biomaterials* 223 (2019) 119477.
- [148] E.E. Falco, M.O. Wang, J.A. Thompson, J.M. Chetta, D.M. Yoon, E.Z. Li, et al., Porous EH and EH-PEG scaffolds as gene delivery vehicles to skeletal muscle, *Pharm. Res. (N. Y.)* 28 (6) (2011) 1306–1316.
- [149] H. Jo, M. Sim, S. Kim, S. Yang, Y. Yoo, J.H. Park, et al., Electrically conductive graphene/polyacrylamide hydrogels produced by mild chemical reduction for enhanced myoblast growth and differentiation, *Acta Biomater.* 48 (2017) 100–109.
- [150] J. Liu, D. Saul, K.O. Boker, J. Ernst, W. Lehman, A.F. Schilling, Current methods for skeletal muscle tissue repair and regeneration, *BioMed Res. Int.* 2018 (2018) 1984879.
- [151] G.X. Zhao, X.H. Zhang, T.J. Lu, F. Xu, Recent advances in electrospun nanofibrous scaffolds for cardiac tissue engineering, *Adv. Funct. Mater.* 25 (36) (2015) 5726–5738.
- [152] A.K. Sharma, P.V. Hota, D.J. Matoka, N.J. Fuller, D. Jandali, H. Thaker, et al., Urinary bladder smooth muscle regeneration utilizing bone marrow derived mesenchymal stem cell seeded elastomeric poly(1,8-octanediol-co-citrate) based thin films, *Biomaterials* 31 (24) (2010) 6207–6217.
- [153] M.P. Prabhakaran, A.S. Nair, D. Kai, S. Ramakrishna, Electrospun composite scaffolds containing poly(octanediol-co-citrate) for cardiac tissue engineering, *Biopolymers* 97 (7) (2012) 529–538.
- [154] Y.Z. Du, J. Ge, Y.N. Li, P.X. Ma, B. Lei, Biomimetic elastomeric, conductive and biodegradable polycitrate-based nanocomposites for guiding myogenic differentiation and skeletal muscle regeneration, *Biomaterials* 157 (2018) 40–50.
- [155] Y. Guo, M. Wang, J. Ge, W. Niu, M. Chen, W. Cheng, et al., Bioactive biodegradable polycitrate nanoclusters enhances the myoblast differentiation and *in vivo* skeletal muscle regeneration via p38 MAPK signaling pathway, *Bioact. Mater.* 5 (3) (2020) 486–495.
- [156] L. Zhou, J. Ge, M. Wang, M. Chen, W. Cheng, W.C. Ji, et al., Injectable muscle-adhesive antioxidant conductive photothermal bioactive nanomatrix for efficiently promoting full-thickness skeletal muscle regeneration, *Bioact. Mater.* 6 (6) (2021) 1605–1617.
- [157] M.I. Quinones-Vico, R.S. de la Torre, M. Sanchez-Diaz, A. Sierra-Sanchez, T. Montero-Vilchez, A. Fernandez-Gonzalez, et al., The role of exosomes derived from mesenchymal stromal cells in dermatology, *Front. Cell Dev. Biol.* 9 (2021), 647012.
- [158] J. Zimoch, D. Zielinska, K. Michalak-Micka, D. Rutsche, R. Boni, T. Biedermann, et al., Bio-engineering a prevascularized human tri-layered skin substitute containing a hypodermis, *Acta Biomater.* 134 (2021) 215–227.
- [159] A.A. Chaudhari, K. Vig, D.R. Baganizi, R. Sahu, S. Dixit, V. Dennis, et al., Future prospects for scaffolding methods and biomaterials in skin tissue engineering: a review, *Int. J. Mol. Sci.* 17 (12) (2016) 1974.
- [160] A.W.C. Chua, Y.C. Khoo, B.K. Tan, K.C. Tan, C.L. Foo, S.J. Chong, Skin tissue engineering advances in severe burns: review and therapeutic applications, *Burns Trauma* 4 (2016) s41038-016-0027-y.
- [161] S.G. Priya, H. Jungvid, A. Kumar, Skin tissue engineering for tissue repair and regeneration, *Tissue Eng., Part B* 14 (1) (2008) 105–118.
- [162] C.G. Wang, M. Wang, T.Z. Xu, X.X. Zhang, C. Lin, W.Y. Gao, et al., Engineering bioactive self-healing antibacterial exosomes hydrogel for promoting chronic diabetic wound healing and complete skin regeneration, *Theranostics* 9 (1) (2019) 65–76.
- [163] X.Y. Wang, Z.P. Wang, S. Fang, Y.Z. Hou, X. Du, Y.L. Xie, et al., Injectable Ag nanoclusters-based hydrogel for wound healing via eliminating bacterial infection and promoting tissue regeneration, *Chem. Eng. J.* 420 (2021), 127589.
- [164] M. Wang, C.G. Wang, M. Chen, Y.W. Xi, W. Cheng, C. Mao, et al., Efficient angiogenesis-based diabetic wound healing/skin reconstruction through bioactive antibacterial adhesive ultraviolet shielding nanodressing with exosome release, *ACS Nano* 13 (9) (2019) 10279–10293.
- [165] G.C. Gurtner, S. Werner, Y. Barrandon, M.T. Longaker, Wound repair and regeneration, *Nature* 453 (7193) (2008) 314–321.

- [166] H. Yin, C.Y. Chen, Y.W. Liu, Y.J. Tan, Z.L. Deng, F. Yang, et al., *Synechococcus elongatus* PCC7942 secretes extracellular vesicles to accelerate cutaneous wound healing by promoting angiogenesis, *Theranostics* 9 (9) (2019) 2678–2693.
- [167] Z.W.B. Zhang, Y. Zhang, W.B. Li, L.L. Ma, E.D. Wang, M. Xing, et al., Curcumin/Fe-SiO₂ nano composites with multi-synergistic effects for scar inhibition and hair follicle regeneration during burn wound healing, *Appl. Mater. Today* 23 (2021), 101065.
- [168] E.A. Kamoun, E.R.S. Kenawy, X. Chen, A review on polymeric hydrogel membranes for wound dressing applications: PVA-based hydrogel dressings, *J. Adv. Res.* 8 (3) (2017) 217–233.
- [169] J. Tavakoli, Y.H. Tang, Honey/PVA hybrid wound dressings with controlled release of antibiotics: structural, physico-mechanical and in-vitro biomedical studies, *Mater. Sci. Eng. C* 77 (2017) 318–325.
- [170] X. Peng, X. Xu, Y.R. Deng, X. Xie, L.M. Xu, X.Y. Xu, et al., Ultrafast self-gelling and wet adhesive powder for acute hemostasis and wound healing, *Adv. Funct. Mater.* 31 (33) (2021), 2102583.
- [171] A. Mohandas, S. Deepthi, R. Biswas, R. Jayakumar, Chitosan based metallic nanocomposite scaffolds as antimicrobial wound dressings, *Bioact. Mater.* 3 (3) (2018) 267–277.
- [172] B. Hu, M.Z. Gao, K.O. Boakye-Yiadom, W. Ho, W. Yu, X.Y. Xu, et al., An intrinsically bioactive hydrogel with on-demand drug release behaviors for diabetic wound healing, *Bioact. Mater.* 6 (12) (2021) 4592–4606.
- [173] A. Goins, V. Ramaswamy, E. Dirr, K. Dulany, S. Irby, A. Webb, et al., Development of poly (1,8 octanediol-co-citrate) and poly (acrylic acid) nanofibrous scaffolds for wound healing applications, *Biomater. Mater.* 13 (1) (2017), 015002.
- [174] Y.W. Xi, J. Ge, Y. Guo, B. Lei, P.X. Ma, Biomimetic elastomeric polypeptide-based nanofibrous matrix for overcoming multidrug-resistant bacteria and enhancing full-thickness wound healing/skin regeneration, *ACS Nano* 12 (11) (2018) 10772–10784.
- [175] Y.W. Xi, J. Ge, M. Wang, M. Chen, W. Niu, W. Cheng, et al., Bioactive anti-inflammatory, antibacterial, antioxidative silicon-based nanofibrous dressing enables cutaneous tumor photothermo-chemo therapy and infection-induced wound healing, *ACS Nano* 14 (3) (2020) 2904–2916.
- [176] S. Garcia-Argüelles, M.C. Serrano, M.C. Gutierrez, M.L. Ferrer, L. Yuste, F. Rojo, et al., Deep eutectic solvent-assisted synthesis of biodegradable polyesters with antibacterial properties, *Langmuir* 29 (30) (2013) 9525–9534.
- [177] C. Xie, M. Luo, M. Chen, M. Wang, X. Qu, B. Lei, Bioactive poly(octanediol-citrate-polyglycol) accelerates skin regeneration through M2 polarization immunomodulating and early angiogenesis, *Adv. Healthc. Mater.* (2022), e2101931.
- [178] W.G. Liu, M. Wang, W. Cheng, W. Niu, M. Chen, M. Luo, et al., Bioactive antiinflammatory antibacterial hemostatic citrate-based dressing with macrophage polarization regulation for accelerating wound healing and hair follicle neogenesis, *Bioact. Mater.* 6 (3) (2021) 721–728.
- [179] W. Cheng, M. Wang, M. Chen, W. Niu, Y.N. Li, Y.D. Wang, et al., Injectable antibacterial antiinflammatory molecular hybrid hydrogel dressing for rapid MDRB-infected wound repair and therapy, *Chem. Eng. J.* 409 (2021), 128140.
- [180] M. Mehdizadeh, H. Weng, D. Gyawali, L.P. Tang, J. Yang, Injectable citrate-based mussel-inspired tissue bioadhesives with high wet strength for sutureless wound closure, *Biomaterials* 33 (32) (2012) 7972–7983.
- [181] J. Guo, G.B. Kim, D.Y. Shan, J.P. Kim, J.Q. Hu, W. Wang, et al., Click chemistry improved wet adhesion strength of mussel-inspired citrate-based antimicrobial bioadhesives, *Biomaterials* 112 (2017) 275–286.
- [182] X. Lu, S. Shi, H. Li, E. Gerhard, Z. Lu, X. Tan, et al., Magnesium oxide-crosslinked low-swelling citrate-based mussel-inspired tissue adhesives, *Biomaterials* 232 (2020) 119719.
- [183] J. Guo, W. Wang, J. Hu, D. Xie, E. Gerhard, M. Nisic, et al., Synthesis and characterization of anti-bacterial and anti-fungal citrate-based mussel-inspired bioadhesives, *Biomaterials* 85 (2016) 204–217.
- [184] F.D. Zou, X.X. Sun, X.H. Wang, Elastic, hydrophilic and biodegradable poly (1, 8-octanediol-co-citric acid)/polylactic acid nanofibrous membranes for potential wound dressing applications, *Polym. Degrad. Stabil.* 166 (2019) 163–173.
- [185] J. Xiao, S. Chen, J. Yi, H. Zhang, G.A. Ameer, A cooperative copper metal-organic framework-hydrogel system improves wound healing in diabetes, *Adv. Funct. Mater.* 27 (1) (2017), 1604872.
- [186] J. Moskow, B. Ferrigno, N. Mistry, D. Jaiswal, K. Bulsara, S. Rudraiah, et al., Review: bioengineering approach for the repair and regeneration of peripheral nerve, *Bioact. Materials* 4 (2019) 107–113.
- [187] R.M. Stassart, W. Mobius, K.A. Nave, J.M. Edgar, The axon-myelin unit in development and degenerative disease, *Front. Neurosci.* 12 (2018) 467.
- [188] H. Yang, Q. Li, L. Li, S. Chen, Y. Zhao, Y. Hu, et al., Gastrodin modified polyurethane conduit promotes nerve repair via optimizing schwann cells function, *Bioact. Mater.* 8 (2022) 355–367.
- [189] R.G. Almeida, S. Pan, K.L.H. Cole, J.M. Williamson, J.J. Early, T. Czopka, et al., Myelination of neuronal cell bodies when myelin supply exceeds axonal demand, *Curr. Biol.* 28 (8) (2018) 1296–1305.
- [190] M.P. Lichtenstein, E. Perez, L. Ballesteros, C. Sunol, N. Casan-Pastor, Short-term electrostimulation enhancing neural repair *in vitro* using large charge capacity nanostructured electrodes, *Appl. Mater. Today* 6 (2017) 29–43.
- [191] M.V. Sofroniew, C.L. Howe, W.C. Mobley, Nerve growth factor signaling, neuroprotection, and neural repair, *Annu. Rev. Neurosci.* 24 (2001) 1217–1281.
- [192] F. Rao, Y.H. Wang, D.Y. Zhang, C.F. Lu, Z. Cao, J.J. Sui, et al., Aligned chitosan nanofiber hydrogel grafted with peptides mimicking bioactive brain-derived neurotrophic factor and vascular endothelial growth factor repair long-distance sciatic nerve defects in rats, *Theranostics* 10 (4) (2020) 1590–1603.
- [193] K.H. Zhang, D.W. Huang, Z.Y. Yan, C.Y. Wang, Heparin/collagen encapsulating nerve growth factor multilayers coated aligned PLLA nanofibrous scaffolds for nerve tissue engineering, *J. Biomed. Mater. Res.* 105 (7) (2017) 1900–1910.
- [194] P. Ginestra, Manufacturing of polycaprolactone-graphene fibers for nerve tissue engineering, *J. Mech. Behav. Biomed. Mater.* 100 (2019) 103387.
- [195] H. Amani, H. Kazerooni, H. Hassanpoor, A. Akbarzadeh, H. Pazoki-Toroudi, Tailoring synthetic polymeric biomaterials towards nerve tissue engineering: a review, *Artif. Cells, Nanomed, Biotechnol.* 47 (1) (2019) 3524–3539.
- [196] S. Mobini, B.S. Spearman, C.S. Lacko, C.E. Schmidt, Recent advances in strategies for peripheral nerve tissue engineering, *Curr. Opin. Biomed. Eng.* 4 (2017) 134–142.
- [197] S. Yi, L. Xu, X.S. Gu, Scaffolds for peripheral nerve repair and reconstruction, *Exp. Neurol.* 319 (2019), 112761.
- [198] D. Shahriari, G. Loke, I. Tafel, S. Park, P.H. Chiang, Y. Fink, et al., Scalable fabrication of porous microchannel nerve guidance scaffolds with complex geometries, *Adv. Mater.* 31 (30) (2019), 1902021.
- [199] G. Courtine, M.V. Sofroniew, Spinal cord repair: advances in biology and technology, *Nat. Med.* 25 (6) (2019) 898–908.
- [200] N. Nishida, F. Jiang, J. Ohgi, A. Tanaka, Y. Imajo, H. Suzuki, et al., Compression analysis of the gray and white matter of the spinal cord, *Neural Regen. Res.* 15 (7) (2020) 1344–1349.
- [201] E. Diaz, H. Morales, Spinal cord anatomy and clinical syndromes, *Semin, Ultrasound CT MRI* 37 (5) (2016) 360–371.
- [202] W. Xue, W. Shi, Y.F. Kong, M. Kuss, B. Duan, Anisotropic scaffolds for peripheral nerve and spinal cord regeneration, *Bioact. Mater.* 6 (11) (2021) 4141–4160.
- [203] J. Koffler, W. Zhu, X. Qu, O. Platoshyin, J.N. Dulin, J. Brock, et al., Biomimetic 3D-printed scaffolds for spinal cord injury repair, *Nat. Med.* 25 (2) (2019) 263–269.
- [204] H. Shen, C.X. Fan, Z.F. You, Z.F. Xiao, Y.N. Zhao, J.W. Dai, Advances in biomaterial-based spinal cord injury repair, *Adv. Funct. Mater.* (2021), 2110628.
- [205] X. Li, D.Y. Liu, Z.F. Xiao, Y.N. Zhao, S.F. Han, B. Chen, et al., Scaffold-facilitated locomotor improvement post complete spinal cord injury: motor axon regeneration versus endogenous neuronal relay formation, *Biomaterials* 197 (2019) 20–31.
- [206] H. Ren, X.R. Chen, M.Y. Tian, J. Zhou, H.W. Ouyang, Z.Y. Zhang, Regulation of inflammatory cytokines for spinal cord injury repair through local delivery of therapeutic agents, *Adv. Sci.* 5 (11) (2018), 1800529.
- [207] K.A. Tran, P.P. Partyka, Y. Jin, J. Bouyer, I. Fischer, P.A. Galie, Vascularization of self-assembled peptide scaffolds for spinal cord injury repair, *Acta Biomater.* 104 (2020) 76–84.
- [208] J.R. Slotkin, C.D. Pritchard, B. Luque, J. Ye, R.T. Layer, M.S. Lawrence, et al., Biodegradable scaffolds promote tissue remodeling and functional improvement in non-human primates with acute spinal cord injury, *Biomaterials* 123 (2017) 63–76.
- [209] D.F. Liu, J. Chen, T. Jiang, W. Li, Y. Huang, X.Y. Lu, et al., Biodegradable spheres protect traumatically injured spinal cord by alleviating the glutamate-induced excitotoxicity, *Adv. Mater.* 30 (14) (2018), 1706032.
- [210] M.B. Orr, J.C. Gensel, Spinal cord injury scarring and inflammation: therapies targeting glial and inflammatory responses, *Neurotherapeutics* 15 (3) (2018) 541–553.
- [211] D.Y. Liu, M.Y. Shu, W.Y. Liu, Y.Y. Shen, G. Long, Y.N. Zhao, et al., Binary scaffold facilitates *in situ* regeneration of axons and neurons for complete spinal cord injury repair, *Biomater. Sci.* 9 (8) (2021) 2955–2971.
- [212] Q.Z. Zhang, B. Shi, J.X. Ding, L.S. Yan, J.P. Thawani, C.F. Fu, et al., Polymer scaffolds facilitate spinal cord injury repair, *Acta Biomater.* 88 (2019) 57–77.
- [213] R.T. Tran, W.M. Choy, H. Cao, I. Qattan, J.C. Chiao, W.Y. Ip, et al., Fabrication and characterization of biomimetic multichanneled crosslinked-urethane-doped polyester tissue engineered nerve guides, *J. Biomed. Mater. Res.* 102 (8) (2014) 2793–2804.
- [214] G.B. Kim, Y. Chen, W. Kang, J. Guo, R. Payne, H. Li, et al., The critical chemical and mechanical regulation of folic acid on neural engineering, *Biomaterials* 178 (2018) 504–516.
- [215] C.G. Wang, M. Wang, K.S. Xia, J.K. Wang, F. Cheng, K.S. Shi, et al., A bioactive injectable self-healing anti-inflammatory hydrogel with ultralong extracellular vesicles release synergistically enhances motor functional recovery of spinal cord injury, *Bioact. Mater.* 6 (8) (2021) 2523–2534.
- [216] R.A. Hoshi, S. Behl, G.A. Ameer, Nanoporous biodegradable elastomers, *Adv. Mater.* 21 (2) (2009) 188–192.
- [217] S. Dolai, S.K. Bhunia, S. Rajendran, V. UshaVipinachandran, S.C. Ray, P. Kluson, Tunable fluorescent carbon dots: synthesis progress, fluorescence origin, selective and sensitive volatile organic compounds detection, *Crit. Rev. Solid State* 46 (4) (2021) 349–370.
- [218] J. Yang, Y. Zhang, S. Gautam, L. Liu, J. Dey, W. Chen, et al., Development of aliphatic biodegradable photoluminescent polymers, *Proc. Natl. Acad. Sci. U. S. A.* 106 (25) (2009) 10086–10091.
- [219] C.A. Serrano, Y. Zhang, J. Yang, K.A. Schug, Matrix-assisted laser desorption/ionization mass spectrometric analysis of aliphatic biodegradable photoluminescent polymers using new ionic liquid matrices, *Rapid Commun. Mass Spectrom.* 25 (9) (2011) 1152–1158.
- [220] Z.W. Xie, J.P.M. Kim, Q. Cai, Y. Zhang, J.S. Guo, R.S. Dhimi, et al., Synthesis and characterization of citrate-based biodegradable small molecules and biodegradable polymers, *Acta Biomater.* 50 (2017) 361–369.
- [221] Y. Zhang, J. Yang, Design strategies for fluorescent biodegradable polymeric biomaterials, *J. Mater. Chem. B* 1 (2) (2013) 132–148.
- [222] M. Wang, Y. Guo, P.X. Ma, B. Lei, Photoluminescent arginine-functionalized polycitrate with enhanced cell activity and hemocompatibility for live cell bioimaging, *J. Biomed. Mater. Res.* 106 (12) (2018) 3175–3184.

- [223] B. Jiang, R. Suen, J.J. Wang, Z.J. Zhang, J.A. Wertheim, G.A. Ameer, Mechanocompatible polymer-extracellular-matrix composites for vascular tissue engineering, *Adv. Healthc. Mater.* 5 (13) (2016) 1594–1605.
- [224] B. Jiang, R. Suen, J.J. Wang, Z.J. Zhang, J.A. Wertheim, G.A. Ameer, Vascular scaffolds with enhanced antioxidant activity inhibit graft calcification, *Biomaterials* 144 (2017) 166–175.
- [225] A.S. Wadajkar, T. Kadapure, Y. Zhang, W.N. Cui, K.T. Nguyen, J. Yang, Dual-imaging enabled cancer-targeting nanoparticles, *Adv. Healthc. Mater.* 1 (4) (2012) 450–456.
- [226] Z.W. Xie, Y.X. Su, G.B. Kim, L. Liu, H. Weng, R.P. Mason, L.P. Tang, et al., Development of intrinsically photoluminescent and photostable polylactones, *Adv. Mater.* 26 (26) (2014) 4491–4496.
- [227] Z.W. Xie, Y.X. Su, G.B. Kim, E. Selvi, C.Y. Ma, V. Aragon-Sanabria, et al., Immune cell-mediated biodegradable theranostic nanoparticles for melanoma targeting and drug delivery, *Small* 13 (10) (2017), 1603121.
- [228] J. Li, Y.C. Tian, D.Y. Shan, A. Gong, L.Y. Zeng, W.Z. Ren, et al., Neuropeptide Y Y1 receptor-mediated biodegradable photoluminescent nanobubbles as ultrasound contrast agents for targeted breast cancer imaging, *Biomaterials* 116 (2017) 106–117.
- [229] J.Q. Hu, J.S. Guo, Z.W. Xie, D.Y. Shan, E. Gerhard, G.Y. Qian, et al., Fluorescence imaging enabled poly(lactide-co-glycolide), *Acta Biomater.* 29 (2016) 307–319.
- [230] Y. Zhang, R.T. Tran, I.S. Qattan, Y.T. Tsai, L.P. Tang, C. Liu, et al., Fluorescence imaging enabled urethane-doped citrate-based biodegradable elastomers, *Biomaterials* 34 (16) (2013) 4048–4056.
- [231] D. Shan, S.R. Kothapalli, D.J. Ravnice, E. Gerhard, J.P. Kim, J. Guo, et al., Development of citrate-based dual-imaging enabled biodegradable electroactive polymers, *Adv. Funct. Mater.* 28 (34) (2018), 1801787.
- [232] Y.H. Tsou, X.Q. Zhang, X. Bai, H. Zhu, Z.Y. Li, Y.L. Liu, et al., Dopant-free hydrogels with intrinsic photoluminescence and biodegradable properties, *Adv. Funct. Mater.* 28 (34) (2018), 1802607.
- [233] Y.Z. Du, Y.M. Xue, P.X. Ma, X.F. Chen, B. Lei, Biodegradable, elastomeric, and intrinsically photoluminescent poly(silicon-citrate)s with high photostability and biocompatibility for tissue regeneration and bioimaging, *Adv. Healthc. Mater.* 5 (3) (2016) 382–392.
- [234] M. Wang, Y. Guo, M. Yu, P.X. Ma, C. Mao, B. Lei, Photoluminescent and biodegradable polycitrate-polyethylene glycol-polyethyleneimine polymers as highly biocompatible and efficient vectors for bioimaging-guided siRNA and miRNA delivery, *Acta Biomater.* 54 (2017) 69–80.
- [235] Y.N. Li, N. Li, J. Ge, Y.M. Xue, W. Niu, M. Chen, et al., Biodegradable thermal imaging-tracked ultralong nanowire-reinforced conductive nanocomposites elastomers with intrinsic efficient antibacterial and anticancer activity for enhanced biomedical application potential, *Biomaterials* 201 (2019) 68–76.
- [236] M.J. Chen, M.Z. Yin, Design and development of fluorescent nanostructures for bioimaging, *Prog. Polym. Sci.* 39 (2) (2014) 365–395.
- [237] F. Li, Y.J. Su, G.F. Pi, P.X. Ma, B. Lei, Biodegradable, biomimetic elastomeric, photoluminescent, and broad-spectrum antibacterial polycitrate-polypeptide-based membrane toward multifunctional biomedical implants, *ACS Biomater. Sci. Eng.* 4 (8) (2018) 3027–3035.
- [238] D.D. Guo, C.Y. Shi, X. Wang, L.L. Wang, S.L. Zhang, J.T. Luo, Riboflavin-containing telodendrimer nanocarriers for efficient doxorubicin delivery: high loading capacity, increased stability, and improved anticancer efficacy, *Biomaterials* 141 (2017) 161–175.
- [239] P. Mi, Stimuli-responsive nanocarriers for drug delivery, tumor imaging, therapy and theranostics, *Theranostics* 10 (10) (2020) 4557–4588.
- [240] M. Kanamala, W.R. Wilson, M.M. Yang, B.D. Palmer, Z.M. Wu, Mechanisms and biomaterials in pH-responsive tumour targeted drug delivery: a review, *Biomaterials* 85 (2016) 152–167.
- [241] J. Zhang, J.P. Jia, J.P. Kim, F. Yang, X. Wang, H. Shen, et al., Construction of versatile multilayered composite nanoparticles from a customized nanogel template, *Bioact. Mater.* 3 (1) (2018) 87–96.
- [242] G.B. Kim, V. Aragon-Sanabria, L. Randolph, H. Jiang, J.A. Reynolds, B.S. Webb, et al., High-affinity mutant interleukin-13 targeted CAR T cells enhance delivery of clickable biodegradable fluorescent nanoparticles to glioblastoma, *Bioact. Mater.* 5 (3) (2020) 624–635.
- [243] Z. Jiang, Y. Tian, D. Shan, Y. Wang, E. Gerhard, J. Xia, et al., pH protective Y1 receptor ligand functionalized antiphagocytosis BPLP-WPU micelles for enhanced tumor imaging and therapy with prolonged survival time, *Biomaterials* 170 (2018) 70–81.
- [244] N. Pandey, J.U. Menon, M. Takahashi, J.T. Hsieh, J. Yang, K.T. Nguyen, et al., Thermo-responsive fluorescent nanoparticles for multimodal imaging and treatment of cancers, *Nanotheranostics* 4 (1) (2020) 1–13.
- [245] R. Iyer, A.E. Kuriakose, S. Yaman, L.C. Su, D.Y. Shan, J. Yang, et al., Nanoparticle eluting-angioplasty balloons to treat cardiovascular diseases, *Int. J. Pharm.* 554 (2019) 212–223.
- [246] A.E. Kuriakose, N. Pandey, D. Shan, S. Banerjee, J. Yang, K.T. Nguyen, Characterization of photoluminescent polylactone-based nanoparticles for their applications in cardiovascular diseases, *Front. Bioeng. Biotechnol.* 7 (2019) 353.
- [247] R. Dimatteo, N.J. Darling, T. Segura, *In situ* forming injectable hydrogels for drug delivery and wound repair, *Adv. Drug Deliv. Rev.* 127 (2018) 167–184.
- [248] Y.N. Sun, D. Nan, H.Q. Jin, X.Z. Qu, Recent advances of injectable hydrogels for drug delivery and tissue engineering applications, *Polym. Test.* 81 (2020), 106283.
- [249] D. Gyawali, P. Nair, Y. Zhang, R.T. Tran, C. Zhang, M. Samchukov, et al., Citric acid-derived *in situ* crosslinkable biodegradable polymers for cell delivery, *Biomaterials* 31 (34) (2010) 9092–9105.
- [250] A. Gonsalves, P. Tambe, D. Le, D. Thakore, A.S. Wadajkar, J. Yang, et al., Synthesis and characterization of a novel pH-responsive drug-releasing nanocomposite hydrogel for skin cancer therapy and wound healing, *J. Mater. Chem. B* 9 (46) (2021) 9533–9546.
- [251] X.Q. Zhang, H.H. Tang, R. Hoshi, L. De Laporte, H.J. Qiu, X.Y. Xu, et al., Sustained transgene expression *via* citric acid-based polyester elastomers, *Biomaterials* 30 (13) (2009) 2632–2641.
- [252] M. Wang, Y. Guo, Y.M. Xue, W. Niu, M. Chen, P.X. Ma, et al., Engineering multifunctional bioactive citric acid-based nanovectors for intrinsic targeted tumor imaging and specific siRNA gene delivery *in vitro/in vivo*, *Biomaterials* 199 (2019) 10–21.
- [253] M. Wang, M. Chen, W. Niu, D.D. Winston, W. Cheng, B. Lei, Injectable biodegradation-visual self-healing citrate hydrogel with high tissue penetration for microenvironment-responsive degradation and local tumor therapy, *Biomaterials* 261 (2020) 120301.
- [254] L. Zhang, M. Wang, M. Chen, W. Niu, W.G. Liu, T.T. Leng, et al., A safe and efficient bioactive citrate-lysine/miRNA33 agonist nanosystem for high fat diet-induced obesity therapy, *Chem. Eng. J.* 408 (2021), 127304.